# MODEL BUILDING INCORPORATING DISCRIMINATION BETWEEN RIVAL MATHEMATICAL MODELS IN HEAT TRANSFER

Thesis for the Degree of Ph. D. MICHIGAN STATE UNIVERSITY GERALD JAMES VAN FOSSEN Jr. 1973



#### ABSTRACT

MODEL BUILDING INCORPORATING DISCRIMINATION

BETWEEN RIVAL MATHEMATICAL MODELS IN HEAT TRANSFER

By

Gerald James Van Fossen, Jr.

The primary concern of this thesis is the development of mathematical models from experimental data in
heat transfer. A model building procedure is proposed
which enables an experimenter to develop several mechanistic, mathematical models that describe a complex phenomenon.
A discrimination criterion is incorporated in the model
building procedure to help an experimenter decide which
of several rival models describes the phenomenon best.

The model building procedure involves performing optimum experiments to estimate the parameters involved in proposed models. A criterion for finding optimum experiments for parameter estimation is discussed. Optimum experimental conditions for estimating the parameters involved in a mathematical model that describes the temperature distribution in a melting solid are found.

To illustrate the procedure proposed for model building including discrimination, a mathematical model is found
for the specific case of a melting solid. An optimum,
transient experiment for parameter estimation is performed
on a finite, one-dimensional, melting, low temperature

alloy. Tr

alloy. The temperature data from this experiment is used to find a mathematical model for the melting solid. The proposed model building procedure is generally applicable to experiments for which, a) large amounts of data are generated for each experiment, b) the model is unknown, c) the model can be solved numerically with reasonable expenditures of computer time and d) optimum experiments can be designed and run.

بایاد حجارت

BETWEE

in

# MODEL BUILDING INCORPORATING DISCRIMINATION BETWEEN RIVAL MATHEMATICAL MODELS IN HEAT TRANSFER

 $\mathbf{B}\mathbf{y}$ 

Gerald James Van Fossen, Jr.

#### A THESIS

Submitted to
Michigan State University
in partial fulfillment of the requirements
for the degree of

DOCTOR OF PHILOSOPHY

Department of Mechanical Engineering

1973

# TABLE OF CONTENTS

CHAPTER	I DESCRIPTION OF THE PROBLEM	1
1.1	Introduction	1
1.2	Definition of model building and descrimination between rival mathematical models	2
	Possible applications of model building and discrimination between rival models	5
<b>%</b> 1.4	Parameter estimation and its use in model building and discrimination	5
1.5	Background of model building and discrimination in other fields	9
1.6	Application to heat transfer	19
1.7	The proposed method	21
CHAPTER	II OPTIMUM EXPERIMENTS FOR PARAMETER ESTIMATION	28
2.1	Introduction	28
2.2	Sensitivity coefficients	29
2.3	The criteria for design of optimum experiments	31
2.4	Results for several sample cases	36
CHAPTER	III EXPERIMENTAL EQUIPMENT AND TECHNIQUE	69
3.1	The data aquisition system	69
3.2	Equipment and test specimens	72
3.3	The experiment	76

CHAPTER

4.1

4.2

4.3

CHAPTER

LIST OF

APPENDIX

A.1

¥.5

WDBENDIN

3.1

2.2

APPENDI

CHAPTER	IV TEST OF THE PROPOSED METHOD	81
4.1	Introduction	81
4.2	The model building process	81
4.3	Discrimination between rival mathematical models	102
CHAPTER	v conclusions	106
LIST OF R	EFERENCES	109
APPENDIX	A FINITE DIFFERENCE METHOD FOR CALCULATING TEMPERATURE DISTRIBUTIONS IN ONE DIMENSIONAL FREEZING-MELTING AND TEMPERATURE VARIABLE PROPERTY PROBLEMS	112
A.1	General finite difference method	112
A.2	The solution of freezing-melting problems	119
APPENDIX	B PARAMETER ESTIMATION PROCEDURE AND THE CALCULATION OF SENSITIVITY COEFFICIENTS.	135
B.1	The Gauss-Newton or linearization method of minimizing the sum of squares function	135
B.2	Calculation of sensitivity coefficients	138
APPENDIX	C THE CALCULATION OF SURFACE HEAT FLUX	142

TABLE

2.4

2.4

2.4

4.

# LIST OF TABLES

TABLE		
2.4.1	$\overline{\Delta}_{\text{opt}}$ for several values of $\mathbf{T}_{\mathbf{T}}^{+}$ with $oldsymbol{ ho}\mathbf{L}$ the parameter to be estimated for the semi-infinite example	44
2.4.2	$\overline{\Delta}_{\text{opt}}$ for several values of $T_{\mathbf{T}}^{+}$ and $L_{\mathbf{T}}^{+}$ with $T_{\mathbf{r}}$ and $\rho$ L being the parameters to be estimated for the semi-infinite example	49
2.4.3	Locations and times for maxima and minima of sensitivity coefficients $S_{\mathbf{p}L}^{\mathbf{T}}$ and $S_{\mathbf{T}_{\mathbf{f}}}^{\mathbf{T}}$	67
4.3.1	Comparison of the likelihood functions of the four models	104

2.4.1(a)

2.4.1(b)

2.4.2

2.4.3

2.4.4

2.4.5

2.4.6

## LIST OF FIGURES

FIGURE		PAGE
1.2.1	Concentration of B versus reaction time for the two models A-B-C and A-B-C	4
1.7.1	Flow diagram of the proposed model building procedure	23
2.4.1(a)	Dimensionless temperature of a freezing semi-infinite body subjected to a step decrease in temperature at the boundary for several values of the dimensionless heat of fusion, L <sub>T</sub> <sup>+</sup>	40
2.4.1(b)	Dimensionless temperature of a freezing semi-infinite body subjected to a step decrease in temperature at the boundary for several values of dimensionless	
	fusion temperature, $T_T^+$	41
2.4.2	Dimensionless sensitivity coefficients for a freezing liquid semi-infinite body with a step decrease in temperature at the surface	42
2.4.3	$\overline{\Delta}_{ m opt}$ versus dimensionless heat of fusion for a single thermocouple with $ ho$ L the	
	property to be estimated	• 45
2.4.4	Merit function, M, versus $\Delta T_{max}$	. 45
2.4.5	Product of merit function, $M$ , and $\overline{\Delta}_{opt}$ .	
	versus $\Delta T_{\text{max}}$ used to determine the optimum $\Delta T_{\text{max}}$ for estimating $\rho L$	47
2.4.6	Sensitivity coefficients at $x/E = 0.0$ for a melting-freezing, finite body with constant heat flux, q, at $x=0$ and insulated at $x=E$	

FIGURE		PAGE
2.4.7	Sensitivity coefficients at $x/E = 0.5$ for a melting-freezing, finite body with constant heat flux, q, at x=0 and insulated at x=E.	51
2.4.8	Sensitivity coefficients at x/E = 1.0 for a melting-freezing, finite body with constant heat flux, q, at x=0 and insulated at x=E	52
2.4.9	Dimensionless, $S_{\mathbf{L}}^{\mathbf{T}}$ , versus dimensionless time, $\mathbf{T}$ , for a finite body with constant heat flux, q, at $\mathbf{x}/\mathbf{E} = 0$ and insulated at $\mathbf{x}/\mathbf{E} = 1$ .	•• 55
2.4.10	$\overline{\Delta}$ versus $\tau_{\rm m}$ for several values of $\Delta \tau_{\rm max}$ for a melting, finite body of solid initially at the fusion temperature with $ ho L$	y
	the parameter to be estimated	58
2.4.11	$\overline{\Delta}_{\text{opt}}$ versus $\Delta T_{\text{max}}$ for finite body of solid initially at the fusion temperature with $ ho L$	
	the parameter to be estimated	59
2.4.12	The product $M\overline{\Delta}_{opt}$ versus $\Delta T_{max}$ used to determine the optimum $\Delta T_{max}$ for estimating	62
	the paramater pl	61
2.4.13	Experimental heat flux from copper heater- calorimeter and heat flux through copper lid versus time	63
2.4.14	Sensitivity coefficients $S_{oldsymbol{ ho}}^{oldsymbol{T}}$ and $S_{oldsymbol{T}_{oldsymbol{f}}}^{oldsymbol{T}}$ at	
	x=0.0 versus time for a finite body insulated at x=E and the heat flux of Figure 2.4.13 prescribed at x=0.0	a · · 64
2.4.15	Sensitivity coefficients $S_{oldsymbol{ h}L}^{oldsymbol{T}}$ and $S_{oldsymbol{T}_{oldsymbol{f}}}^{oldsymbol{T}}$ at	
	<pre>x/E = 0.5 versus time for a finite body insulated at x=E and the heat flux of Figure 2.4.13 prescribed at x=0.0</pre>	65
2.4.16	Sensitivity coefficients $S_{m{p}^{ar{L}}}^{m{T}}$ and $S_{m{T}}^{m{T}}$ at	
	<pre>x/E = 1.0 versus time for a finite body insulated at x=E and the heat flux of Figure 2.4.13 prescribed at x=0.0</pre>	66

FIGURE		PAGE
3.2.1	The experimental equipment	74
3.3.1	Partial section view of nylon cup specimen showing copper lid in place and location of thermocouples	77
4.2.1	Constant thermal conductivity and heat capacity model and the data versus time	
4.2.2	Residuals for constant thermal conductivity and heat capacity model versus time	84
4.2.3	Residuals for the constant thermal conductivity and heat capacity model versus measured temperature	
4.2.4	Step change in thermal properties model and data versus time	87
4.2.5	Residuals for the step change in thermal property model versus time	89
4.2.6	Residuals for the step change in thermal properties model versus measured temperature	90
4.2.7	Energy absorbed by melting over a range of temperature model	92
4.2.8	Melting over a range of temperature model and the data versus time	93
4.2.9	Residuals for the melting over a range of temperature model versus time	95
4.2.10	Residuals for the melting over a range of temperature model versus measured temperature.	97
4.2.11	Isothermal melting-freezing model and the data versus time	98
4.2.12	Residuals for the isothermal melting-freezing model versus time	99
4.2.13	Residuals for the isothermal melting-freezing model versus measured temperature	100

FIGURE

**A.**1

**A.**2

A.3

A.4

**A.**5

B.1

£.2

0.1

• 5

0,3

FIGURE

A.1	Node geometry and nomenclature for the finite difference solution to the heat conduction equation at the interface between dissimilar materials
<b>A.</b> 2	Node geometry and nomenclature for the finite difference solution to the heat conduction equation at the heated surface with a known heat flux
A.3	Node geometry and nomenclature for the floating node used in the finite difference solution of the freezing-melting problem114
A.4	A comparison of the finite difference solution to an exact solution of the freezing-melting problem
<b>A.</b> 5	A comparison of the finite difference solution to an approximate solution of the freezing-melting problem
B.1	A comparison of exact and numerical approximation of the dimensionless sensitivity coefficient $S_{\mathbf{k}}^{T}(\mathbf{x},\mathbf{t})$ for a finite body with constant heat flux, q, at $\mathbf{x}=0$ and insulated at $\mathbf{x}=E$
B.2	A comparison of exact and numerical approximation of the dimensionless sensitivity coefficients $S_{pc}^{T}(\mathbf{x},t)$ for a finite body with constant heat flux, q, at $\mathbf{x}=0$ and insulated at $\mathbf{x}=E$
C.1	Ratio of temperature rise to maximum temperature rise versus ratio of dimensionless time to dimensionless duration of heat pulse at the insulated surface of a plate with heat applied to the other side
C.2	Illustration of how a time varying heat flux is broken up into a series of heat pulses144
C.3	Comparison of heat flux calculated from temperature data accurate to six places for 1, 2, and 3 future temperatures for a slab with a step in flux at one surface and the other surface insulated

FIGURE		PAGE
C.4	Heat flux calculated from noisy data for 2 future temperatures for a slab with a step in flux at one surface and insulated at the other surface	148

# LIST OF SYMBOLS

A(n), B(n), C(n), D(n)	Coefficients used in numerical approximation to heat conduction equation defined by equations [A.1.1]
CNBD	Finite difference parameter defined in Appendix A
<b>c</b> <sub>p</sub>	Specific heat at constant pressure
E	Length of finite body
erf(x)	Error function $erf(x) = \sqrt{\pi} \int_{0}^{x} e^{-t^{2}} dt$
erfc(x)	Complementary error function $erfc(x) = 1-erf(x)$
Fo	Constant heat flux applied to surface of a semi-infinite body
k	Thermal conductivity
k <sup>†</sup>	Ratio of thermal conductivity of liquid phase to thermal conductivity of solid phase
L	Heat of fusion
L(model i/d	ata) Likelihood function for model i given the data
L <sub>T</sub> , L <sub>q</sub>	Heat of fusion non-dimensionalized with respect to temperature and heat flux respectively
M	Merit function for maximum temperature rise
m	Number of discreet times in data
N	Number of data points
n	Number of thermocouples
<u>P</u>	Vector of parameters with elements pi
q	Heat flux

 $s_{p_i}^{r}$ 

T(x,t)

X

$\mathbf{s}_{\mathbf{p_i}}^{\mathtt{T}}$	Sensitivity coefficient - derivative of temperature T with respect to parameter pi
Ti	Initial temperature
T <sub>f</sub>	Fusion temperature
To	Surface temperature $(x = 0)$
T <sub>T</sub> , T <sub>q</sub>	Fusion temperature non-dimensionalized with respect to temperature and heat flux respectively
Ts, T	Dimensionless temperature of solid and liquid phase respectively
T(x,t)	Temperature at location x and time t
t	Time
M	Vector of predictions with elements $\mathbf{w}_{\mathbf{u}}$
x	Location
<u>Y</u>	Vector of observations with elements yu
<u>z</u>	Sensitivity matrix with elements z

ε λ ξ ρ ο τ ¥

# GREEK SYMBOLS

a	Thermal diffusivity
a+	Ratio of thermal diffusivity of solid phase to thermal diffusivity of liquid phase
<u>r</u>	Matrix formed by the product $\underline{Z}'\underline{Z}$
Δ	Matrix whose elements are $\delta_{ij}$ defined by equation [2.3.2]
$\Sigma$	Determinant of the matrix $\Delta$
$\Delta_{ t opt}$	Optimum $\overline{\Delta}$ as defined by equation [2.3.6]
$\Delta$ T <sub>max</sub>	Maximum temperature rise experienced during an experiment
€	Location of solid-liquid interface
λ	Root of equation [2.4.4] or finite difference parameter defined in Appendix A
<u><b>ξ</b></u>	Vector of controllable variables
ρ	Density
σ	Variance of observations
7	Dimensionless time
<u>\<b>Y</b></u>	Weighting matrix used in likelihood function

#### CHAPTER I

#### DESCRIPTION OF THE PROBLEM

#### 1.1 Introduction

One of the most fundamental problems in science is that of obtaining mathematical models from observations. The basic objective of this thesis is to propose and demonstrate a procedure that can be used to develop an adequate mathematical model for certain types of physical Processes. The procedure is successfully applied to the Specific case of finding a mathematical model from experimental data for a melting, one-dimensional solid which is heated at one surface and insulated at the other. This re-Presents a complex heat transfer process. The proposed procedure could be used to find an adequate mathematical model for any process where one can obtain large amounts of data from a single transient experiment at a relatively low cost. The individual parts of the proposed procedure are not new; however, the idea of using optimum experiments and Ciscrimination coupled with actual heat transfer data for finding a mathematical model is original.

The proposed process is called <u>model building</u> which incorporates <u>discrimination</u> between rival mathematical models, these terms are defined in section 1.2 of this

chapter
which d
some ex
in heat
paramet
ature c
ematical
describe
discrim:
posed pr
model is
outlines

ables an

process.

thesis c

te able

Which is

Tertal da

the defic

chapter. Model building procedures have been suggested which do not include discrimination. Section 1.3 contains some examples of how the proposed procedure would be of use in heat transfer. Section 1.4 discusses the importance of parameter estimation in model building. A review of literature concerned with model building between rival mathematical models is contained in section 1.5. Section 1.6 describes how the existing methods for model building and discrimination can be applied to heat transfer. The proposed procedure for developing an adequate mathematical model is given in section 1.7 along with a flow chart that outlines the proposed procedure.

# 1.2 Definition of model building and discrimination between rival mathematical models.

## Model Building

Model building is the complete procedure which enables an experimenter to develop a "best" model for the Process. It is not simply the derivation of mathematical models from conservation principles. All the models in this thesis can be so derived. The experimenter may; however, be able to derive several of these models without knowing which is the correct one.

In the model building procedure the simplest reasonable "first cut" model is proposed and fitted to the experimental data (i.e., the parameters in the model are estimated). The quality of fit is then examined to learn the nature of the deficiencies in the model. based on this knowledge,

a modified model is proposed to better describe the process.

#### Discrimination

A very important part of model building is called discrimination. Discrimination involves the <u>design of experiments</u> so that differences between the predicted responses of two or more models is the greatest. By using such experiments along with a <u>decision-making criteria</u>, one can better decide which is the correct model. Various criteria are presented in section 1.5.

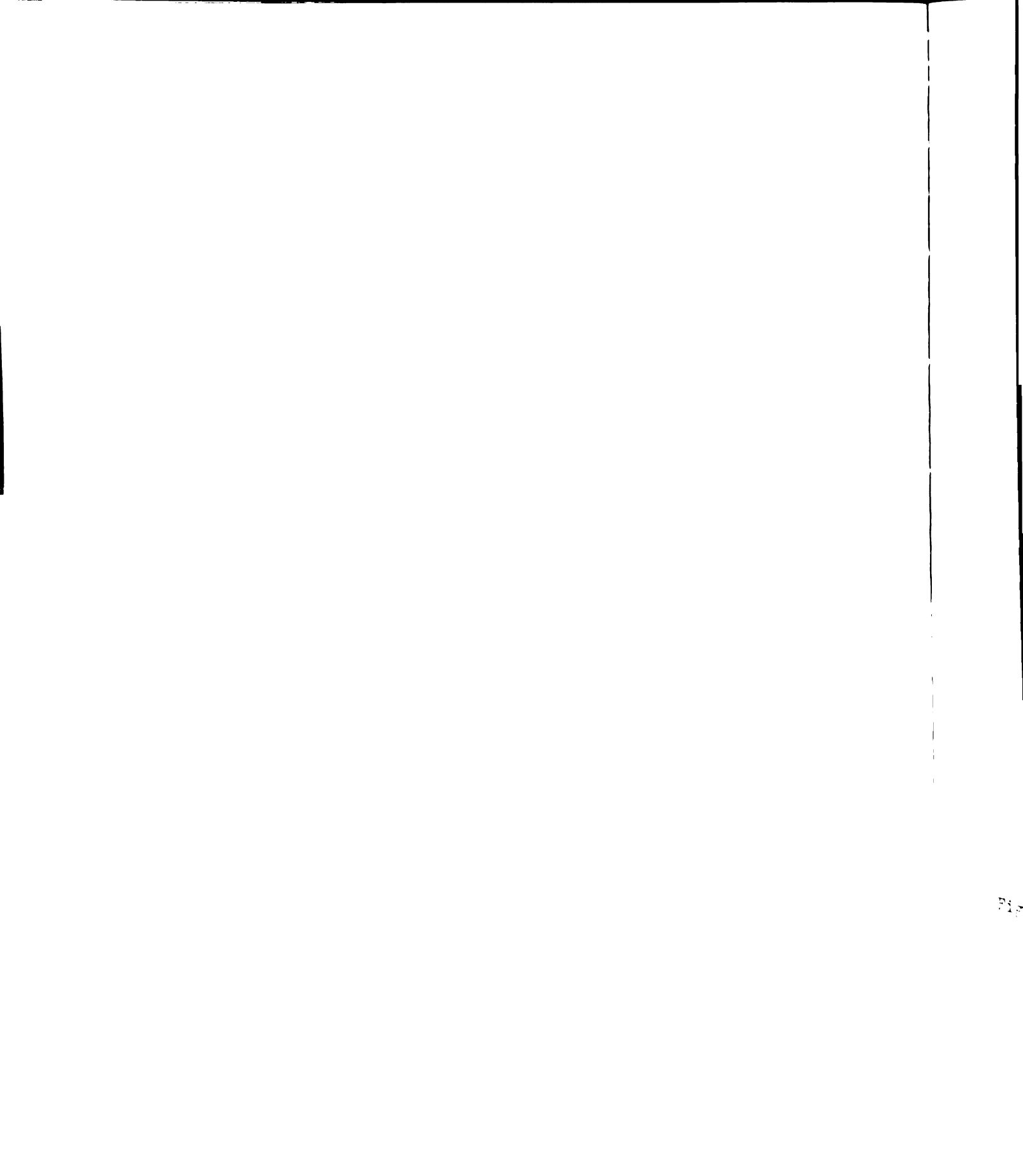
An example of the need for design of experiments for discrimination has been given by chemical engineers (1). A substance "A" reacts in the presence of a catalyst to form substance "B" which in turn forms "C". One possible model for this is given by

$$A \longrightarrow B \longrightarrow C \qquad [1.2.1]$$

Another possible model is

$$A \longrightarrow B \longrightarrow C$$
 [1.2.2]

The concentration of "B" versus reaction time is shown in Figure 1.2.1. If the reaction is observed only until time t<sub>1</sub>, no discrimination can be accomplished because the predicted responses and the data are essentially the same until t<sub>1</sub>. All the parameters in the model represented by equation [1.2.2] cannot be determined accurately if the reaction is observed only until time t<sub>1</sub>, because there has been no significant production of "B" from "C" for O≤t≤t<sub>1</sub>. If the



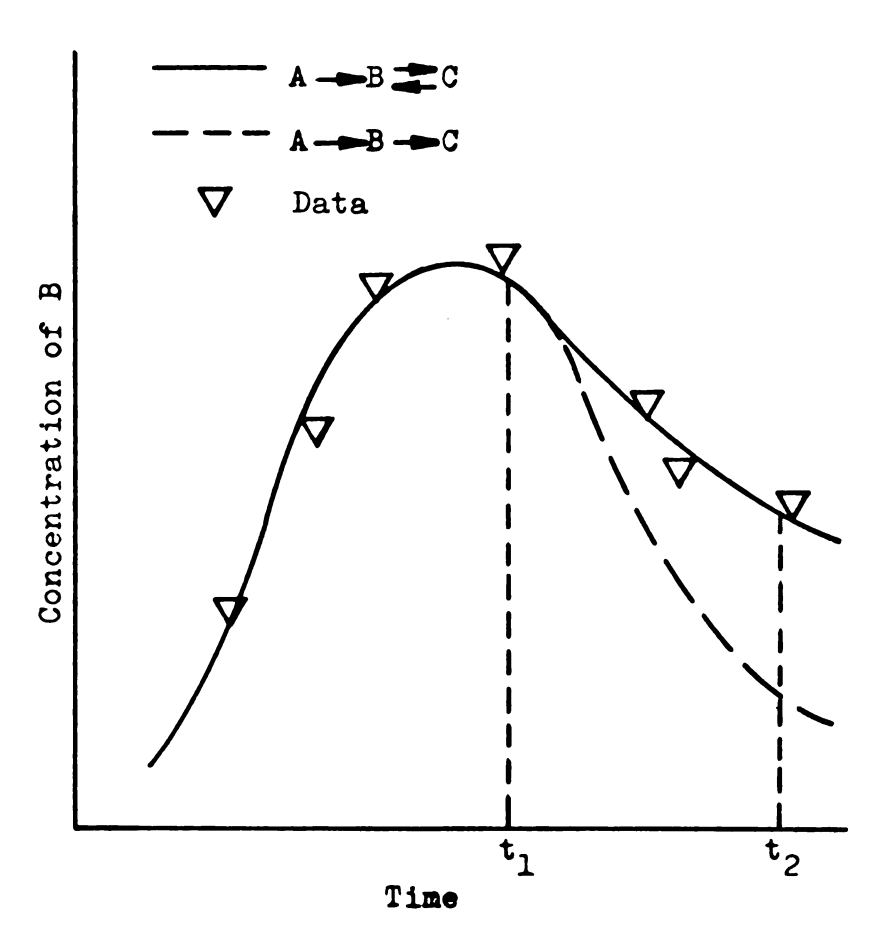


Figure 1.2.1 Concentration of B versus reaction time for the two models A—B—C and A—B—C.

reactic the mod propose

1.3 Pos

applied number of the application of the chauses a Model contract of the chauses a model contr

1.4 Par

any sit

needs t

ensine ensine

ي. پينهرو reaction is allowed to proceed until time  $t_2$ , we see that the model of equation [1.2.2] is the better of the two proposed.

#### 1.3 Possible application of model building.

Model building, including discrimination, can be applied to many areas in heat transfer. For example, a number of models have been proposed for ablating solids. One application to this area is to determine if significant radiant heat transfer exists within the ablating material and, if present, should be included in the model. Another application relates to the work of Pfahl and Mitchel (2). They used an isothermal change of phase model to describe the charring of cork but a competing and untested model uses a chemical reaction to describe the charring process. Model building, including discrimination, can be used in any situation where the mathematical model is unknown or needs to be improved.

### 1.4 Parameter estimation and its use in model building.

Parameter estimation is a discipline that provides techniques for calculating many of the parameters in a mathematical model from a single complex experiment. Some engineers use the terms nonlinear estimation, identification, nonlinear regression and nonlinear least squares instead of parameter estimation.

appeari to desi by a si "comple perimen

meters.

two para If a sta thermal

for a sp

ematical

adequate change di these ch

be possi

The classical method of determining parameters appearing in a relatively complex mathematical model is to design several experiments, each of which is described by a simple model involving one parameter. Thus if the "complex" model contains two parameters, two separate experiments would be conducted in order to find both parameters.

An example is linear heat conduction involving two parameters, thermal conductivity and heat capacity. If a steady state experiment is performed, only the thermal conductivity is involved in the reduced mathematical model. If a transient experiment is performed for a specimen with no temperature gradients, only the heat capacity is involved in another reduced model.

In most cases such separate experiments would be adequate, but there are materials which dry or otherwise change during the prolonged tests usually involved. When these changes occur, a rapid transient experiment might be possible that would permit the estimation (using parameter estimation) of the properties.

1.4.1

should

quality other v the phy functic tained

the case

one may

Where k(
and k ar

1.4.2 p

physical with exp

lodel ca

zation o

#### 1.4.1 Distinction between parameters and properties

The distinction between parameters and properties should be made clear. A property is a characteristic quality of a system and may be a function of any of the other variables in the problem. A parameter need not have the physical significance of a property and it is not a function of any other variable. A parameter may be contained in the expression for a property; for example, in the case of temperature dependent thermal conductivity one may write

$$k(T) = k_a + kT \qquad [1.4.1]$$

where k(T) is the property thermal conductivity and  $k_{\mathbf{a}}$  and k are parameters.

#### 1.4.2 Parameter estimation criterion

In testing a model's ability to describe a physical phenomenon, the predicted response is compared with experimental data taken from the actual physical system. In making this comparison, the parameters in the model can be estimated from the data if they are unknown.

A basic tool of parameter estimation is the minimization of a weighted sum of squared differences between the measurements and predicted values from the mathematical

model. (See Appendix B for a more complete description.)

The parameters in the model are varied until the combination is found that minimizes the weighted sum of squares. The ability of the digital computer to solve complex mathematical models has allowed parameter estimation to become more widely used. Box and co-workers (3,4) have developed the method from a statistical viewpoint. Beck(5,6) was the first to apply the method to finding parameters involved in a partial differential equation in heat transfer. He used the method to find thermal conductivity and heat capacity simultaneously from a single transient experiment. Pfahl(7,8) used the method to find seven parameters at once in charring cork.

# 1.4.3 Importance of optimum experiments in parameter estimation.

It is important that parameter estimation experiments be carefully planned in advance. The best or optimum ones should be run in order to obtain the greatest accuracy. One might think that experimentalists always do this. This is not usually true in the sense meant here, however. One can run the best experiment in terms of careful specimen preparation, placement of sensors, test procedure, and data aquisition and still have a poor experiment for simultaneously estimating several parameters. It may be clear how to design an experiment for estimating a single parameter. It is not obvious; however, how to design an optimum experiment when several parameters are to be estimated. Optimum parameter estimation experiments are discussed further in

Chapter II.

# 1.5 Background of model building and discrimination in other fields.

Model building is the name of the general procedure that we are discussing. It has a number of components including selecting optimum experimental designs, performing the experiments, analyzing the data, etc. These are discussed as a whole in Section 1.7. An essential step in model building is discrimination. It is so important a step that there is a tendency to confuse discrimination with the the entire process. Discrimination is only a part of model building, but it is a crucial part in the proposed procedure.

## 1.5.1 Model building

There is extensive literature on the mathematical modeling of different phenomena. There are cases; however, for which the usual continuum mechanics approach can produce several competing models. Model building is needed to choose the "best" one of these rival models. The model building literature is much smaller than the mathematical modeling literature.

#### Box and Hunter

Most of the model building work was done by chemical engineers and chemists in cooperation with statisticians.

Box and Hunter (9) proposed a method for use in model building. They suggested treating the estimated parameters in the

model as observations and the controllable variables as independent variables. Controllable variables are the variables an experimenter is able to change or control. If the model is correct, the estimated parameters should not change as the settings of the controllable variables change, i.e., parameters should stay constant. Factorial design is used to choose the setting of the controllable variables (the factors) and the parameters are estimated for each setting of the factors. Statistical analysis is used to determine the effect of the factors on the parameters thus giving the experimenter important clues as to how the model should be modified.

In another paper Box and Hunter (1) state "all information relating to the possible inadequacy of a tentatively entertained model is contained in the residuals". Residuals are the difference between the measured response and the response predicted by the model. Examination of plots of the residuals can aid one in telling where improvements should be made. Residuals should be plotted in any way that might shed light on pertinent questions. Anscombe (11) Anscombe and Tukey, and Draper and Smith, in addition to Box and Hunter, all recommend graphical examination of the residuals to show deficiencies in the model.

## 1.5.2 Discrimination

Discrimination has several aspects. These include,

Factorial design is a statistical procedure that allows one to determine efficiently the effect of the factors on the response; see reference (10) page 122.

a) the development of a discrimination criterion, b) the use of this criterion and c) the optimum design of experiments to promote the discrimination. Parts a) and c) can be confused because the optimum experiment design can involve a criterion based upon the discrimination criterion.

Discrimination between rival mathematical models is an area known to statisticians as hypothesis testing. Work has been done by statisticians and engineers on both the discrimination criterion and on designing the most efficient experiment to accomplish the discrimination.

#### Hunter and Reiner

Hunter and Reiner (14) proposed a design scheme for the case of two rival models. Their experimental design consists of making n initial runs to estimate the parameters in each model (n must be greater than the number of parameters in each model). The n+1<sup>st</sup> setting of the controllable variables is chosen so that the predicted responses of the two models are farthest apart. The n+1<sup>st</sup> data point is taken, the parameters estimated again, and the n+2<sup>nd</sup> setting of the controllable variables determined in the same manner. The procedure is thus sequential.

The discrimination is accomplished by making replicate runs to get an estimate of the variance which is a measure of the experimental error. The sum of squares of the residuals compared to the variance in an F-test is the discrimination criterion. An F-test is a statistical test used to guard against making the wrong decision by comparing the residual sum of squares with an estimate of experimental error.

Hun Bay

where tor

chos to s

leas

acco

Wher Tode

Į t

ity

3/20

to f

•

÷e ÷:e ÷:e ÷:e ;;;

prob

tii.

ion :

:8 g:

Roth

Roth (15) extended the <u>experiment design</u> criterion of Hunter and Reiner to any number of rival models and used a Bayesian approach for the discrimination. Roth defined

$$C_{ij} = |w_{j}^{(1)} - w_{j}^{(1)}||w_{j}^{(2)} - w_{j}^{(i)}||w_{j}^{(3)} - w_{j}^{(i)}|... \qquad [1.5.1]$$

where  $w_j^{(1)}$  is the predicted response of model i with the vector of controllable variables set at  $x_j$ .  $C_{ij}$  is a direct measure of spread between the predicted responses. Roth chose to select  $x_j$ , the setting of the controllable variables, to subject the current "best" model to the severest test; to accomplish this he defined the utility function

$$U(x_j) = \sum_{i} P(\text{model } i) \cdot C_{ij}$$
 [1.5.2]

where P(model i) is the probability or degree of belief in model i. The experiment design procedure is to select the  $x_j$  that maximizes  $U(x_j)$ .

Roth used Bayes' theorem to combine a prior probability for each model and the likelihood function for each model to find a posterior probability for each model; i.e.,

P(model i/data) = P(model i)·L(model i/data)/P(data) [1.5.3]

The maximization of this posterior probability is Roth's discrimination criterion. P(model i/data) is the posterior probability of model i or simply the degree of belief in model i in light of the data; P(model i) is the prior probability for model i; L(model i/data) is the likelihood function for model i which will be discussed shortly; and P(data) is given by

$$P(data) = \sum_{i} P(model i) \cdot L(model i/data) \qquad [1.5.4]$$

If the errors in the measurements are assumed independent and normally distributed with zero mean and constant variance,  $\sigma^2$ , the likelihood function can be expressed as

$$L(\text{model i/data}) = \left[ \frac{1}{\sqrt{\pi} \sigma} \right]^{N} \exp \left[ -\frac{1}{2\sigma^{2}} \sum_{u=1}^{N} (y_{u} - w_{u})^{2} \right]$$

$$[1.5.5]$$

Where N is the number of measurements,  $y_u$  are the measurements and  $w_{ij}$  are the predicted responses.

If no prior information is available P(model i) can be set to 1/m for all i where m is the number of rival models. The decision of calling one model best is made by comparing the magnitudes of the posterior probabilities for different models. The posterior probability not only helps choose between models but gives the probability of each model in light of the data. This is also a sequential procedure.

#### Box and Hill

Reiner or Roth do not take into account the magnitude of the experimental error; thus, it could be possible for the next design point to be in a region where the confidence regions for the predicted response for each model overlapped

Wh 8 and no real discrimination could be accomplished. A confidence region is a band around the predicted response from a model where one has a certain degree of confidence that, if the model is correct, measurements will fall within this band.

Box and Hill (16) used the concept of entropy from communication theory to develop an experiment design procedure to correct this fault. Entropy can be defined as

$$S = -\sum_{i=1}^{m} \boldsymbol{\pi}_{i} \ln \boldsymbol{\pi}_{i} \qquad [1.5.6]$$

where m is the number of rival models and  $\pi_i$  is the probability associated with model i. The least possible information regarding discrimination occurs when entropy is maximum; it can be shown that this happens when

$$\pi_{i} = 1/m \qquad [1.5.7]$$

for all i. The criterion of Box and Hill is then to maximize the expected change in entropy between input and output; that is, to perform the experiment which will cause the greatest change in entropy. An upper bound for the expected change in entropy was given by Box and Hill as

$$D = \frac{1}{2} \sum_{i=1}^{m} \sum_{j=i+1}^{m} \boldsymbol{\pi}_{i,n-1} \boldsymbol{\pi}_{j,n-1} \left\{ \frac{(\sigma_{i}^{2} + \sigma_{j}^{2})}{(\sigma^{2} + \sigma_{i}^{2})(\sigma^{2} + \sigma_{j}^{2})} + (y_{n}^{(i)} - y_{n}^{(j)})^{2} \frac{1}{(\sigma^{2} + \sigma_{i}^{2})} + \frac{1}{(\sigma^{2} + \sigma_{j}^{2})} \right\} [1.5.8]$$

 $\pi_{i,n-1}$  and  $\pi_{j,n-1}$  are the prior probabilities of models i and j respectively after n-1 runs have been performed,  $\sigma^2$  is the constant variance of the data,  $\sigma_i$  and  $\sigma_j$  are the variances under models i and j respectively, and  $y_n^{(i)}$  and  $y_n^{(j)}$  are the predicted responses from models i and j respectively for the n<sup>th</sup> or next data point. This expression contains the term  $(y_n^{(i)}-y_n^{(j)})^2$  which is similar to the criteria of both Hunter and Reiner and Roth; that is, the next data point is taken at the setting of the controllable variables where the predicted responses are the farthest apart. The Eox and Hill criterion also includes the variance of the data and of each model.

Hunter and  $\operatorname{Hill}^{(17)}$  propose exactly the same criterion but they use repeated runs to obtain an estimate of the variance,  $\sigma^2$ . The <u>discrimination criterion</u> used by Box and Hill is the same as that of Roth, i.e., the Bayesian posterior probability for each model.

Meeter, Pirie, and Elot (18) compared the method of Box and Hill with a somewhat similar method developed by Chernoff (19). They favor the Chernoff procedure because the Box and Hill criterion requires maximization of an upper bound; it would seem more logical to maximize a lower bound but this is not easily obtained. Results on several test cases done by Meeter, Pirie and Blot; however, show the Box and Hill procedure superior. Chernoff's criterion was developed assuming the cost of making measurements was zero. This is not the case in most engineering problems where the cost of experiments is generally high.

### Hunter, Hill and Wichern

Hunter, Hill and Wichern (20) presented a joint design criterion for model discrimination and parameter estimation. Their experiment design criterion is to maximize

$$C = w_1 D + w_2 E$$
 [1.5.9]

with respect to the controllable variables. Here  $\mathbf{w}_1$  and  $\mathbf{w}_2$  are non-negative weights, D is essentially the Box and Hill criterion described above, and E is a parameter estimation criterion. Initially  $\mathbf{w}_1$ D is made larger but as experimentation progresses and one model begins to emerge superior  $\mathbf{w}_2$ E begins to dominate. The discrimination criterion is the Bayesian posterior probability for each model.

#### Atkinson

Atkinson (21) gave a <u>discrimination criterion</u> which is a statistical test for determining if there is any evidence that the models give significantly different fits to the data; in other words, it tests the hypothesis that all the models are the same. The test statistic is

$$\frac{N-p}{p-1} \frac{(Y\hat{F})^2 - (Y\hat{F})^2}{(Y\hat{F})^2}$$
 [1.5.10]

where N is the number of measurements, p is the number of models,  $(YF)^2$  is defined by

$$(Y\hat{F})^2 = \sum_{j=1}^{N} (y_j - \hat{f})^2$$
 [1.5.10(a)]

 $\hat{f}$  is the model formed by regression using the observations or measurements as the dependent variable and the predictions from each model as the independent variables.  $\hat{f}$  combines the predictions from <u>all</u> the models into a single set of predictions that describe the data.  $(YF)^2$  is defined by

$$(Y\tilde{F})^2 = \sum_{j=1}^{N} (y_j - \tilde{f})^2$$
 [1.5.10(b)]

with f defined by

$$\sum_{j=1}^{N} (f_{ij} - \hat{f})^2 = 2, \quad i=1,2,...,p \qquad [1.5.10(c)]$$

f<sub>ij</sub> is the predicted value from model i for data point j. L is any constant. Thus f is equally distant from each model. (Yf)<sup>2</sup> is used as an estimate of error. The test statistic is tested by an F-test with N-p and p-l degrees of freedom to determine if there is any significant difference in the way the models fit the data.

Atkinson does not consider the problem of designing experiments to make discrimination more efficient; his method merely treats each model as a formula that is supposed to represent some aspect of the data and tests to see if they are different.

## Reilly

The ratio of likelihood functions was used by Reilly (22) as his discrimination criterion. The likelihood function can be defined in terms of the probability density function (23). Let  $f(\underline{Y},\underline{P})$  be the joint probability density function of the independent, random variables  $\underline{Y}$  and parameters  $\underline{P}$ . Suppose that N observations are made on  $\underline{Y}$ , and let  $(Y_1,Y_2,Y_3,\ldots,Y_N)$  be the observations; then the function given by

$$L(Y_{1}, Y_{2}, Y_{3}, \dots, Y_{N}: \underline{P}) = f(Y_{1}, \underline{P})f(Y_{2}, \underline{P})f(Y_{3}, \underline{P}) \dots f(Y_{N}, \underline{P})$$

$$[1.5.11]$$

is called the likelihood function. A maximum likelihood estimator  $\frac{\Delta}{P}$  is an estimator that maximizes the likelihood function with respect to the parameters  $\underline{P}$ . If the errors are independent and gaussian with zero mean and constant variance, maximum likelihood parameter estimates are the same as those given by least squares.

For the purpose of comparing the relative plausibilities of two parameter vectors  $\underline{P}_1$  and  $\underline{P}_2$  it is convenient to compare their likelihoods by examining the ratio. The likelihood ratio  $L(\underline{P}_1)/L(\underline{P}_2)$  is sometimes called the odds ratio and is a direct measure of the relative plausibilities of  $\underline{P}_1$  and  $\underline{P}_2$  in light of the data. According to Reilly, a likelihood ratio of 10 is ordinarily taken as showing a real difference while a ratio of 100 shows strong preference for one parameter over the other (22).

To discriminate between two rival mathematical models, Reilly suggests that we examine the ratio  $L_1(\underline{P}_1)/L_2(\underline{P}_2)$  where  $L_1(\underline{P}_1)$  and  $L_2(\underline{P}_2)$  are m ximum likelihood functions for models 1 and 2 respectively. This gives a comparison of models at their individual best.

## 1.6 Application to heat transfer.

All the methods described above with the exception of the last two were developed for a different type of experimental technique than that used in our heat transfer experiments. In chemical engineering an experiment to study a reaction rate mechanism, for example, may consist of several runs. A typical experimental run might be to start with a known initial concentration of reactants; fix the temperature, pressure, catlyst, etc. and let the reaction proceed for a certain length of time. The reaction is then stopped and the reactants analysed to find the concentrations of reactant and product. Thus each run may contain only a single data point, and several runs must usually be made before one may estimate all the parameters in the proposed model.

In transient heat transfer, however, it may be possible to obtain all the necessary data from a single run. The experiment might consist of heating a sample of the "unknown" material and measuring the temperature as a function of time for several locations on the sample. The temperature measurements are usually obtained with thermocouples. Several thermocouples may be used which allows

several locations at one time to be recorded. The signal from each thermocouple may be recorded continuously or it may be discretized at this point. A number of parameters in the model are estimated from a single experiment.

The method for model building proposed by Box and Hunter (1); i.e., treating the estimated parameters in the model as observations, may be misleading in many cases in heat transfer. It is demonstrated in Chapter II that if the settings of the controllable variables are not chosen carefully, the estimated parameters may be inaccurate or it may not be possible to find them all simultaneously. Therefore, this method is not recommended for model building in heat transfer.

Many researchers recommend graphical examination of the residuals for model building. (1, 11, 12, 13) This seems to be a most useful tool for model building. By plotting the residuals against different variables one may learn where deficiencies in the model exist and propose a new or modified model that will correct them. This process will be illustrated by example in Chapter IV.

In situations like the example of the reaction rate study discussed in the beginning of this section, many experiments are required to obtain the data. If one wishes to discriminate between two or more models that are supposed to describe the reaction mechanism, some method of conserving (minimizing the number) experiments is needed. For this reason the design strategies outlined in section 1.5 were developed. All the experimental designs developed thus far

are concerned with finding the setting of the controllable variables at which to take the <u>next</u> data point for best discrimination, thus all the designs are sequential. In many cases in heat transfer there are a relatively limited number of controllable variables. Frequently all the data necessary for discrimination can be obtained from a single experiment; in such cases sequential designs are not needed.

The Bayesian approach used by Roth and also Box and Hill allows prior knowledge or belief about each model to enter the design criterion. The experimenter usually has no prior preference for any one model initially, but as experimentation and sequential discrimination proceed concurrently he may gain evidence that one or more models is superior to the others. This evidence or belief is allowed to enter the decision criterion. Without sequential experimentation, one has no way to gain sufficient a priori knowledge to allow it to enter the discrimination decision. While the Bayesian approach is a very powerful tool, it will not be employed here because of the difficulty of performing different sequential experiments.

On the other hand, both the method for discrimination proposed by Atkinson and the method of maximum likelihood ratios described by Reilly seem to be directly applicable here. Both these methods involve the residuals in some manner. The method of Reilly is to be employed.

1.7 The proposed model building method.

The proposed model building procedure is illustrated

in the flow diagram of Figure 1.7.1. If the experimenter lacks sufficient knowledge about the process to propose a complex model, it is recommended that a simple mechanistic model be proposed for the process even though the model is suspected to be deficient. This is block 1. of Figure 1.7.1. in block 2. the optimum experiment for parameter estimation is found. Estimating the parameters utilizing data from the optimum experiment will cause the model to describe the process as adequately as it can. The optimum experiment is then performed (block 3.) and the parameters estimated from the data (block 4.). In block 5. the model and the data plotted together are examined visually to try and extract information about the model. The residuals should be plotted against any pertinent variables and examined visually. Valuable clues as to the nature of the deficiencies in the model can be gained in this manner. is a very important step. In block 6. the experimenter must decide if the model or models he has to this point in the process are plausible or capable of describing the features of the process he is interested in. There is no formal criterion for this decision; it is left to the judgement of the experimenter. If they are plausible, he proceeds to block 8. the discrimination stage; if they are not, he procedes to block 7. In block 7. the experimenter must evaluate the information he gained in block 5. and propose a new or modified model based on this information. experimenter then proceeds back to block 2. and repeats the process until he has one or more plausible models.



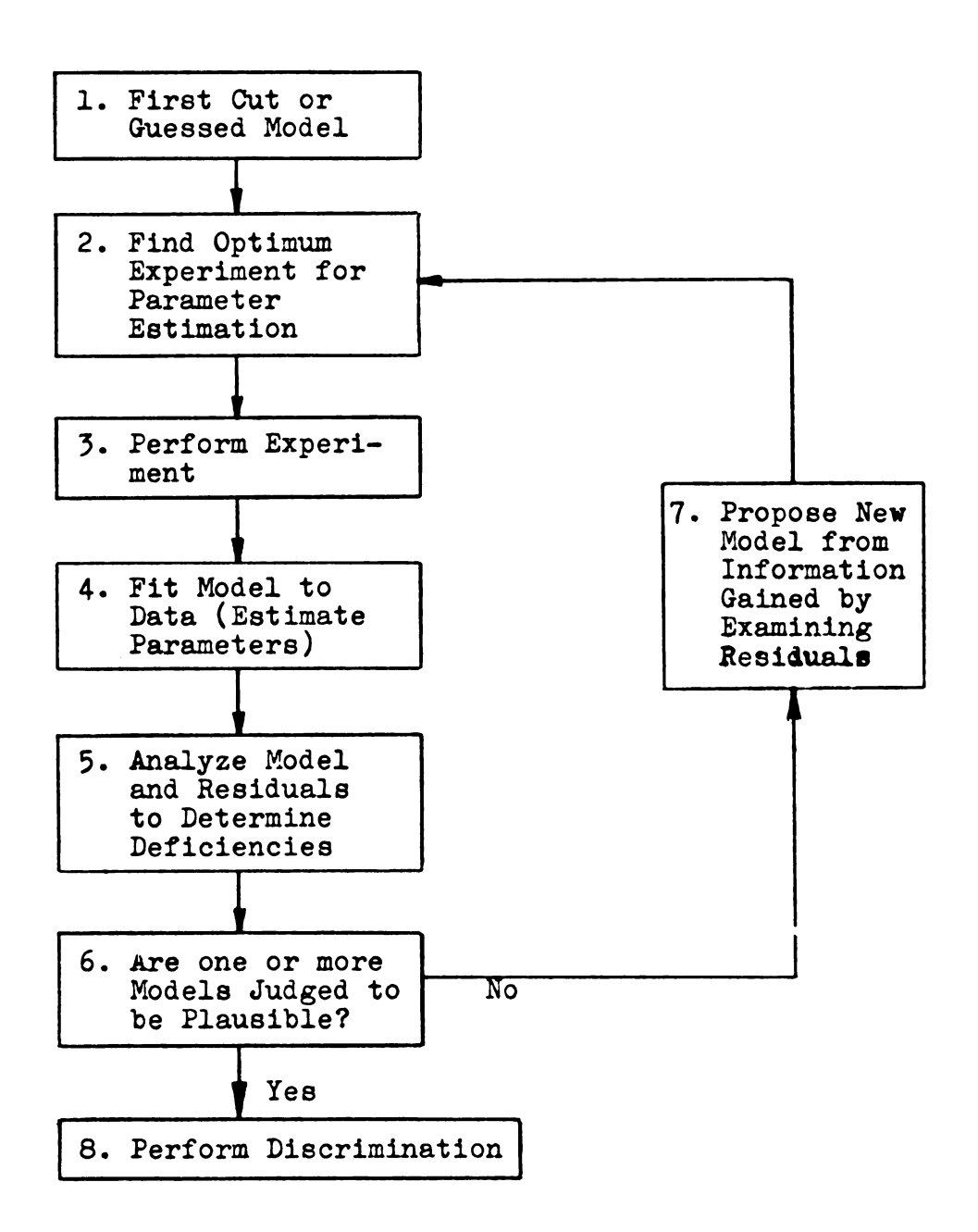


Figure 1.7.1 Flow diagram of the proposed model building procedure.

This procedure will be illustrated in Chapter IV.

In many cases the experimenter has some prior knowledge about the process. If enough information is available
to propose one or more mathematical models, then the building of competing models may be skipped entirely and one
may go on to discrimination. It is highly recommended that
the residuals be examined in any case; they contain all the
information about the "goodness of fit" of the models.

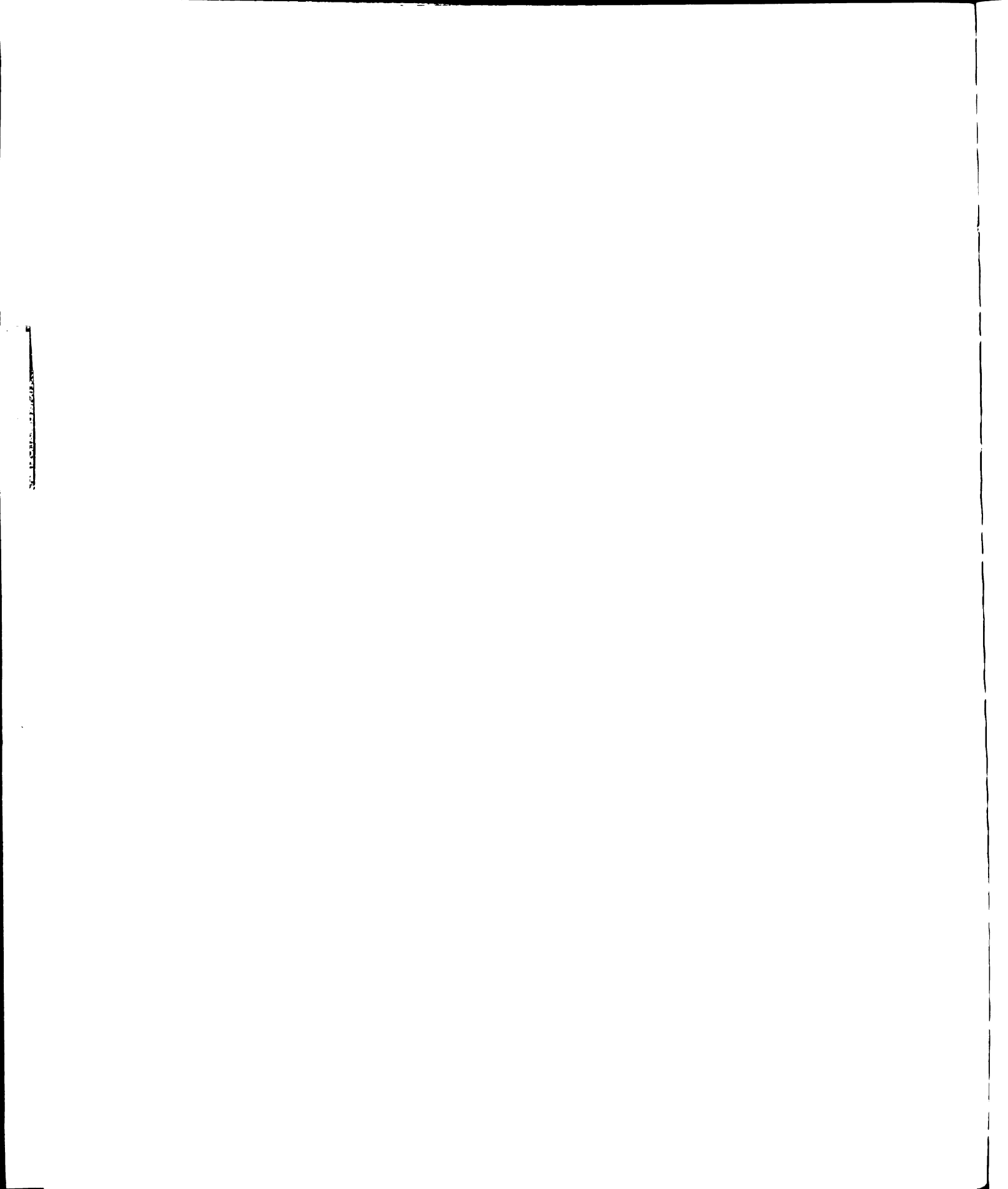
The next step after proposing new models is to test them to determine which fits the data adequately. This is the discrimination process (block 8. of Figure 1.7.1). Three possible cases arise here: 1.) none of the models is adequate. 2.) one of the models is adequate or 3.) more than one of the models is adequate. Should Case 1.) occur, more models should be developed. Case 2.) is the most desirable case; if this should occur, the investigation can be concluded. For Case 3.) two explanations are possible; either one model is a special case of the other or the data is not sufficiently accurate to allow discrimination. If the former is true, the experimenter should be the judge of which model suits his purpose best based on other considerations. If the latter is true, methods of improving the experiment should be sought.

To improve discrimination the experimenter might want to devise some special experiment to discriminate between the models. As an example of this, suppose two rival models that describe the temperature history of a solid being heated are: 1.) a model that has change of

phase and 2.) a model that has a chemical reaction. Since both models might describe the temperature equally well during heating, the experimenter should devise another experiment to discriminate. Change of phase is reversible; that is, the specimen can melt during heating and solidify during cooling. Thus for change of phase, the measured temperatures should exhibit the same behavior while heating or cooling. The chemical reaction is irreversible; that is, the reaction occurs during heating but the reactants do not return to their original state during cooling. Hence the measured temperature for the chemical reaction should exhibit considerably different behavior during cooling than it did during heating. With this information the experimenter could discriminate more effectively by performing an experiment that involved both heating and cooling.

All statistical tests are based on comparing the residuals with some measure of experimental error to determine if the model is adequate in light of the data. The method proposed by Atkinson does not require the experimenter to supply an estimate of the experimental error. This method, however, tests the hypothesis that all the models fit the data equally well; one could just as well say it tests the hypothesis that all the models fit the data equally poorly. It provides no means to test how well the models fit the data on an individual basis.

The likelihood ratio test requires the experimenter to supply an estimate of the experimental error which can sometimes be difficult to obtain. If a reasonable



estimate of experimental error is available, this method can be used effectively in discrimination since only the ratio of likelihoods is of concern. The experimenter who is familiar with his equipment can usually supply an estimate of experimental error that is good enough for this purpose. The alternative is to perform replicate runs to obtain an estimate of variance. Although replication is generally to be recommended, it will not be used in this work.

The likelihood function for zero mean and gaussian error is

$$L(\text{model i/data}) = \frac{1}{(2\pi)^{N/2} \left[\det \underline{\Psi}\right]^{\frac{1}{2}}} EXP \left[-\frac{1}{2}(\underline{Y}-\underline{W})^{2}\underline{\Psi}^{-1}(\underline{Y}-\underline{W})\right]$$

$$[1.7.1]$$

where \(\begin{align\*} \text{ is the covariance matrix of the errors. For independent errors \(\begin{align\*} \begin{align\*} \text{ reduces to a diagonal matrix with the diagonal elements equal to the square of the variance. If the variance is constant then equation [1.7.1] reduces to [1.5.5]. For correlated errors \(\begin{align\*} \begin{align\*} \text{ can be a full N x N} \end{align\*} \) matrix. Unfortunately the errors are correlated in a transient experiment involving temperature measurements when the sampling rate is relatively high. This is the type of experiment that we have.

We have no way to evaluate the elements of the co-variance matrix; all we can do is provide an estimate of the constant variance (experimental error). When errors are correlated it is known that (24,25)

$$\frac{1}{\sigma^2} \sum_{u=1}^{\mathbf{N}} (y_u - w_u)^2 > (\underline{Y} - \underline{W})' \underline{\Psi}^{-1} (\underline{Y} - \underline{W}) \qquad [1.7.2]$$

Considering this we will define a new likelihood function in an attempt to approximate the true value of the likelihood function from [1.7.1]. Let the new likelihood function be

$$L(\text{model i/data}) = EXP \left[ -\frac{1}{2\sigma^2 N} \sum_{u=1}^{N} (y_u - w_u)^2 \right]$$
[1.7.3]

This is not the correct form of the likelihood function but it is the best we can do at this time. Equation [1.7.3] will be used in the likelihood ratio test to discriminate between rival models.

#### CHAPTER II

#### OPTIMUM EXPERIMENTS FOR PARAMETER ESTIMATION

### 2.1 Introduction

An optimum experiment is defined as the experiment which allows the parameters in a mathematical model to be calculated with the greatest accuracy. The combination of experimental conditions yielding predicted responses that are most sensitive to changes in the parameters are usually the optimim conditions. This will be demonstrated later. If experiments are not carefully planned, the experimental points may be so situated in the space of controllable variables that the calculated parameters may not only be imprecise but also highly correlated (1). Controllable variables are defined to be the variables the experimenter has the ability to change; some examples might be location of sensors, maximum run time for transient experiments, boundary conditions, and initial conditions. If parameters are correlated for certain settings of the controllable variables, they cannot be determined simultaneously. Seinfeld (26) calls this condition the observability problem while others call it the identifiability condition.

An example of an experiment with correlated parameters is a semi-infinite body heated by a constant heat flux.

 $F_0$ , at the surface x=0. Here the controllable variable is the location, x, of the measurement. At the heated surface the temperature at time t is given by (27)

$$T(0,t) = 2F_0(t/\pi \rho c_p k)^{\frac{1}{2}}$$
 [2.1.1]

where  $\rho_{c_p}$  is the volumetric heat capacity and k is the thermal conductivity. If a single thermocouple were located at the surface x = 0, k and  $\rho_{c_p}$  can not be found simultaneously; they are said to be correlated at this location since only their product can be estimated. If the single thermocouple were placed at any position, x, other than zero, then both k and  $\rho_{c_p}$  can be simultaneously estimated provided the heating is continued long enough to cause the temperature to change at the sensor location.

More complex mathematical models such as those describing heat commuction with temperature dependent thermal properties or those describing heat conduction with change of phase do not reveal correlations between the parameters as simply as the example given above. This is because simple exact solutions are not known for these more general cases. Nevertheless, numerical solutions can be utilized to find optimum experiments in such cases.

# 2.2 Sensitivity coefficients.

Sensitivity coefficients can be utilized to aid in finding optimum conditions. A sensitivity coefficient is defined as the derivative of the predicted value of a measured quantity with respect to the parameter  $\mathbf{p_i}$ ,

Sensitivity coefficient = 
$$S_{p_i}^T(\underline{\xi},t) = \frac{\partial T(\underline{P},\underline{\xi},t)}{\partial p_i}$$
 [2.2.1]

where  $\underline{\boldsymbol{\xi}}$  is a vector of controllable variables and  $\underline{P}$  is a vector of parameters.  $T(\underline{P},\underline{\boldsymbol{\xi}},t)$  is the predicted response for the controllable variables set at  $\boldsymbol{\xi}$  and time t.

If for any fixed  $\xi$  and all values of t the relation

$$\sum_{\mathbf{j}} \mathbf{A}_{\mathbf{j}} \mathbf{S}_{\mathbf{p}_{\mathbf{j}}}^{\mathbf{T}} (\boldsymbol{\xi}, \mathbf{t}) = 0 \qquad [2.2.2]$$

is satisfied and any one of the constant coefficients  $A_j$  is nonzero the sensitivity coefficients are said to be linearly dependent. For cases where the sensitivity coefficients are linearly dependent all the parameters cannot be found simultaneously (28). This is illustrated by differentiating equation [2.1.1] with respect to k to obtain

$$S_k^T(0,t) = \frac{\partial T(0,t)}{\partial k} = -\frac{F_0}{k} (t/\pi \rho c_p k)^{\frac{1}{2}}$$
 [2.2.3]

and with respect to  $ho c_p$  to obtain

$$S^{T}_{c_{p}}(0,t) = \frac{\partial T(0,t)}{\partial \rho^{c_{p}}} = -\frac{F_{o}}{\rho^{c_{p}}}(t/\pi \rho c_{p}k)^{\frac{1}{2}}$$
 [2.2.4]

we see that for all values of t

$$A_1 S_k^T(0,t) + A_2 S_p^T(0,t) = 0$$
 [2.2.5]

Where

$$\mathbf{A}_{1} = \mathbf{k} \qquad \qquad \left[ 2.2.5(\mathbf{a}) \right]$$

and

$$A_2 = -\rho c_p \qquad [2.2.5(b)]$$

Any criteria for finding optimum experimental conditions should alert the experimenter to linear dependence of the sensitivity coefficients.

## 2.3 Criteria for design of optimum experiments.

while there is much work in the literature on parameter estimation, few researchers have considered the problem of experimental design. Seinfeld (26) states that there may be cases where the parameters in a mathematical model cannot be estimated but does not consider the problem of designing experiments to avoid these cases. G.E.P. Box and co-workers seem to have been the first to realize the need for experimental design in parameter estimation.

Box and Lucas (29) suggested maximizing the determinant of the matrix  $\Gamma$ 

$$\underline{\Gamma} = \underline{Z}'\underline{Z}$$
 [2.3.1]

as a criterion. The elements of the sensitivity matrix  $\underline{z}$  are

$$z_{ij} = S_{p_i}^T(\underline{P}, \underline{\xi}_j, t)_{\underline{P} = \underline{\widehat{P}}}$$

[2.3.1(a)]

 $\widehat{\underline{P}}$  is a least squares estimate of  $\underline{\underline{P}}$ , the vector of parameters.

Note the prime (') means transposition.

ę)

If the errors in the measurements are independent and normally distributed with zero mean and constant variance then the volume of the confidence region in parameter space is inversly proportional to the square root of det  $\Gamma$ . By designing the experiment to maximize det  $\Gamma$  the confidence region for  $\Gamma$  is minimized if these conditions are valid.

These assumptions are not all valid in our case since the experimental errors are correlated rather than being independent. The nature of this correlation is not understood at this time. Other justification for maximizing the determinant of  $\Gamma$  that is not dependent on these assumptions has been presented in (5). No better criterion is available at this time.

One justification of the criterion is to note that if any two or more sensitivity coefficients for a given experiment are linearly dependent as discussed in section 2.2, the criterion, det  $\Gamma$ , is identically zero. This results from the rows of the matrix  $\Gamma$  being proportional  $\Gamma$ . If det  $\Gamma$  = 0, the confidence region in parameter space is infinite whether or not all the assumptions are valid.

Most models in heat transfer are <u>nonlinear in the</u> <u>parameters</u>. For such cases the sensitivity coefficients are dependent on the value of the parameters and thus an initial estimate of  $\underline{P}$  is needed to design the best experiment for estimating  $\underline{P}$ . It may seem strange that in order to use this scheme one must have initial estimates of the parameters that are to be found; however, any experimental design uses the experimenter's prior knowledge of the subject. The better

his initial guess the better and more efficient the experimental design will be.

The criterion can be made arbitrarily large by increasing the number of observations and the range of the measured variable(s). Physically the experimenter is restricted to finite quantities, hence constraints must be imposed. For a large number of equally spaced measurements in time and a model that is linear in the dependent variable  $\operatorname{Beck}^{(5)}$  modified the criterion to include constraints of a fixed number of observations and a fixed temperature range. The resulting criterion is to maximize the determinant of the matrix  $\Delta$  whose elements are

$$\delta_{ij} = \frac{1}{N \tau_{m}} \sum_{k=1}^{n} \int_{0}^{\tau_{m}} \left[ \frac{p_{i}}{\Delta T_{max} p_{i}} S_{i}^{T}(x_{k}, \tau) \right] \left[ \frac{p_{j}}{\Delta T_{max} p_{j}} (x_{k}, \tau) \right] d\tau$$
[2.3.2]

 $au_m$  is the maximum dimensionless duration of the transient experiment, n is the number of thermocouples,  $S_{p_i}^T(\mathbf{x_l}, \mathbf{7})$  and  $S_{p_j}^T(\mathbf{x_l}, \mathbf{7})$  are the sensitivity coefficients at location  $\mathbf{x_l}$  for parameters  $\mathbf{p_i}$  and  $\mathbf{p_j}$  respectively.  $\Delta T_{max}$  is the constraint of the maximum temperature rise occurring. In the experiment.

Beck considered models that are linear in the dependent variables although the dependent variables may be nonlinear in the parameters. This can be a confusing but important distinction. For models that are linear in the dependent variable the dimensionless sensitivity coefficients

are independent of temperature rise. Thus for models which are linear in the dependent variable it becomes unnecessary to consider temperature rise as a separate constraint. If the model is nonlinear in the dependent variable, the sensitivity coefficients are also nonlinear in the dependent variable. Consequently the choice of maximum temperature rise must be considered as a separate constraint. For nonlinear problems there may exist an optimum temperature rise. Heinekin, Tsuchiya, and Aris (31) proposed a criterion for systems of ordinary differential equations that is similar to the criterion given by Beck.

For the types of experiments conducted in heat transfer investigations, examples of controllable variables are thickness of sample, initial conditions, type of boundary condition (i.e., heat flux or temperature), maximum temperature rise, and to a limited extent the functional form of the boundary conditions. These controllable variables must be adjusted to maximize the determinant of the matrix  $\Delta$ .

For a finite body the sample length, E, enters the optimization criterion through the dimensionless time,

$$\tau = \alpha t/E^2$$
 [2.3.3]

If the thermal diffusivity,  $\mathbf{Q}$ , is not constant it can be evaluated at some reference temperature for convenience. Thus once the optimum value of  $\mathbf{T}_{\mathrm{m}}$  is known, the sample length can be chosen from other considerations and the maximum run time, t, can be found from equation  $\begin{bmatrix} 2.3.3 \end{bmatrix}$ . For a semi-infinite body with only a single thermocouple

the thermocouple location, x, enters the criterion through the dimensionless time,

$$\tau = at/x^2 \qquad [2.3.4]$$

After  $\tau_{m}$  is determined, the duration of the experiment and thermocouple location(s) can be chosen from other considerations.

The procedure then is to fix all the controllable variables except  $au_{\rm m}$  and calculate

$$\overline{\Delta} = \det \underline{\Delta}$$
 [2.3.5]

as a function of  $\boldsymbol{\tau}_{\mathrm{m}}$ . The maximum temperature rise,  $\Delta \mathrm{T}_{\mathrm{max}}$ , must be attained for each value of  $\boldsymbol{\tau}_{\mathrm{m}}$ . For the case of a step change in temperature at a boundary, this is automatically satisfied. For the case of a heat flux boundary condition; however, the heat flux must be adjusted for each value of  $\boldsymbol{\tau}_{\mathrm{m}}$  so that the given  $\Delta \mathrm{T}_{\mathrm{max}}$  is attained in time  $\boldsymbol{\tau}_{\mathrm{m}}$ . The maximum value of  $\overline{\Delta}$ 

$$\max_{\boldsymbol{\tau}_{m}} \left[ \Delta \right] = \Delta_{\text{opt}} \qquad [2.3.6]$$

indicates the best value of  $\tau_{\rm m}$  for that particular setting of the other controllable variables. This procedure is repeated for different settings of the other controllable variables until the best combination is found. The procedure is illustrated for several test cases below.

Any optimum experiment must be a compromise between theory and practice. Practical considerations play an

important role in the choice of the controllable variables. One of the most important of these is the choice of the functional form of the boundary conditions. Only those conditions which are readily attainable and measureable in the laboratory need be considered. Other practical considerations that should be taken into account when planning an experiment are the capabilities of the measuring equipment used. All measuring equipment introduces some error into the measurement whether in the form of random electronic noise or a biased error due to inaccurate calibration, for example. To minimize the effect of measurement errors from noise on the calculated parameters, the overall temperature rise for the experiment should be kept as large as practical. This is introduced into the optimization criterion later in the form of a "merit" function for the temperature rise. When thermocouples are attached to a body there is always some question as to the exact location of the measuring junction. In Chapter III, the experimental technique will be discussed and it can be seen that the possible uncertainty in thermocouple location is equal to the radius of the thermocouple wire used. This effect can be minimized by using relatively thick specimens and the smallest practical thermocouple wire diameter.

## 2.4 Results for several sample cases.

#### Semi-infinite case

Several test cases were investigated to find the optimum experimental conditions. The first case was that

of a semi-infinite body of liquid having constant thermal properties that freezes when subjected to a step decrease in temperature at the surface x = 0. The initial fluid temperature is  $T_i$  and the surface temperature becomes  $T_o$ . The solution for the temperature distribution is (27)

$$T_{s} = \frac{T_{s}(x,t)-T_{o}}{T_{i}-T_{o}} = \frac{T_{T}^{+}}{erf(\lambda)}erf\left[\left(\frac{1}{4\tau}\right)^{\frac{1}{2}}\right] \qquad [2.4.1]$$

in the solid and

$$\overline{T}_{\mathbf{z}} = \frac{T(\mathbf{x}, \mathbf{t}) - T_{0}}{T_{1} - T_{0}} = 1 - \frac{(1 - T_{T}^{+})}{\operatorname{erfc}\left[\lambda(\alpha^{+})^{\frac{1}{2}}\right]} \operatorname{erfc}\left[\left(\frac{\alpha^{+}}{\tau}\right)^{\frac{1}{2}}\right]$$

$$[2.4.2]$$

in the liquid. The dimensionless position of the solidliquid interface is given by

$$\epsilon^+(\tau) = \frac{\epsilon(t)}{x} = 2\lambda \tau^{\frac{1}{2}}$$
 [2.4.3]

The constant  $\lambda$  is found as the root of

$$\frac{e^{-\lambda^{2}}}{\operatorname{erf}(\lambda)} - \frac{(a^{+})^{\frac{1}{2}}k^{+}(1-T_{T}^{+})e^{-\lambda^{2}}a^{+}}{T_{T}^{+}\operatorname{erfc}\left[\lambda(a^{+})^{\frac{1}{2}}\right]} = \pi^{\frac{1}{2}}\lambda L_{T}^{+} \quad [2.4.4]$$

where the five dimensionless properties are defined by

$$T_{T}^{+} = \frac{T_{f} - T_{o}}{T_{i} - T_{o}}$$
 [2.4.5]

$$L_{T}^{+} = \frac{\rho^{L}}{(\rho c_{p})_{s}(T_{f}-T_{o})}$$
 [2.4.6]

$$\tau = \frac{\alpha_s^t}{x^2} \qquad [2.4.7]$$

$$\mathbf{a}^{+} = \mathbf{a}_{s}/\mathbf{a}_{s}$$
 [2.4.8]  
$$\mathbf{k}^{+} = \mathbf{k}_{s}/\mathbf{k}_{s}$$
 [2.4.9]

$$k^+ = k_{\ell}/k_{s} \qquad [2.4.9]$$

The subscripts s and & refer to the solid and liquid respectively. The heat of fusion is L and the fusion temperature is T<sub>f</sub>.

Figure 2.4.1 (a) shows the dimensionless temperatures  $\overline{\mathbf{T}}_{\mathbf{Q}}$  and  $\overline{\mathbf{T}}_{\mathbf{S}}$ , versus dimensionless time,  $\boldsymbol{\mathcal{T}}$ , for several values of the dimensionless heat of fusion,  $L_{\rm T}^{+}$ , with the dimensionless fusion temperature,  $T_T^+$ , held at 0.5. Note that the larger the heat of fusion, the longer it takes the temperature at a given location to drop below the fusion temperature. Figure 2.4.1 (b) shows the dimensionless temperatures versus dimensionless time for several values of the dimensionless fusion temperature,  $T_{T}^{+}$ , with the dimensionless heat of fusion equal to 1.0. Note that as  $T_{\mathrm{T}}^{+}$  approaches 1.0, there is a more pronounced effect of the phase change upon the temperature history.

Sensitivity coefficients for all the properties are shown in Figure 2.4.2, for the common case of Figure 2.4.1(a) and (b). A number of observations can be made from an inspection of this figure. For example, the curves for  $S_{\mathbf{k}}^{\mathbf{T}}$  and ST have almost identical shape which means they are almost linearly dependent. Because this case of a semi-infinite body has these curves plotted in terms of a similarity variable 7 which includes both the independent variables x and t, an observed linear dependence in Figure 2.4.2

means that the dependence is true for <u>any</u> nonzero x and all t's. If the body were finite, the sensitivities would not be a function of only one independent variable. Another observation is that the magnitude of  $\mathbf{S}_{\mathbf{C}_{\mathbf{PS}}}^{\mathbf{T}}$  is small which means this experiment would be ineffective for estimating the heat capacity of the solid phase. Another observation is that  $\mathbf{S}_{\mathbf{PL}}^{\mathbf{T}}$  and  $\mathbf{S}_{\mathbf{T}_{\mathbf{f}}}^{\mathbf{T}}$  are not correlated indicating that this experiment would be successful in simultaneously determining  $\mathbf{PL}$  and  $\mathbf{T}_{\mathbf{f}}$ .

If one calculates  $\overline{\Delta}_{\mathrm{opt}}$  for this experiment for all six properties as explained in section 2.3, the magnitude is on the order of  $10^{-22}$  indicating a very small chance of simultaneously estimating all six parameters. Three or four parameters could be estimated simultaneously, however. An examination of Figure 2.4.2 can tell which ones. As noted above  $\mathbf{S}_{\mathrm{ps}}^{\mathrm{T}}$  is always small and thus  $\mathbf{pc}_{\mathrm{ps}}$  has little effect upon the predicted temperatures. Hence one should not try to estimate  $\mathbf{pc}_{\mathrm{ps}}$  from such an experiment; if one does, then all the parameters calculated at the same time could be quite inaccurate. Also  $\mathbf{k}_{\mathrm{s}}$  and  $\mathbf{pL}$  should not be simultaneously estimated due to near linear dependence. A group of three that could be estimated together is  $\mathbf{T}_{\mathrm{f}}$ ,  $\mathbf{pL}$ , and  $\mathbf{k}_{\mathrm{l}}$ . By examining sensitivity curves such as Figure 2.4.2 one can learn a great deal in terms of possible optimum experiments.

One estimation problem is to find the density-heat of fusion product,  $\rho$ L, when the other properties are known. The controllable variables for this case are thermocouple location, maximum run time, initial temperature  $T_i$ , boundary

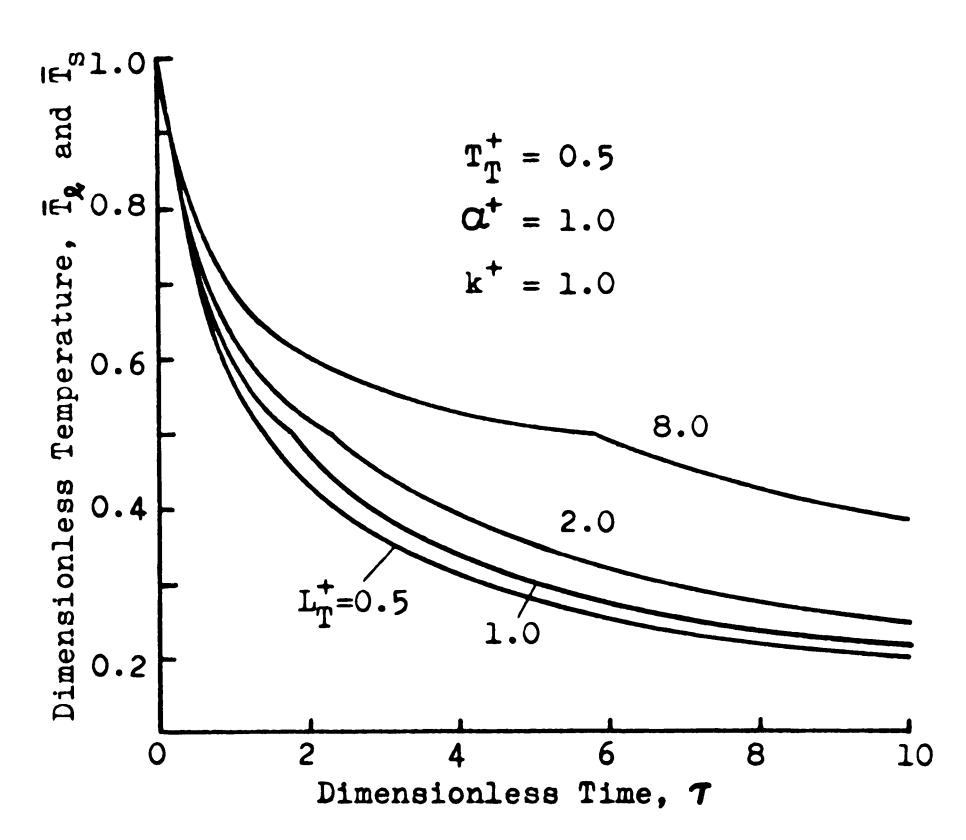


Figure 2.4.1 (a) Dimensionless temperature of a freezing semi-infinite body subjected to a step decrease in temperature at the boundary for several values of the dimensionless heat of fusion,  $L_{\rm T}^+$ .

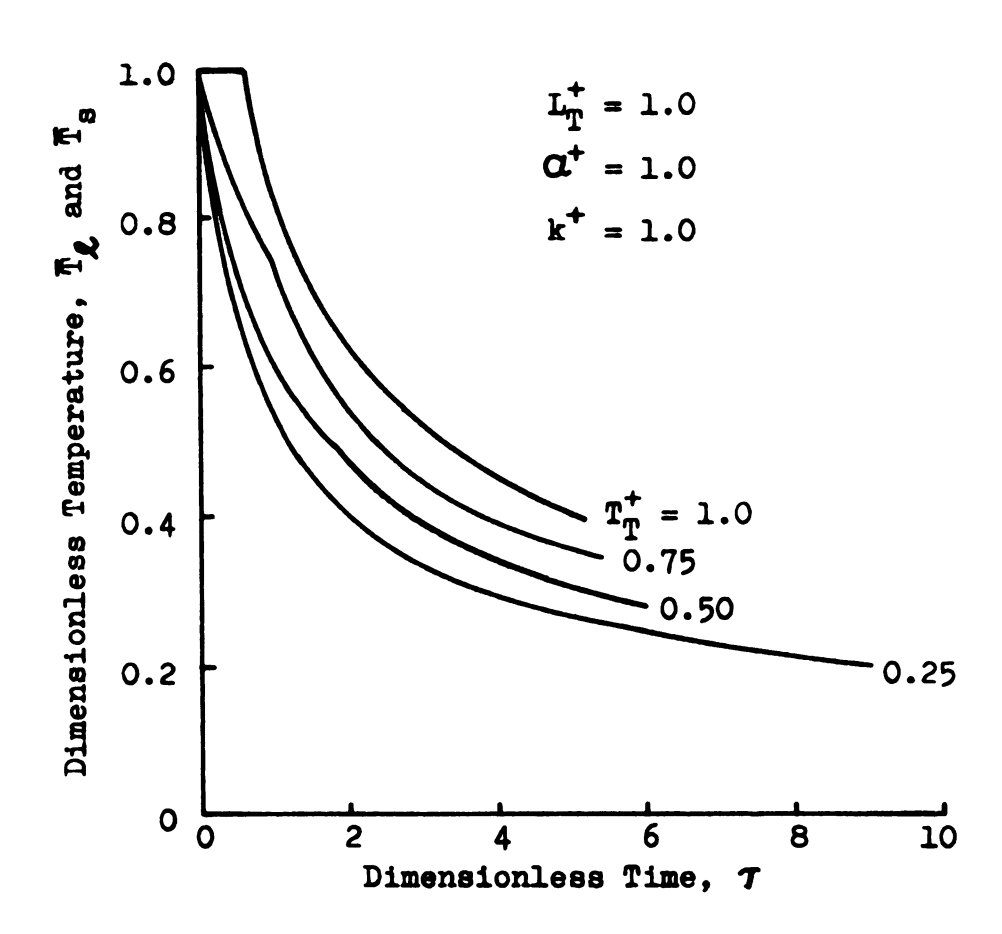


Figure 2.4.1(b) Dimensionless temperature of a freezing semi-infinite body subjected to a step decrease in temperature at the boundary for several values of dimensionless fusion temperature,  $T_{\rm T}$ .

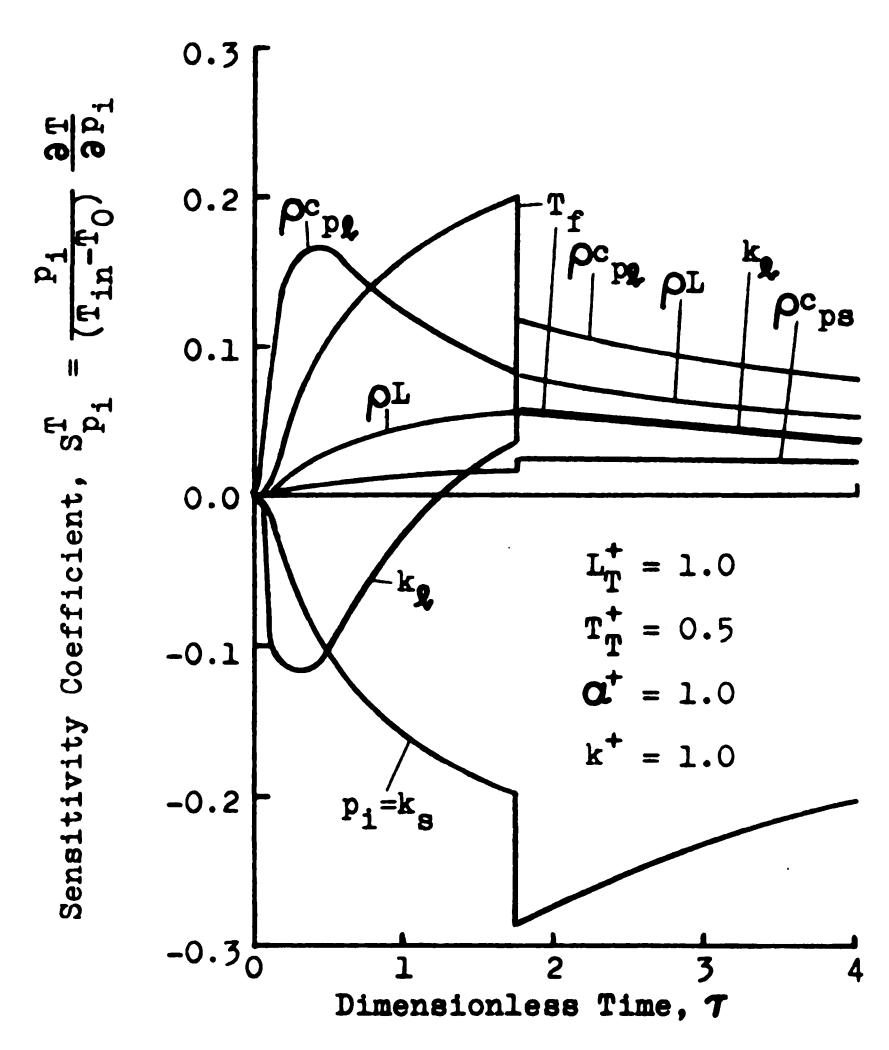


Figure 2.4.2 Dimensionless sensitivity coefficients for a freezing liquid semi-infinite body with a step decrease in temperature at the surface.

temperature To, and maximum temperature rise. In order to find an optimum experiment for estimating  $\rho$ L, each of these controllable variables must be considered. Thermocouple location and maximum run time are both included in the dimensionless time given by equation [2.4.7] (for a single thermocouple). Hence maximizing  $\overline{\Delta}$  with respect to au considers both location and run time for a single thermocouple. The initial temperature and boundary temperature are included in the dimensionless parameters  $\textbf{T}_{T}^{+}$  and  $\textbf{L}_{T}^{+}.$  The range of  $\textbf{T}_{T}^{+}$  is from zero to one. If  $\textbf{T}_{T}^{+}$  is zero, i.e., the boundary temperature at x = 0 is equal to the fusion temperature, no freezing can occur and hence no information related to the heat of fusion could be contained in the data. Table 2.4.1 shows the value of  $\overline{\Delta}_{\text{opt}}$  with  $L_{\text{T}}^{+}$ =1 for several values of  $T_T^+$ . For a single thermocouple,  $T_T^+$ =1 (the initial temperature  $T_i$  equal to the fusion temperature  $T_f$ ) seems to be a desirable experimental condition. The value of  $\mathbf{L}_{\mathrm{T}}^{+}$ can be controlled by an appropriate choice of the quantity  $(T_f-T_o)$ , or since  $T_T^+$  will be set equal to one,  $(T_i-T_o)$ . The best value of  $L_T^+$  may be chosen by examining  $\overline{\Delta}_{opt}$ versus  $L_T^+$ . Figure 2.4.3 shows  $\overline{\Delta}_{opt}$  versus  $L_T^+$ , we see that the optimum experiment for a single thermocouple with  $T_{T}^{+}$ =1 is one for which  $L_T^+$  is larger, or in other words,  $(T_i-T_o)$ should be chosen as small as practical.

At this point, one may decide just what the optimum value of  $\Delta T_{max} = (T_i - T_o)$  should be given some information about the experimental equipment. In Chapter III the experimental equipment will be discussed. The maximum

Table 2.4.1  $\overline{\Delta}_{opt}$  for several values of  $T_T^+$  with  $\rho L$  the parameter to be estimated for the semi-infinite example.

$L_{\mathrm{T}}^{+} = 1$	<b>a</b> <sup>+</sup> = 1	k <sup>+</sup> = 1
T <sub>T</sub> <sup>+</sup>	$\Delta_{ t opt}$	$ au_{ t opt}$
0.00	0.00000	
0.25	0.00015	8.86
0.50	0.00312	3.84
0.75	0.01476	2.52
1.00	0.03709	1.91

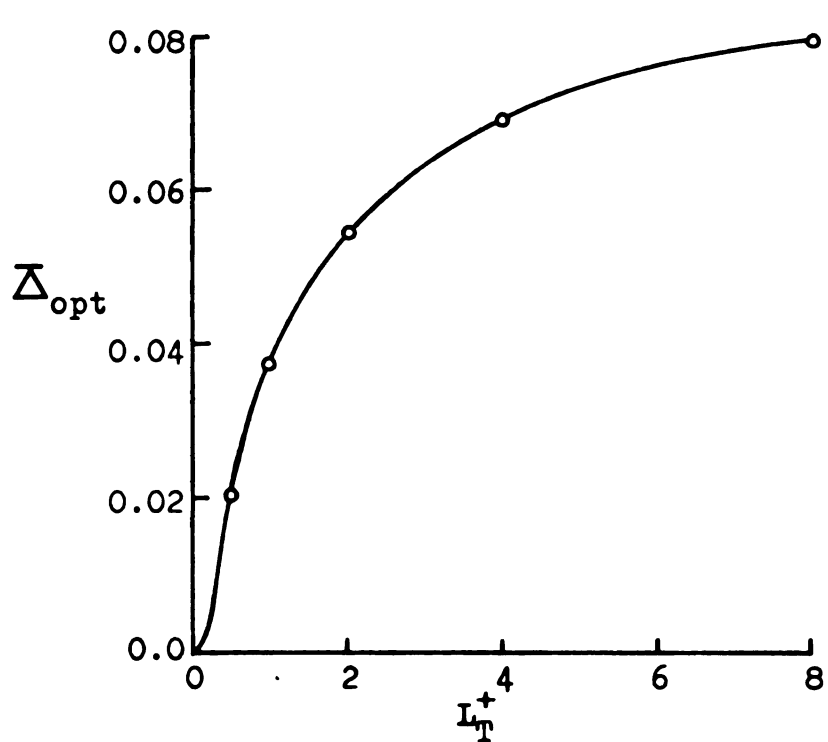


Figure 2.4.3  $\Delta_{\text{opt}}$  versus dimensionless heat of fusion for a single thermocouple with  $e^L$  the property to be estimated.

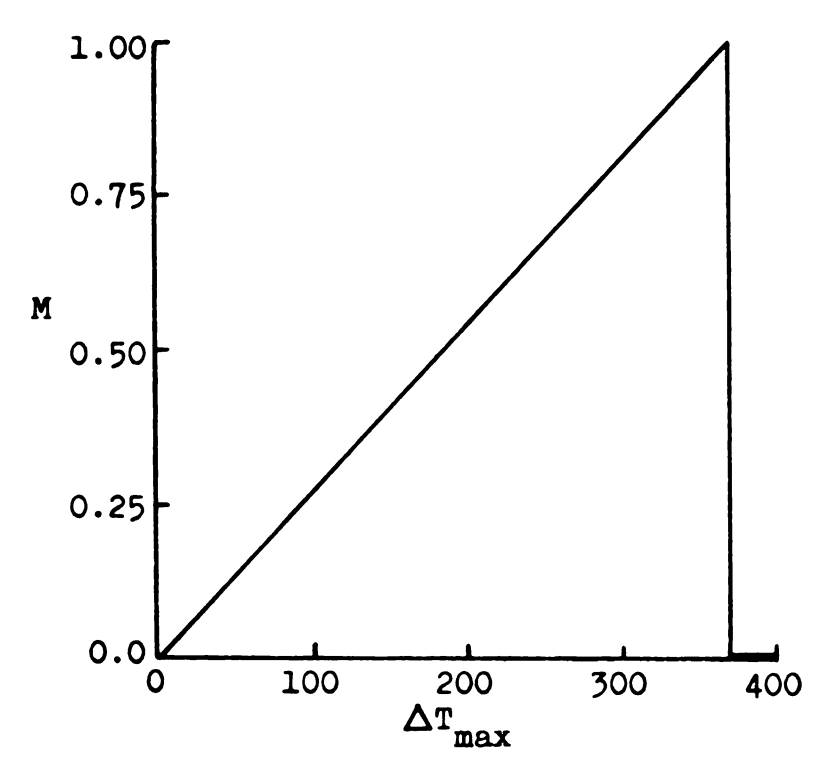


Figure 2.4.4 Merit function, M, versus  $\Delta T_{max}$ 

temperature rise for the equipment at the highest gain setting of the DC amplifiers is about  $370^{\circ}F$ . Electronic noise introduced by various components is on the order of about  $\frac{1}{2}^{\circ}F$ . Thus if our experiment were planned with a  $1^{\circ}F$  temperature rise say, any information in the signal would be masked by the noise in the signal.

To aid in selecting the optimum temperature rise, we now define a "merit function" (32) for the temperature rise based on the characteristics of the equipment used. This idea of a merit function for the experimental equipment is new in the field of optimum experiments for parameter estimation. Since the noise introduced into the signal is not a function of the temperature rise but remains constant, a linear function was selected. The value of the merit function at a  $\Delta T_{max}$  of  $0^{\circ}F$  is chosen as zero and at a  $\Delta T_{max}$  of 370°F the value of the merit function is chosen as one. If the temperature rise goes beyond 370°F the output of the DC amplifier goes beyond the range of the analog to digital converter in the computer and a lower gain must be selected; it is not convenient to do this in the middle of a test so the merit function is assigned a value of zero for  $\Delta T_{\text{max}}$  greater than 370°F. Figure 2.4.4 shows the merit function, M, versus  $\Delta T_{max}$ .

To select the optimum temperature rise, the criterion of the maximum of the product of the merit function and  $\overline{\Delta}_{\rm opt}$  is chosen and is shown in Figure 2.4.5. A  $\Delta T_{\rm max}$  of about 350°F is the best using this criterion.

If one wishes to calculate both the density-heat of

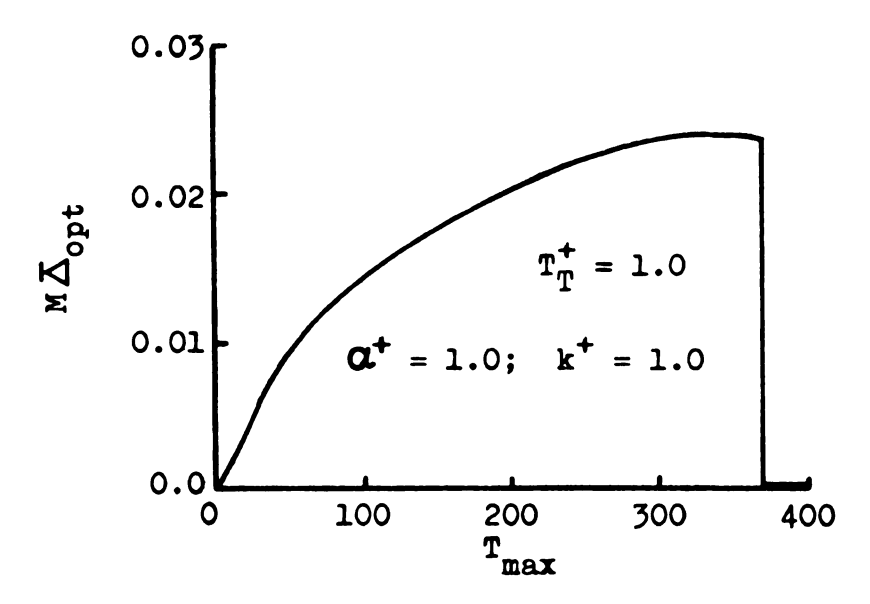


Figure 2.4.5 Product of merit function, M, and  $\Delta_{\rm opt}$  versus  $\Delta T_{\rm max}$  used to determine the optimum  $\Delta T_{\rm max}$  for estimating  $\epsilon$ .

fusion product and the fusion temperature using this experiment, Table 2.4.2 indicates that  $T_{\rm T}^+$ =1 and large  $L_{\rm T}^+$  still provide the best experiment. The optimum temperature rise was not computed for this case.

# Finite solid insulated at x=E

The next example is that of a finite body of solid material that is insulated at the surface x=E. A constant heat flux, q, is applied at the surface x=O and the solid melts. Sensitivity coefficients for this case were calculated using the finite difference methods described in Appendices A and B. The dimensionless heat of fusion is given by

$$L_{q}^{+} = \frac{\rho L}{\rho c_{p,q} qE/k} \qquad [2.4.10]$$

and the dimensionless fusion temperature is given by

$$T_{q}^{+} = \frac{T_{f} - T_{i}}{qE/k_{g}}$$
 [2.4.11]

Figures 2.4.6 through 2.4.8 show the dimensionless sensitivity coefficients for values of  $L_q^+$ =1 and  $T_q^+$ =0.5 at locations x/E=0.0, 0.5, and 1.0 respectively. No attempt to find the optimum experiment for this case was made.

Visual examination of the sensitivity coefficients in Figures 2.4.6 through 2.4.8 shows that all the curves have distinct shapes at each location which means that they are linearly independent at least in pairs and thus pairs of parameters are not correlated. Closer examination reveals that the sensitivity coefficient  $S_{\mathbf{k}_{\mathbf{k}}}^{T}$  has a significant



Table 2.4.2  $\overline{\Delta}_{opt}$  for several values of  $T_T^+$  and  $L_T^+$  with  $T_f$  and  $\rho L$  being the parameters to be estimated for the semi-infinite example.

	<b>a</b> <sup>+</sup> = 1.	$0   k^+ = 1.0$	
T <sub>T</sub> +	L <b>T</b>	$\Delta_{ t opt}$	$ au_{ exttt{opt}}$
0.0		0.0	
0.5	0.5	5.857x10 <sup>-5</sup>	1.60
0.5	1.0	1.310x10 <sup>-4</sup>	2.94
1.0	0.5	2.720x10 <sup>-3</sup>	0.675
1.0	1.0	6.627x10 <sup>-3</sup>	1.08

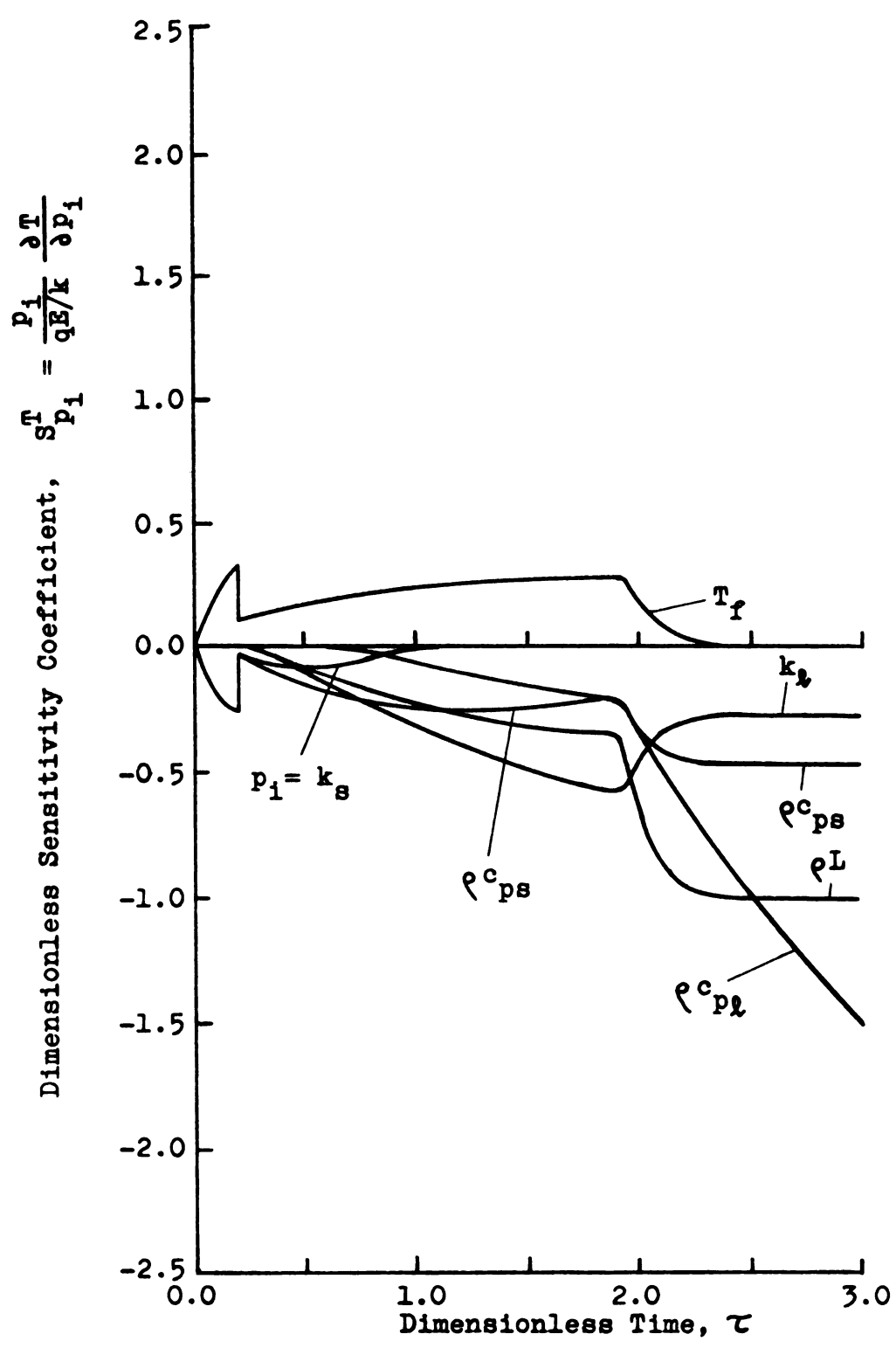


Figure 2.4.6 Sensitivity coefficients at x/E=0.0 for a melting-freezing, finite body with constant heat flux, q, at x=0 and insulated at x=E.

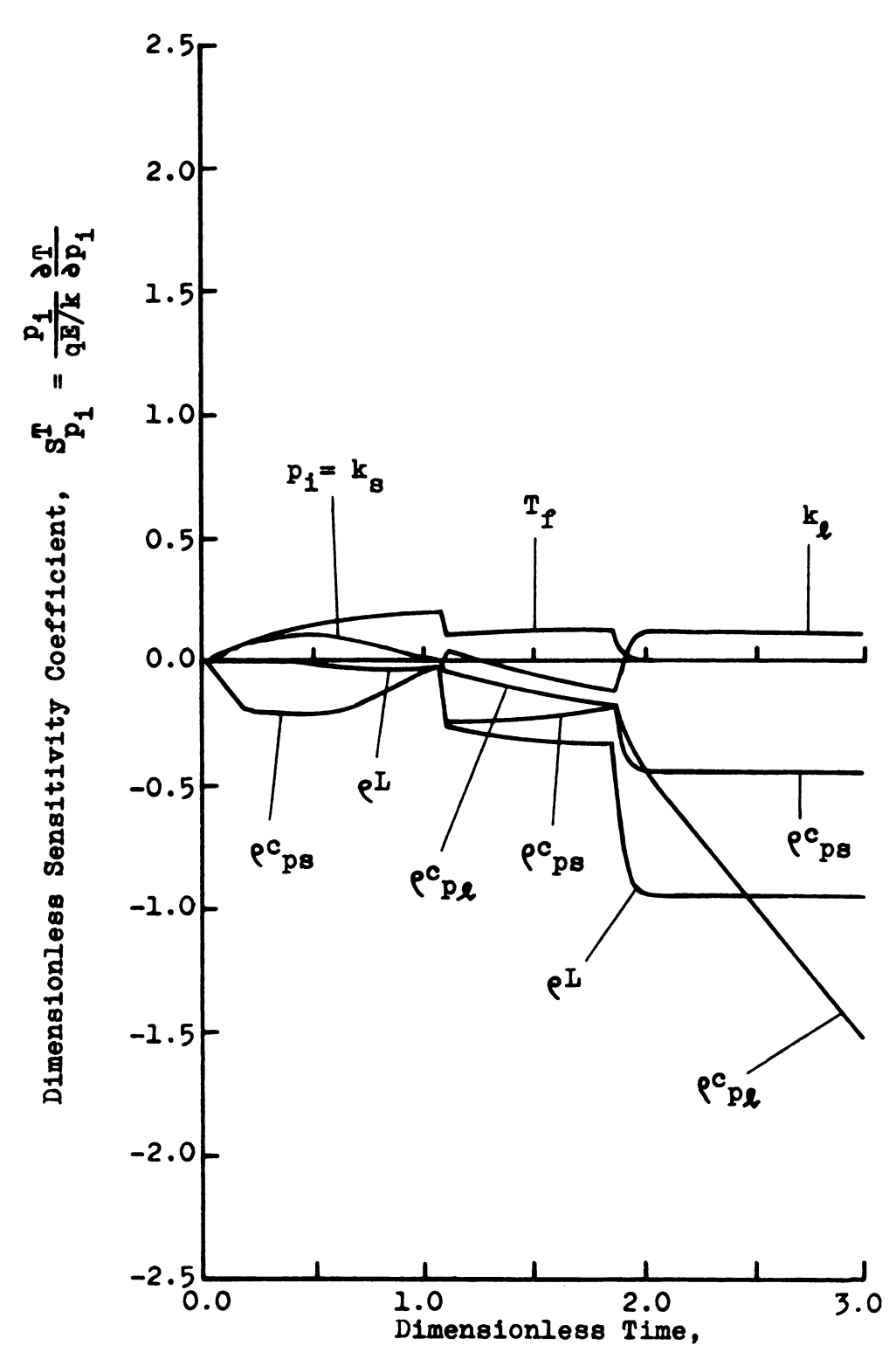


Figure 2.4.7 Sensitivity Coefficients at x/E=0.5 for a melting-freezing, finite body with constant heat flux, q, at x=0 and insulated at x=E.

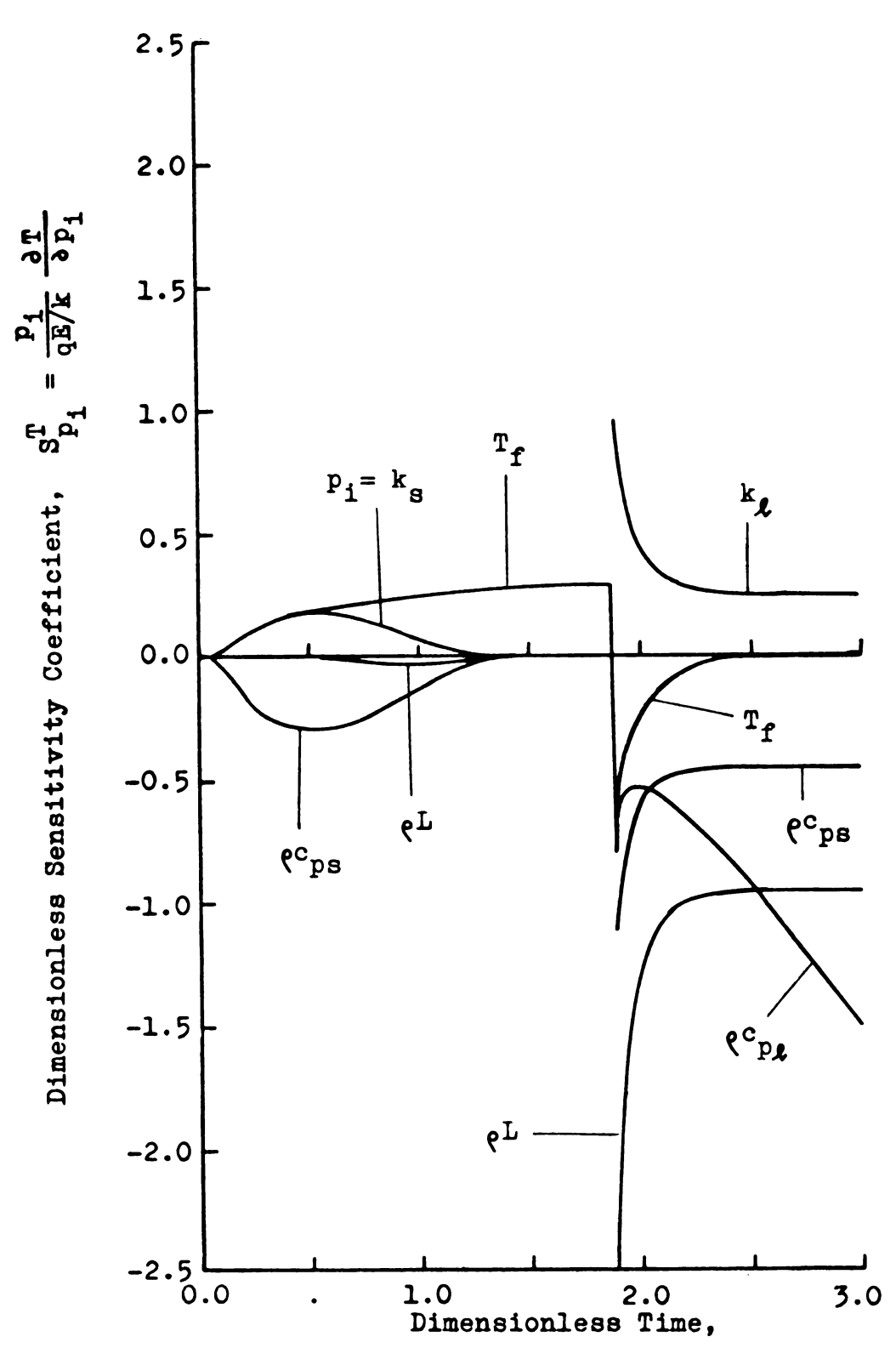


Figure 2.4.8 Sensitivity coefficients at x/E=1.0 for a melting-freezing, finite body with constant heat flux, q, at x=0 and insulated at x=E.



magnitude for only a short time relative to the other parameters and thus may be the least accurate of all the parameters estimated from this experiment.

Experience has shown that it is generally easier to estimate accurately a few parameters simultaneously than many. Thus we will concentrate on estimating the parameters  $\rho$ L and  $T_f$  simultaneously. These two parameters are directly involved in model building and discrimination for the experiments analyzed herein. The other parameters will be measured using other experimental techniques which are described in Chapter III.

At the heated surface, x/E=0.0, both  $S_{T_s}^T$  and  $S_{T_s}^T$ have nonzero magnitudes and distinct shapes with SpL finally approaching a constant value of about -1.0 and  $S_{T_p}^T$  going to zero after the entire body melts. This would be an excellent thermocouple location to estimate  $\rho$ L and T<sub>f</sub> simultaneously for these experimental conditions. At x/E=0.5 both  $S_{\rho L}^{T}$  and  $S_{T_{\bullet}}^{T}$  again have nonzero magnitudes and different shapes. Both are somewhat smaller in magnitude for this location than at x/E=0.0. This location is good out not as good as the heated surface. At  $x/E=1.0 S_{pL}^{T}$  and  $S_{T_{f}}^{T}$  are again not correlated but  $S_{\rho L}^{T}$  has a very small magnitude until the entire body melts and then becomes very large for a short time.  $S_{T_{\mathcal{L}}}^{T}$  has a fairly large magnitude until the entire body melts and then becomes zero. Thus x=E is also a very good thermocouple location, if the experiment is allowed to run until some time after the entire body melts. Thus one can conclude that the heat of fusion  $\rho$ L, and the fusion temperature, T<sub>f</sub>, can be estimated simultaneously

using these experimental conditions and a single thermocouple at many locations in the body. If more than one thermocouple is used, the accuracy of the estimate can be improved.

Figure 2.4.9 shows the dimensionless sensitivity coefficient  $S_{\mathbf{L}}^{\mathbf{T}}$  calculated in the same manner as the previous figures but with  $L_{\mathbf{q}}^{+}=0.445$  and  $T_{\mathbf{q}}^{+}=0.0$ . It is apparent from Figures 2.4.6 through 2.4.8 and Figure 2.4.9 that if one wanted to estimate only the heat of fusion,  $\rho$ L, using a constant heat flux at one boundary and the other boundary insulated, the most desirable location for a thermocouple would be at x=E, the insulated surface. The sensitivity coefficient  $S_{\mathbf{L}}^{\mathbf{T}}$  has, by far, the largest magnitude at this location. An approximate solution to the freezing-melting problem is used to study this case in more detail.

# New approximate solution

An approximate solution can sometimes give greater insight into a problem than a more accurate solution that is unwieldy. For this reason, an approximate solution is obtained using an integral energy equation method given by  $Goodman^{(33)}$ . The simple approximation of a straight line for the temperature distribution is used. In the approximate solution the body is initially a solid at the fusion temperature,  $T_r$ . The solution is

$$\frac{\mathbf{T}-\mathbf{T}_{\mathbf{f}}}{\mathbf{q}\mathbf{B}/\mathbf{k}} = \begin{cases}
-\frac{\mathbf{X}}{\mathbf{E}} + \mathbf{L}_{\mathbf{q}}^{+} + \left[ (\mathbf{L}_{\mathbf{q}}^{+})^{2} + 2\mathbf{T} \right]^{\frac{1}{2}} & 0 \leq \mathbf{x} \leq \mathbf{\epsilon}(\mathbf{T}); \\
0 & \mathbf{\epsilon}(\mathbf{T}) \leq \mathbf{x} \leq \mathbf{E}; & \mathbf{T} \leq \mathbf{T}_{\mathbf{E}}
\end{cases}$$
[2.4.12]

where  $\epsilon(7)$  is the position of the liquid-solid interface

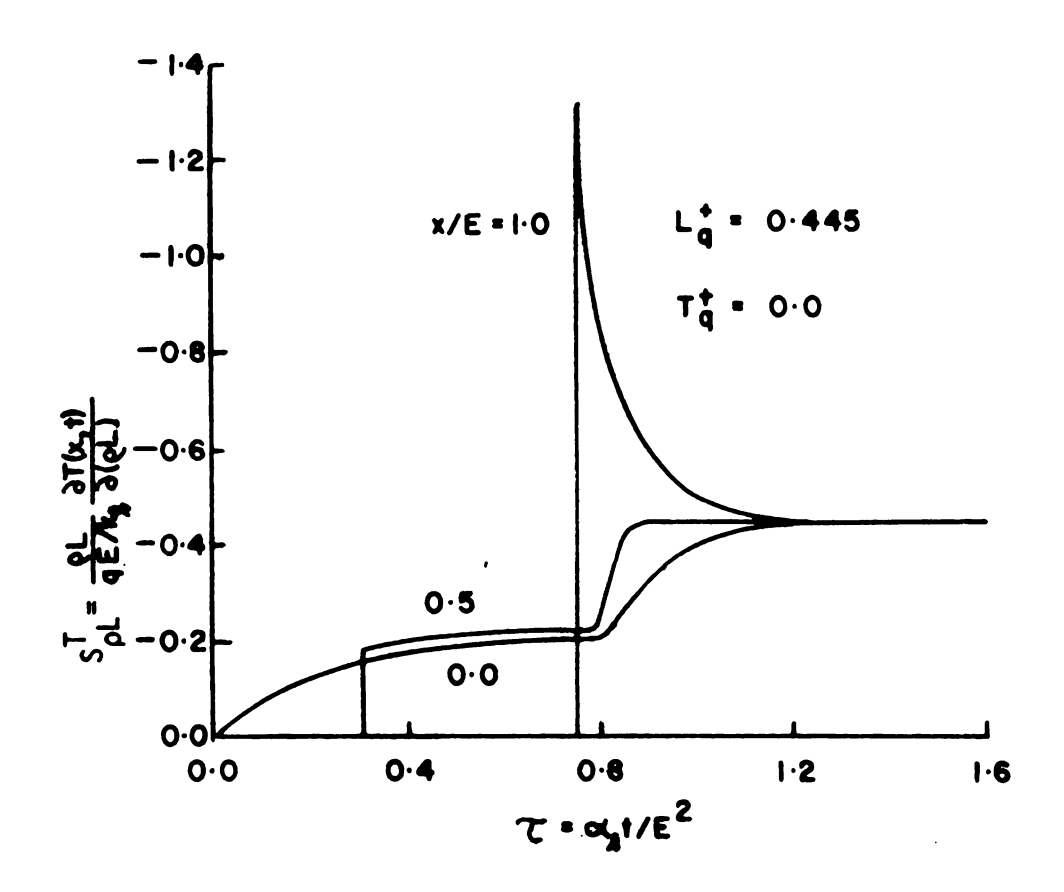


Figure 2.4.9 Dimensionless sensitivity coefficient,  $S_{\text{QL}}^{\text{T}}$ , versus dimensionless time,  $\mathcal{T}$ , for a finite body with constant heat flux, q, at x/E=0 and insulated at x/E=1.



and is given by

$$\boldsymbol{\epsilon}^+(\boldsymbol{\tau}) = \frac{\boldsymbol{\epsilon}(\boldsymbol{\tau})}{\mathbb{E}} = -L_q^+ + \left[ (L_q^+)^2 + 2\boldsymbol{\tau} \right]^{\frac{1}{2}} \quad \left[ 2.4.13 \right]$$

7 is the dimensionless time,

$$\tau = \frac{\alpha_{\ell}^{t}}{\epsilon^{2}}.$$
 [2.4.14]

 $\mathbf{L}_{\mathbf{q}}^{+}$  is the dimensionless heat of fusion and is given by

$$L_{q}^{+} = \frac{\rho^{L}}{\rho^{c}_{p2} (qE/k2)}$$
 [2.4.15]

At the instant the entire body is melted, the temperature distribution is still linear; an exact solution for the problem of a body subjected to a constant heat flux on one side, insulated on the other side and with a linear temperature distribution at  $\boldsymbol{\tau} = \boldsymbol{\tau}_{\rm E}$  is

$$\frac{\mathbf{T}-\mathbf{T_{f}}}{\mathbf{qE/k}} = \mathbf{\tau} + \frac{5}{6} - \frac{2}{\pi} \sum_{n=1}^{\infty} \frac{(-1)^{n}}{n^{2}} e^{-n^{2} \pi^{2} (\mathbf{\tau} - \mathbf{\tau_{E}})} \cos \left(\frac{n \pi x}{E}\right);$$

$$0 \le x \le E, \ \mathbf{\tau} > \mathbf{\tau_{E}}$$
[2.4.16]

 $au_{E}$  is the time taken to melt the entire body and is obtained from [2.4.12] by letting x=E and T-T<sub>f</sub>=0; the result is

$$T_{\rm E} = \frac{1}{2} + L_{\rm q}^{+}.$$
 [2.4.17]

The approximate solution [2.4.12], is differentiated with respect to  $\rho$ L to find  $S_{\rho L}^{T}(x,t)$ ,

$$\mathbf{S}_{\mathbf{p}\mathbf{L}}^{\mathbf{T}}(\mathbf{x},\mathbf{t}) = \frac{\mathbf{p}\mathbf{L}}{\mathbf{q}\mathbf{E}/\mathbf{k}} \frac{\mathbf{d}\mathbf{T}(\mathbf{x},\mathbf{t})}{\mathbf{d}(\mathbf{p}\mathbf{L})} = \begin{cases} -\mathbf{L}_{\mathbf{q}}^{+} + \frac{\mathbf{L}_{\mathbf{q}}^{+}}{\mathbf{L}_{\mathbf{q}}^{+}} \frac{0 \leq \mathbf{x} \leq \mathbf{\epsilon}(\mathbf{\tau}),}{\mathbf{\tau} < \mathbf{\tau}_{\mathbf{E}}}, & \mathbf{\tau} < \mathbf{\tau}_{\mathbf{E}} \\ 0; & \mathbf{\epsilon}(\mathbf{\tau}) \leq \mathbf{x} \leq \mathbf{E}, & \mathbf{\tau} < \mathbf{\tau}_{\mathbf{E}} \\ & [2.4.18] \end{cases}$$

For times greater than  $\tau_{\rm E}$  the solution is found from [2.4.16] to be

$$S_{\mathbf{p}L}^{\mathbf{T}}(\mathbf{x},\mathbf{t}) = -L_{\mathbf{q}}^{+} - 2L_{\mathbf{q}}^{+} \sum_{n=1}^{\infty} (-1)^{n} e^{-n^{2} \pi^{2} (\tau - \tau_{E})} \cos \left(\frac{n\pi x}{E}\right)$$
[2.4.19]

The only thermocouple location considered here is the insulated surface. Only times greater than  $\tau_E$  are of interest because  $S_{\text{pl}}^{\text{T}}(E,t)$  is zero until  $\tau=\tau_E$ . The maximum temperature rise in the liquid occurs at the heated surface x=0 and can be shown to be

$$\frac{\Delta T_{\text{max}}}{qE/k_{\text{g}}} = (\tau - \tau_{E}) + \frac{5}{6} - \frac{2}{\pi^{2}} \sum_{n=1}^{\infty} \frac{(-1)^{n}}{n^{2}} e^{-n^{2} \pi^{2} (\tau - \tau_{E})} [2.4.20]$$

Equations [2.4.19] and [2.4.20] are employed in calculating  $\overline{\Delta}$  as described in section 2.3. Figure 2.4.10 shows  $\overline{\Delta}$  versus dimensionless time for several values of  $\Delta T_{max}$ . Remember that the maximum temperature rise,  $\Delta T_{max}$ , is an experimental constraint. For each value of  $\tau_m$  the heat flux, q, must be adjusted so that  $\Delta T_{max}$  is attained in time  $\tau_m$ .

To determine the optimum temperature rise for this experiment the value of  $\overline{\Delta}_{\rm opt}$ , i.e., the value of  $\overline{\Delta}$  at the optimum  $\tau_{\rm m}$ , is plotted versus  $\Delta T_{\rm max}$  in Figure 2.4.11.

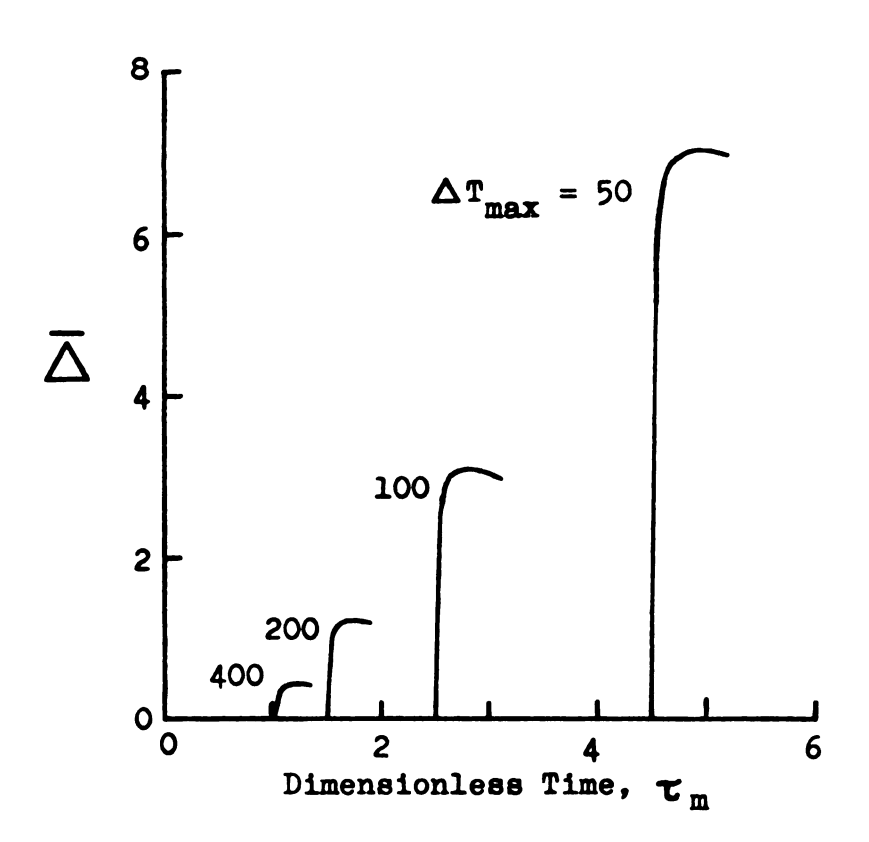


Figure 2.4.10  $\overline{\Delta}$  versus  $\tau_{\rm m}$  for several values of  $\Delta T_{\rm max}$  for a melting, finite body of solid initially at the fusion temperature with  $\epsilon$ L the parameter to be estimated.

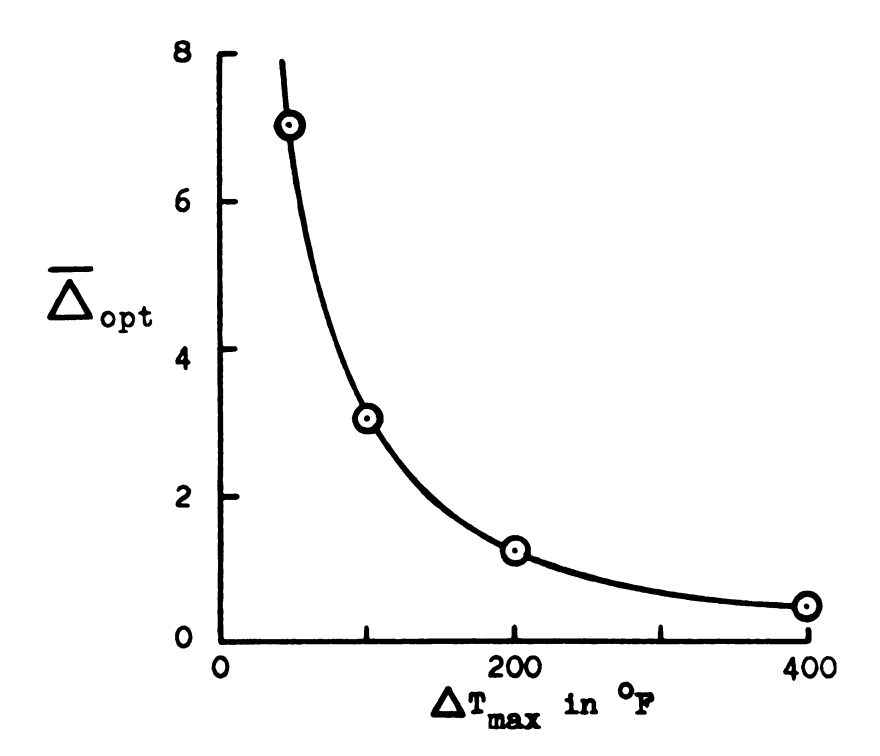


Figure 2.4.11  $\overline{\Delta}_{opt}$  versus  $\Delta T_{max}$  for finite body of solid initially at the fusion temperature with  $\ell$ L the parameter to be estimated.

Figure 2.4.11 indicates that  $\Delta T_{max}$  o is the ideal condition; however, arguments have already been presented to show that this is not the case in practice. To complete this case study, we refer to the merit function of Figure 2.4.3. Again the optimum criterion is to be the maximum value of the M and  $\Delta_{opt}$  product. The product M x  $\Delta_{opt}$  versus  $\Delta T_{max}$  is shown in Figure 2.4.12. From this figure the optimum temperature rise is found to be about 33°F.

The optimum dimensionless time,  $\tau_{\rm m,opt}$ , is now fixed and can be determined by calculating  $\Delta_{\rm opt}$  for a  $\Delta \tau_{\rm max}$  of 33°F as in Figure 2.4.10. Given  $\tau_{\rm m,opt}$ , the value of E can be selected and then q can be determined from equation [2.4.20].

It should be emphasized again that if it were not for the existance of a relation between the maximum temperature rise and the heat flux, such as equation [2.4.20], this optimization process would be more difficult. In the case of a more accurate or more general solution such as a numerical solution, no such relation exists. The process thus becomes a more time consuming iterative type calculation. For each value of  $\tau_{\rm m}$  some other method of finding the heat flux that will cause a maximim temperature rise  $\Delta \tau_{\rm max}$  in time  $\tau_{\rm m}$  must be found. Instead of attempting this costly preliminary procedure, the lessons learned from this simple model and visual examination of the sensitivity coefficients will be used to design our experiment.

# Heat flux approximating the actual case

One other test case was examined. The actual form of

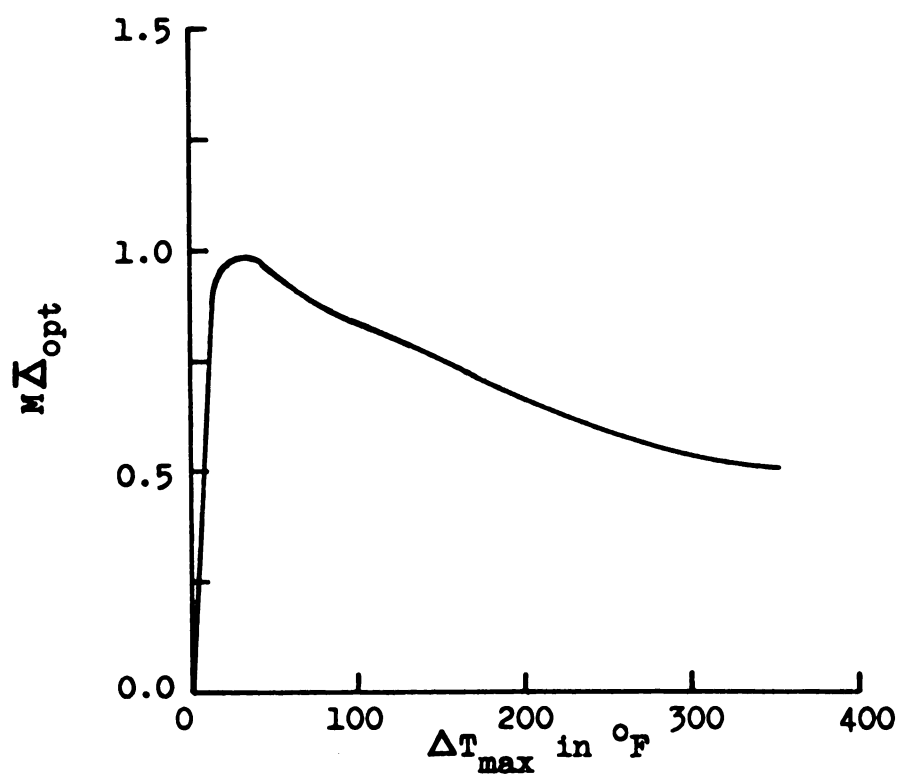


Figure 2.4.12 The product  $M\overline{\Delta}_{opt}$  versus  $\Delta T_{max}$  used to determine the optimum  $\Delta T_{max}$  for estimating the parameter eL.

the heat flux expected from the experiment was used to calculate the sensitivity coefficients  $S_{\mathbf{L}}^{T}(\mathbf{x},t)$  and  $S_{\mathbf{T}_{\mathbf{f}}}^{T}(\mathbf{x},t)$  for a finite body with the surface  $\mathbf{x}=\mathbf{E}$  insulated. The heat flux used is that shown in Figure 2.4.13. The sensitivity coefficients  $S_{\mathbf{L}}^{T}(\mathbf{x},t)$  and  $S_{\mathbf{T}_{\mathbf{f}}}^{T}(\mathbf{x},t)$  versus time are shown for  $\mathbf{x}/\mathbf{E}=0.0$ , 0.5, and 1.0 in Figures 2.4.14, 2.4.15, and 2.4.16 respectively. Examination of these figures again indicates that the heat of fusion,  $\mathbf{\rho}\mathbf{L}$ , and the fusion temperature,  $\mathbf{T}_{\mathbf{f}}$ , can be estimated simultaneously from this experiment since the sensitivity coefficients  $S_{\mathbf{L}}^{T}(\mathbf{x},t)$  and  $S_{\mathbf{T}_{\mathbf{f}}}^{T}(\mathbf{x},t)$  are not correlated at any of the three locations shown.

Table 2.4.3 gives the locations and times for the maxima and minima of the sensitivity coefficients  ${}^T_{\rho L}$  and  ${}^T_{T_{f}}$  for all the cases that were computed. For the semi-infinite body with a step decrease in the surface temperature the maxima occurs at the solid-liquid interface. The only zero values are at the surface x=0 which is what one would expect because the temperature is prescribed there and changes in the properties can have no effect on it.

For the cases using finite bodies all the maxima occur at either the insulated surface or at the heated surface and in most cases at times after the entire body has melted. Zero values of both  $S_{\mathbf{L}}^{\mathbf{T}}$  and  $S_{\mathbf{T}_{\mathbf{f}}}^{\mathbf{T}}$  occur but not at the same time.  $S_{\mathbf{L}}^{\mathbf{T}}$  is zero (actually not identically zero but relatively small) for times less than  $\mathbf{T}_{\mathbf{M}}$  and  $S_{\mathbf{T}_{\mathbf{f}}}^{\mathbf{T}}$  is zero for times greater than  $\mathbf{T}_{\mathbf{E}}$ .  $S_{\mathbf{L}}^{\mathbf{T}}$  being zero while  $S_{\mathbf{T}_{\mathbf{f}}}^{\mathbf{T}}$  is not and vice versa permits the simultaneous estimation of  $\mathbf{P}L$  and  $\mathbf{T}_{\mathbf{f}}$ .

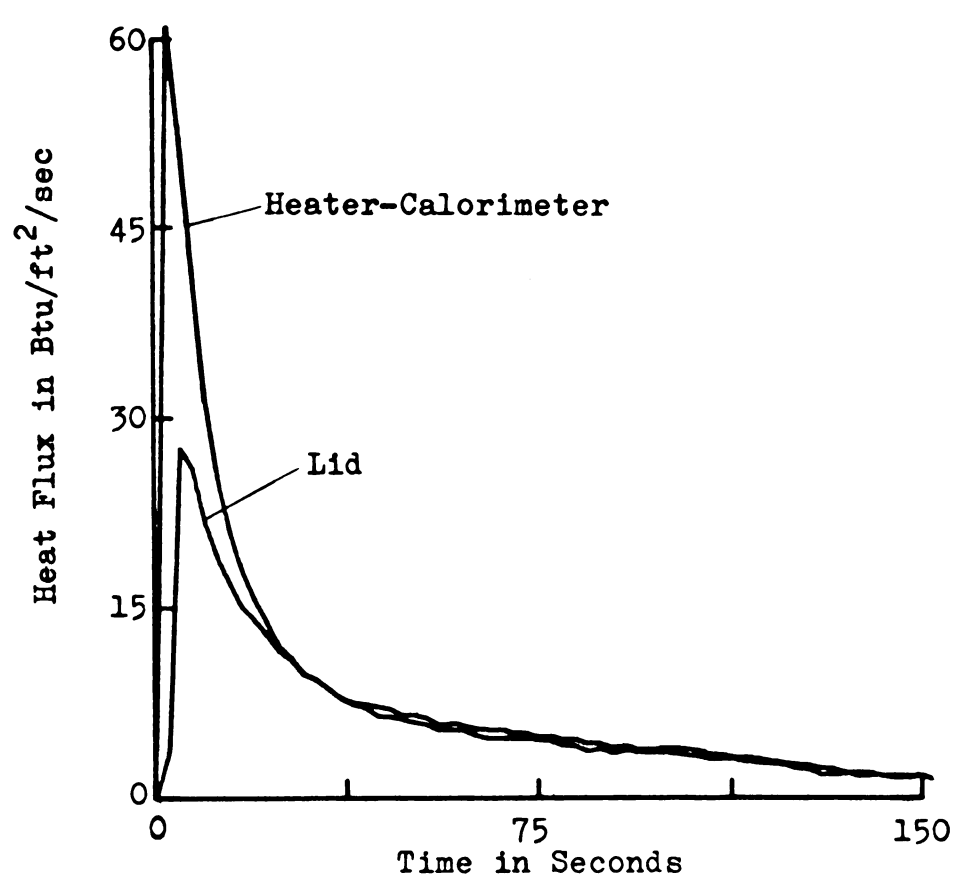


Figure 2.4.13 Experimental heat flux from copper heater-calorimeter and heat flux through copper lid versus time.

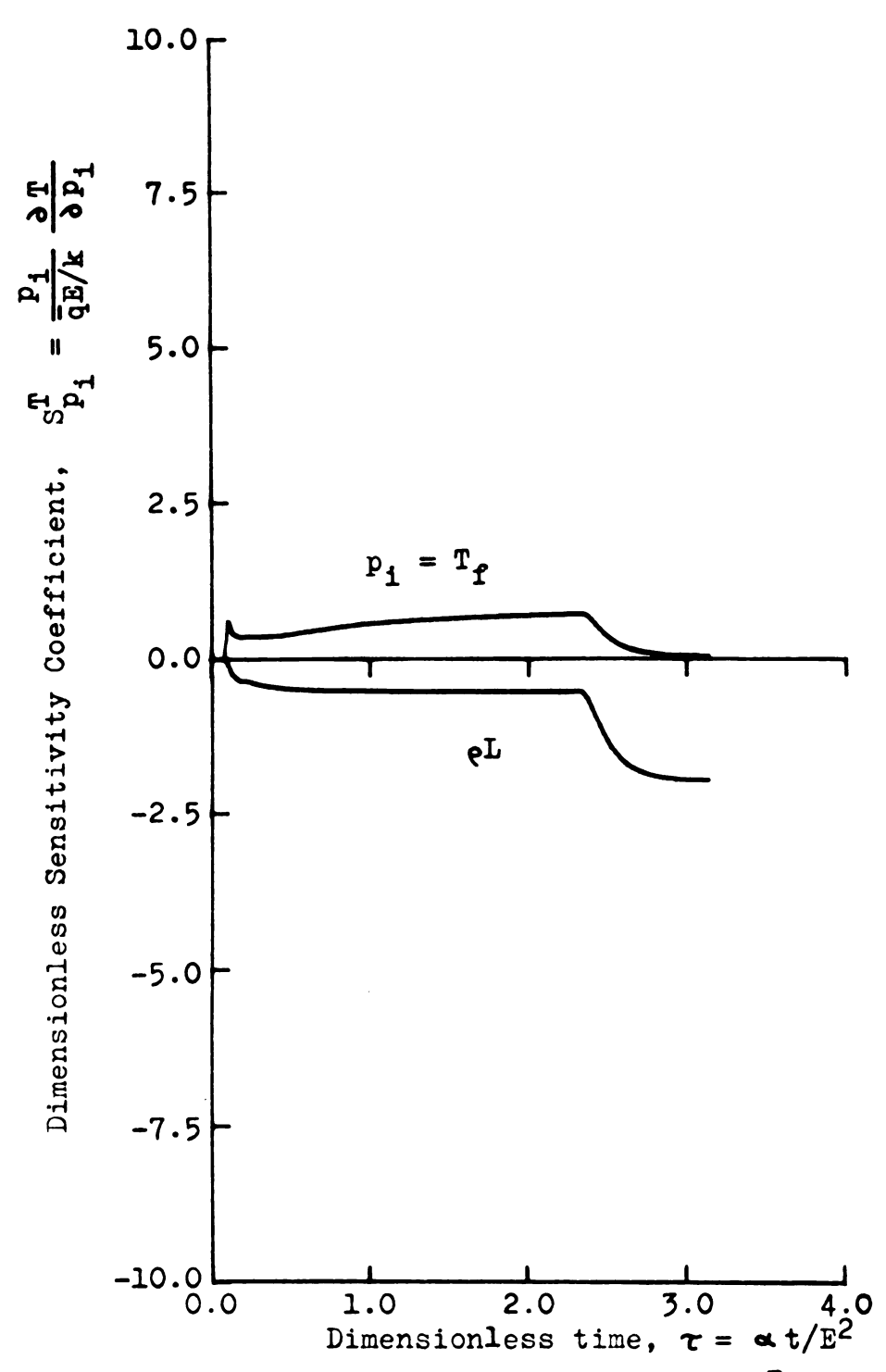


Figure 2.4.14 Sensitivity coefficients  $S_{eL}^T$  and  $S_{T_e}^T$  at x=0.0 versus time for a finite body insulated at x=E and the heat flux of Figure 2.4.12 prescribed at x=0.0.

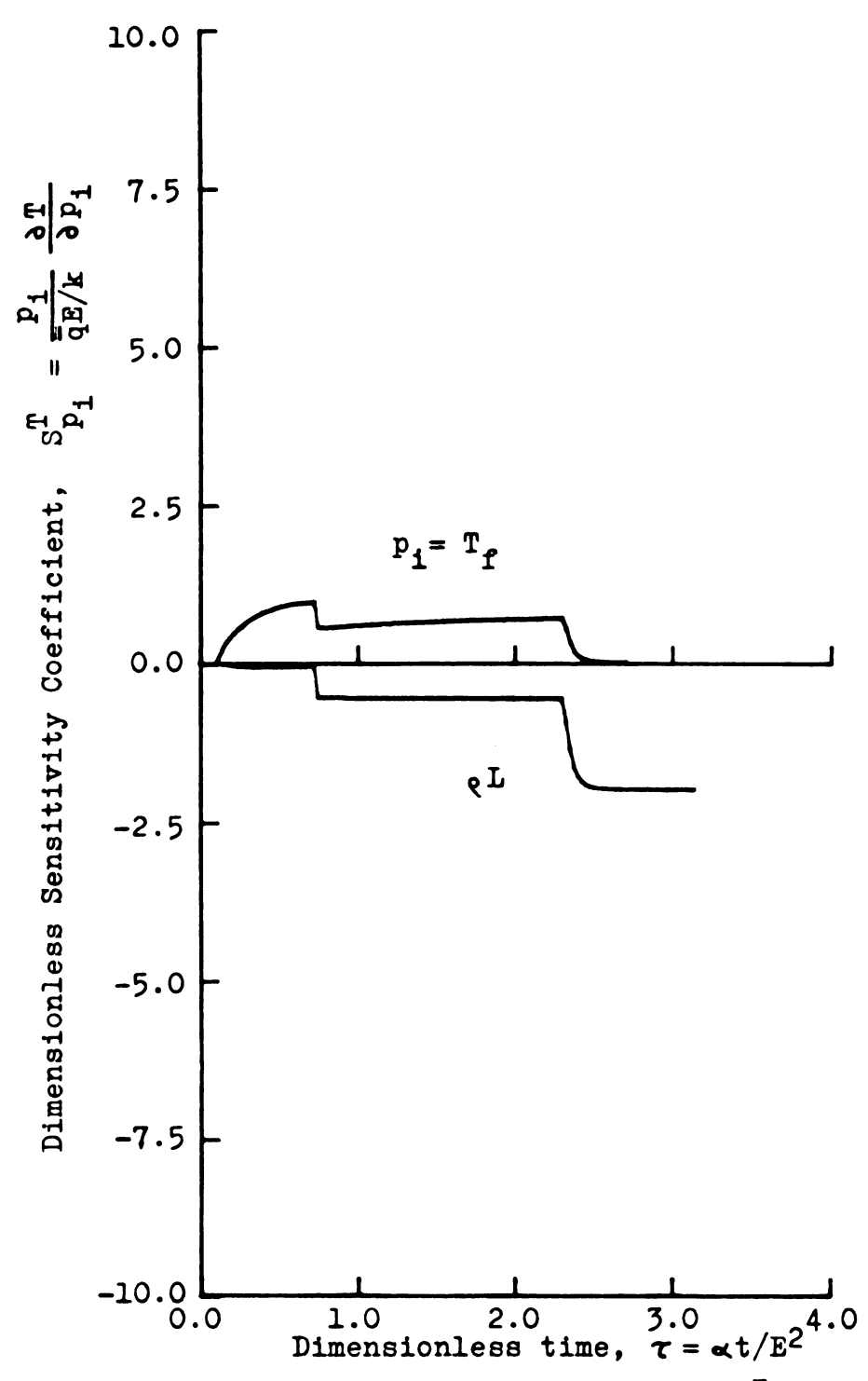


Figure 2.4.15 Sensitivity coefficients  $S_{eL}^T$  and  $S_{T}^T$  at x/E=0.5 versus time for a finite body insulated at x=E and the heat flux of Figure 2.4.12 prescribed at x=0.0.

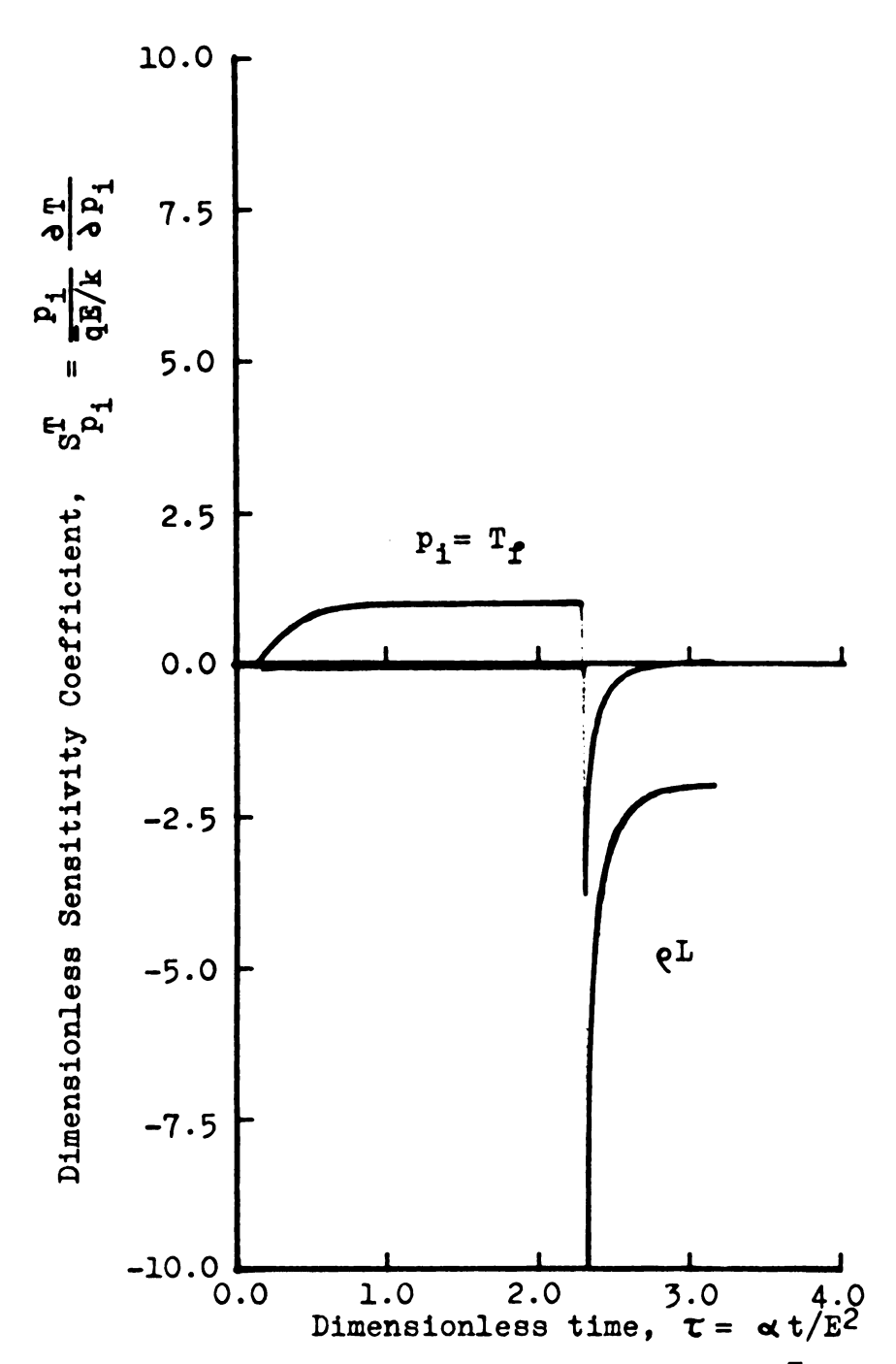


Figure 2.4.16 Sensitivity coefficients  $S_{\mathbf{qL}}^{\mathbf{T}}$  and  $S_{\mathbf{T}_{\mathbf{f}}}^{\mathbf{T}}$  at  $\mathbf{x}/\mathbf{E}=1.0$  versus time for a finite body insulated at  $\mathbf{x}=\mathbf{E}$  and the heat flux of Figure 2.4.12 prescribed at  $\mathbf{x}=0.0$ .

Locations and times for maxima and minima of sensitivity coefficients  $S^T$  and  $S^T_f$  . Table 2.4.3

	To xem	ST	max	gr T	large $\mathbf{S}_{\mathbf{e}L}^{\mathbf{T}}$	$\mathbf{s}^{\mathbf{r}}_{\mathbf{e}^{\mathbf{L}}}$	large	E E	$zero \frac{\mathbf{S}^{\mathbf{T}}}{\mathbf{\phi}\mathbf{L}}$	ST OL	zero S <sub>T</sub>	SE EI
e de la companya de l	x/E	4	x/B	٦	x/B	٦	x/E	L	x/B	٦	x/B	ہ
Semi-infinite body temperature boundary condition at x=0 initially all liquid		И́2 =		W2 =		near TM		near T <b>H</b>	0.0	all	0.0	all
Finite body, constant heat flux at x=0 insulated at x=E L_q^=1, T_q^=0.5	1.0	الا ق	0.0	WД.>	all	> T.H	a11	<t.b< td=""><td>a11</td><td>ИД&gt;</td><td>811</td><td>۶۲B</td></t.b<>	a11	ИД>	811	۶۲B
Finite body, constant heat flux at x=0 insulated at x=E L <sub>q</sub> <sup>+</sup> =0.445, T <sub>q</sub> <sup>+</sup> =0.0	1.0	= 7 <sub>B</sub>		-	811	> T.M			811	ИД>		
Finite body, heat flux of Figure 2.4.12 at x=0, insulated at x=E	1.0	= 7.	1.0	= 7.	811	W2<	811	¥2>	811	ИД>	811	>TB
	ľ											

 $\tau_M$  is defined as the dimensionless time at which the fusion front crosses location  $x_M$  is defined as the dimensionless time it takes to melt the entire body.

The sensitivity coefficient  ${}^{T}_{\rho L}$  has a relatively large magnitude at all locations in the body for times greater than  ${\boldsymbol{\tau}_{M}}$ . The sensitivity coefficient  ${}^{T}_{T}$  has a relatively large magnitude for all locations up until time  ${\boldsymbol{\tau}_{R}}$ .

From the above considerations one can draw several conclusions as to the best experiment to estimate the parameters  $\rho L$  and  $T_{\rho}$  simultaneously.

- A finite body with one surface insulated and a known heat flux at the other surface is desired.
- 2. The best locations for measurement are at the heated surface and the insulated surface.
- 3. The experiment should last somewhat longer than the time it takes to melt the entire body.
- 4. To estimate the parameter  $\rho$ L only,  $\Delta$ T<sub>max</sub> should be kept as small as possible within the limits of the experimental equipment. This may not be true if one wants to find both  $\rho$ L and T<sub>f</sub> simultaneously.

These conclusions were used to design an experiment to estimate the parameters in a melting-freezing model. The experiment will be described in Chapter III.

#### CHAPTER III

### EXPERIMENTAL EQUIPMENT AND TECHNIQUE

# 3.1. The data acquisition system.

The data acquisition system of Michigan State
University Thermal Properties Measurement Facility consists of three basic parts: Thermocouple sensors, a computer signal conditioner, and an IBM 1800 computer. The type and mounting technique of the thermocouple sensors is discussed in Section 3.2.

The computer signal conditioner contains an electronic reference junction compensator and a DC amplifier for each thermocouple. The electronic reference junction compensators are made by Consolidated Ohmic Devices, Inc. model number EZT 213-A9. The function of the electronic reference junction compensator is to add to the voltage produced by the measuring junction of each thermocouple a voltage that compensates for the actual reference junction temperature not being at the standard 32°F. Thus, the electronic reference junctions are supposed to compensate for changes in ambient temperature and eliminate the need for bothersome ice baths or alternatively, calibrating before each use. It was found that they did not perform as expected and calibration before each experiment was necessary.

The DC amplifiers are the Dana Laboratories Incorporated Model 3400. The purpose of the amplifiers, which have a maximum gain setting of 1000, is to boost the voltage produced by the thermocouples, which is in the millivolt range, to a level which the computer can read accurately. Some of the specifications for the Model 3400 are (34) frequency response DC to 100 Hz - ± 0.01%, linearity AC to 2 kHz - ±0.01%, noise at a gain of 1000 - 4 microvolts, input impedence - 10 megohms. The low noise figure is highly desirable and the large imput impedence allows great freedom in the choice of thermocouple wire size and lead length. There are nine separate reference junction-compensator-DC amplifier combinations allowing up to nine separate channels of data.

The IEM 1800 computer is equipped with an analog to digital converter with multiplexer and an interval timer that allow the data from each thermocouple to be automatically discretized and recorded. The minimum time step between data points is about 50 milliseconds. Data is stored on a magnetic disk storage unit and the maximum number of data points is limited only by the available disk storage of the computer. A typical run may contain 2500 data points; without the computer, it would be a nearly impossible task to discretize and record this many data points.

It was discovered that the reference junction compensators introduced 60 Hz noise to the signal to be amplified. Two readings from each channel are taken 1/120 of a

second apart and then averaged to eliminate this 60 Hz noise. This was found to be a very effective method of eliminating the 60 Hz noise since the frequency of the signal from the thermocouple is much much less than 60 Hz. The data acquisition system is calibrated on-line before each experiment. Four separate constant temperature sources are employed in the calibration, they are a Leeds and Northrup thermocouple checking and calibrating furnace Model 9009, boiling distilled water, a large copper block at room temperature and an ice bath. The furnace is set to a temperature of about 360°F and a Leeds and Northrup certified Platinum versus 10% Platinum-Rhodium thermocouple with a Leeds and Northrup guarded six dial potentiometer Model 7556 are used to read the true temperature of the furnace. The true temperature of the boiling water is read using a Tagliabue certified mercury-inglass thermometer with a range from 167°F to 221°F and graduations of 0.2°F. Similar Tagliabue certified mercury-inglass thermometers with appropriate ranges were used to read the temperature of the copper block at room temperature and to check the temperature of the ice bath (32°F).

Thermocouples made from the same spool as used in the specimens are also placed in the furnace, the boiling water, etc. These thermocouples are connected to a Leeds and Northrup rotary switch Model 8248 which allows one at a time to be connected to the computer signal conditioner. The computer reads each thermocouple ten times and stores the average voltage. When all four calibration points are read for all nine channels, the least squares quadratic.

$$T = A(i)v(i)^2 + B(i)v(i) + C(i)$$
 [3.1.1]

is passed through the data. v(i) is the voltage read by the computer for channel i and T is the temperature read from one of the four standards.

Thus the results of the calibration procedure is a set of coefficients A(i), B(i), and C(i) for each data channel. When the experiment is run, the voltages, v(i), are read and stored on the disk and equation [3.1.1] is used to convert them to temperatures at a later time.

## 3.2 Equipment and test specimens.

The test specimens consist of short, solid cylinders of the "unknown" material three inches in diameter and of various heights. The cylinder is insulated on the perimeter and at the bottom. Thermocouples are placed on the outer radial surface of the cylinder at various locations. Several thermocouples are located at the same height around the perimeter of the cylinder and connected to the computer signal conditioner in parallel to read an average temperature for that level. Thermocouples are attached to the surface of the cylinder in various ways depending on the type of material. For metallic specimens a small groove 0.010 inches wide and 0.010 inches deep is machined in the specimen at the desired point of attachment; number 30 gage wire (0.010 inches in diameter) is placed in the groove and the sides of the groove peened over to pinch the wire and hold it in place. A junction between the two dissimilar metals of the thermocouple wire is not formed

before the wire is attached to the specimen; the metal in the specimen becomes part of the actual measuring junction. This method eliminates the need for the usual adhesives which add mass and may possibly insulate the thermocouple from the specimen. For non-metallic specimens a junction is formed by electrically welding the thermocouple wire to form a "bead"; a shallow hole is drilled in the sample and the bead inserted and glued in the hole. Non-metalic substances usually have much lower thermal conductivity than metallic substances so the adhesives usually will not cause problems by insulating the thermocouple since the conductivity of the adhesive may be chosen to be near that of the specimen.

The specimen is mounted on the hydraulic cylinder in the loading frame shown in Figure 3.2.1. Mounted in the loading frame above the specimen of "unknown" material is a similar specimen of OFHC copper. The copper specimen or calorimeter is brought to some elevated temperature with the electric heater shown in Figure 3.2.1. When the desired temperature is reached, the bifurcated heater moves out from between the two specimens and the hydraulic cylinder brings the unknown and the standard into contact; the switch that controls the hydraulic cylinder also gives a command to the computer to initiate data aquisition. The sides of both the specimen and the calorimeter are insulated and the heat flux from the copper is nearly uniform over the surface. Thus a one dimensional heat flow analysis can be utilized. For specimens which have a relatively high thermal

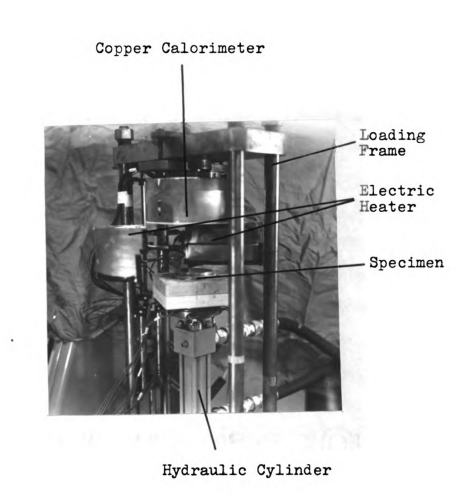


Figure 3.2.1 The experimental equipment.

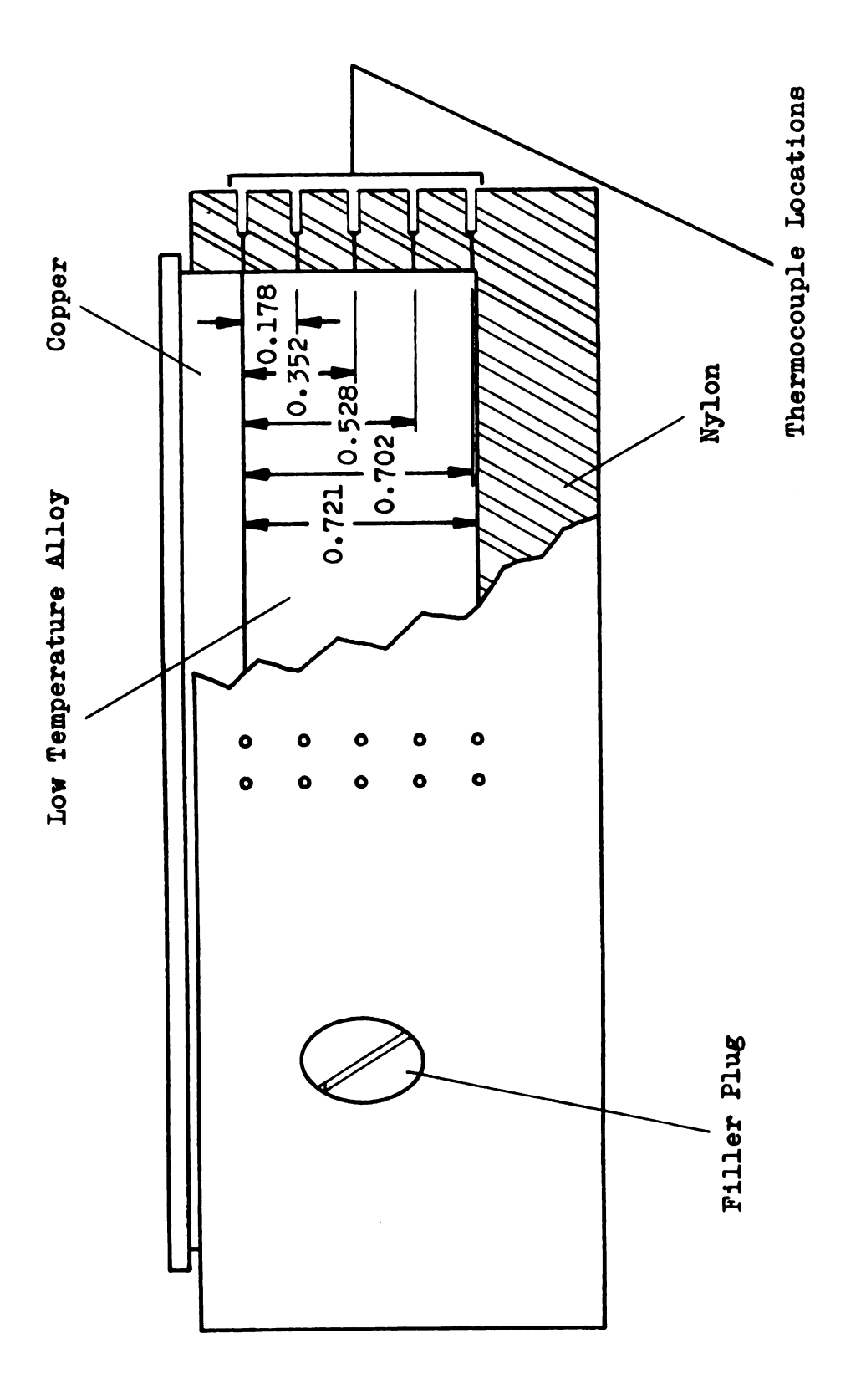
conductivity the assumption of perfect insulation is reasonable. The heat losses from the sides of a high conductivity specimen such as used in this research are a small fraction of the heat flow through it. The applied heat flux over a surface is made as uniform as possible by carefully preparing flat specimens and providing a uniform layer of silicon grease. A "comb" can be made to provide uniform film thicknesses of about 0.015 inch.

One can choose either a temperature boundary condition or a heat flux boundary condition. If a temperature boundary condition is chosen, the data from the extreme thermocouples are used as the boundary temperatures. If; however, a heat flux boundary condition is required for parameter estimation, the procedure is more involved. The copper calorimeter whose thermal properties are wellknown is instrumented with thermocouples for this case. We have found that the one dimensional heat conduction equation describes the temperature distribution adequately. Thus the describing differential equation, the temperature history at several locations, the initial conditions, and the insulation boundary condition are all known for the copper calorimeter. The problem is now the inverse of the normal boundary value problem; that is, the boundary condition at the heated surface is to be found using the given temperature history. Beck (35) has developed a successful technique for solving this problem and it is discussed in Appendix C.

## 3.3 The experiment.

The experiment chosen to illustrate the model building and discrimination techniques proposed in Chapter I was designed to take maximum advantage of the previously developed experimental techniques and equipment available. It was decided to illustrate the techniques for a melting material which is more complex behavior than linear heat conduction. A eutectic alloy of 50% bismuth, 26.6% lead, 13.3% tin, and 10% cadmium was selected; this alloy melts or changes phase at 160°F which is well within the range of the equipment available.

A nylon cup was designed to contain the liquid metal and hold the thermocduples in place. A  $\frac{1}{4}$  inch thick copper lid was pressed into the top of the nylon cup to keep the liquid metal from overflowing when the copper heater was pressed into place, see Figure 3.3.1. A nylon plug with pipe threads was used to seal the filler hole in the side of the nylon cup. The thermocouple wire was 26 gage iron versus constantan. These thermocouples gave a voltage of about 10 millivolts for a temperature of about 370°F; for a gain of 1000 the computer signal conditioner will then supply a maximum of 10 volts to the computer. The IBM 1800 computer at MSU can digitize signals only between ± 10 volts. wire size chosen was 26 gage or 0.0159 inches in diameter. Two 0.0160 inch diameter holes were drilled through the side of the nylon cup at the location of each measuring junction; the iron wire was inserted in one hole and the constantan wire



Partial section view of nylon cup specimen showing copper lid in place and location of thermocouples. Figure 3.3.1

inserted in the other and both were epoxied in place as shown in Figure 3.3.1. The measuring junctions were completed when the nylon cup was filled with liquid metal. The nylon cup was insulated on the sides with transite and fastened to an insulating base, also made of transite, which allowed it to be mounted on the hydraulic cylinder.

The conclusions obtained in Chapter II were utilized in designing the experiment to estimate the parameters in the melting-freezing metal alloy. A finite body with a known heat flux at one surface and insulated at the other surface is desired. The insulation boundary condition is approximated as closely as possible by the low conductivity material used for the cup. (Nylon has a thermal conductivity of about 0.14 Btu/hr/ft<sup>o</sup>F). The heat flux from the copper calorimeter-heater can be calculated as explained in Appendix C. As shown on Figure 3.3.1, there are thermocouples as close as physically possible to the insulated and heated surfaces which are the best locations for measurement. experiment should run for some time longer than it takes to melt the entire specimen. The actual run time was determined from this criterion and the thickness of the sample. sample thickness was chosen large enough to keep the effect of the inaccurately known thermocouple locations to a minimum but small enough so that enough energy could be stored in the copper heater to melt the entire specimen. ness was chosen as 0.75 inches and the experimental run time was then calculated from the optimum conditions described in Chapter II to be about 150 seconds.

The computer program for calculating temperature distributions in the case of melting-freezing problems with a heat flux boundary condition requires the front boundary condition to be applied to the melting or freezing material. thus the heat flux leaving the copper lid must be calculated. The copper lid cannot be considered as part of the copper heater-calorimeter in the heat flux calculation because contact resistance between the two causes a discontinuity in the temperature distribution. avoid this problem, the heat flux from the copper heatercalorimeter was computed separately using the method in Appendix C. The method in Appendix C was also used to compute the heat flux leaving the copper lid. The temperature history in the copper lid was obtained from a thermocouple at the surface nearest the copper heater-calorimeter and the boundary condition at that surface is assumed to be the heat flux that leaves the copper heater-calorimeter.

Experience has shown that the larger the number of properties that are estimated simultaneously, the greater is the probability that there is correlation between them. This results in inaccuracy. To reduce this possibility, a second specimen was constructed to be used in estimating the thermal conductivity and density-specific heat product of the solid phase.

A three inch diameter by one inch high cylinder was cast of the low-temperature alloy. It was machined smooth and thermocouples attached as described in Section 3.2.

Beck (5) recommends that thermocouples be located at both the

heated and insulated surfaces for determining constant thermal conductivity and heat capacity simultaneously. Three thermocouple locations were used with this specimen, they were 0.0625 and 0.125 inches from the heated surface and 0.0625 inches from the insulated surface. Prior to using this sample it was soaked in a refrigerator so the initial temperature was about 45°F. This allowed a greater temperature rise during the experiment before approaching the melting temperature which was avoided in this test.

A separate experiment was also run using the nylon cup specimen to determine the thermal conductivity and density-specific heat product of the liquid phase. The sample was heated to about 180°F initially and the copper calorimeter heated with the electric heater to 400°F.

Since heating of the sample is from above, natural convection effects in the liquid are negligible. One test was run with the copper calorimeter at a lower temperature than the liquid and the results showed natural convection causes a 30% higher "effective" thermal conductivity to be calculated.

The final run was made to determine the fusion temperature and the density-heat of fusion product (or for the melting-over-a-range-of-temperature model the range and the height of the "spike" in the density-specific heat product) and to obtain data against which to compare all the proposed models. The nylon cup specimen was heated from above from an initial temperature of 75°F to a maximum temperature of almost 300°F.

#### CHAPTER IV

#### TEST OF THE PROPOSED METHOD

# 4.1 Introduction

In this chapter the methods for model building and discrimination proposed in Chapter I, the results of the sample cases on optimum experiments for parameter estimation in Chapter II, and the experimental equipment described in Chapter III are used to illustrate the model building and discrimination procedure. Even though we know the sample material is a low melting point alloy, we initially assume ignorace of this fact.

Data used to test the model building-discrimination procedure was obtained as described in Chapter III. Both the heat flux from the copper heater and the heat flux into the specimen (through the copper lid) are shown in Figure 2.4.13. These were calculated by the method outlined in Appendix C.

## 4.2 The model building process

As a first step in the model building process, a simple constant thermal property model was fitted to the data. This corresponds to Block 1. of Figure 1.7.1.

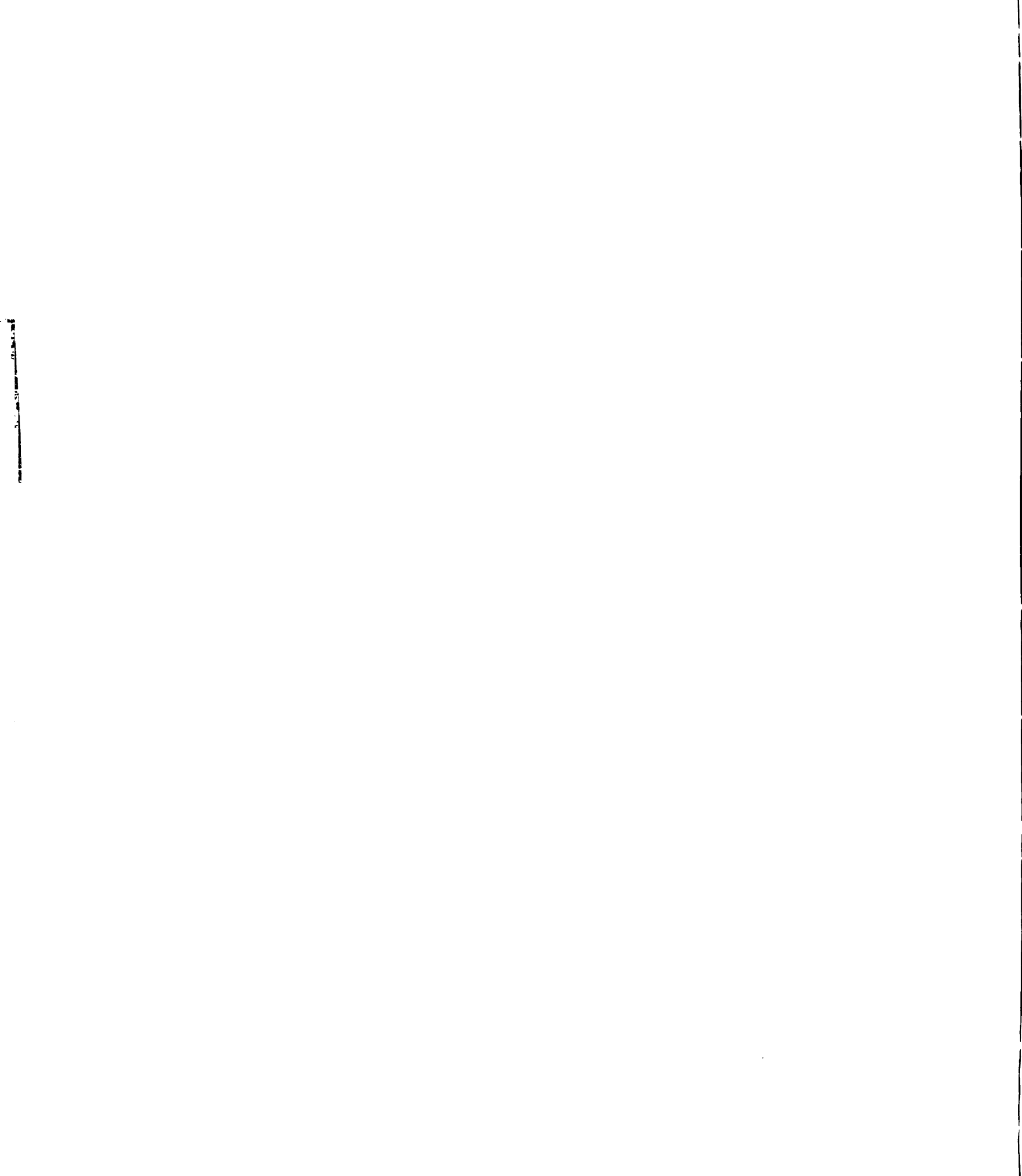
Beck (5) has shown that the optimum experiment for a constant thermal property heat conduction model has one surface

heated and the other insulated with thermocouples at the heated and insulated surfaces. These conditions are met by the experiment described in Chapter III. This satisfies Block 2. of Figure 1.7.1. The experiment was performed and the parameters estimated as in Blocks 3. and 4. of Figure 1.7.1 respectively. The property values that minimized the sum of squares function (see Appendix B) are 5.82 Btu/hr/ft/°F for thermal conductivity and 90.37 Btu/ft<sup>3</sup>/°F for heat capacity.

We now proceed to Block 5. the examination of the model and the residuals. The data and the model shown versus time in Figure 4.2.1. From this plot one can see the lack of fit for all thermocouples away from the heated surface. This plot clearly shows that the model is inadequate but it does not present the information on the deficiencies in the model in a form that is easy to interpret.

Figure 4.2.2 shows the residuals, the difference between the experimental and calculated temperatures, plotted against time. Note that except for the first thermocouple (x=0) positive peaks in the residuals for each thermocouple occur in chronological order moving from the heated surface toward the insulated surface. This may indicate a front moving through the body causing large errors in the predicted response.

Figure 4.2.3 shows the residuals for each thermocouple plotted against the measured temperature of that thermocouple. This plot shows the residuals below a temperature of about 160°F to be nearly identical in both



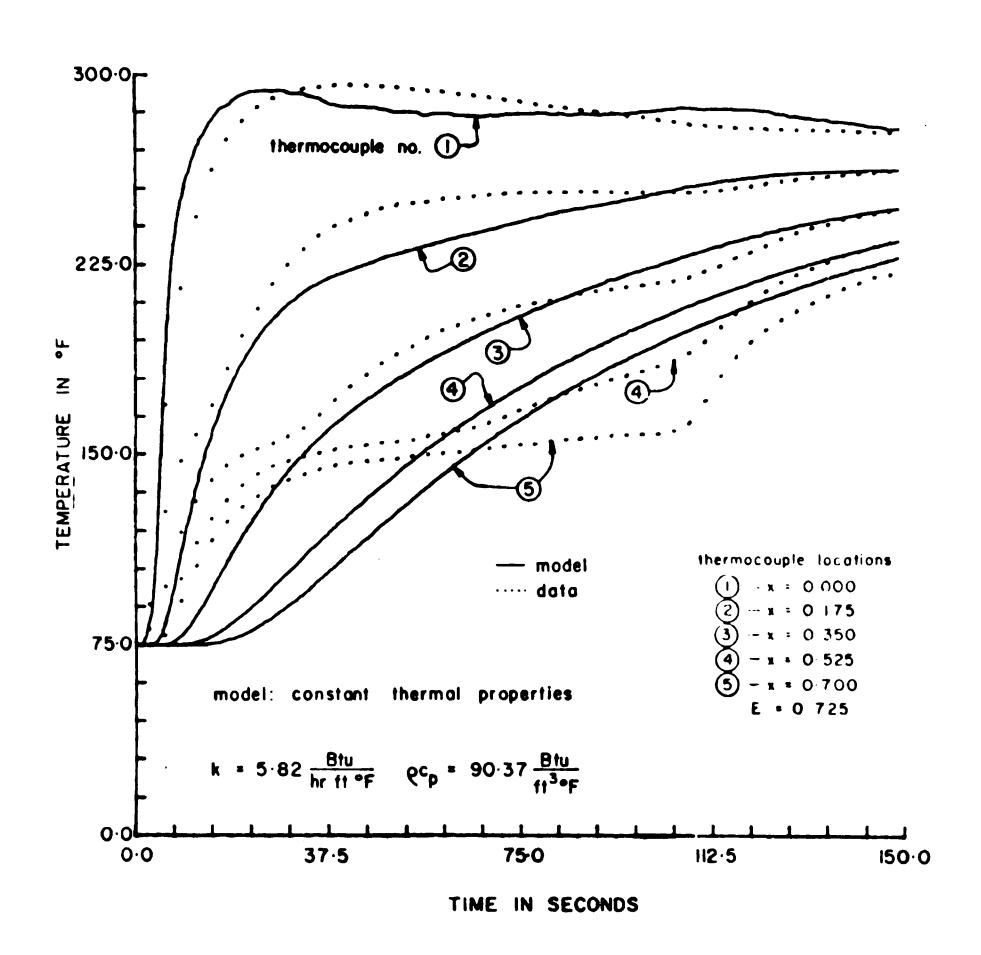


Figure 4.2.1 Constant thermal conductivity and heat capacity model and the data versus time.

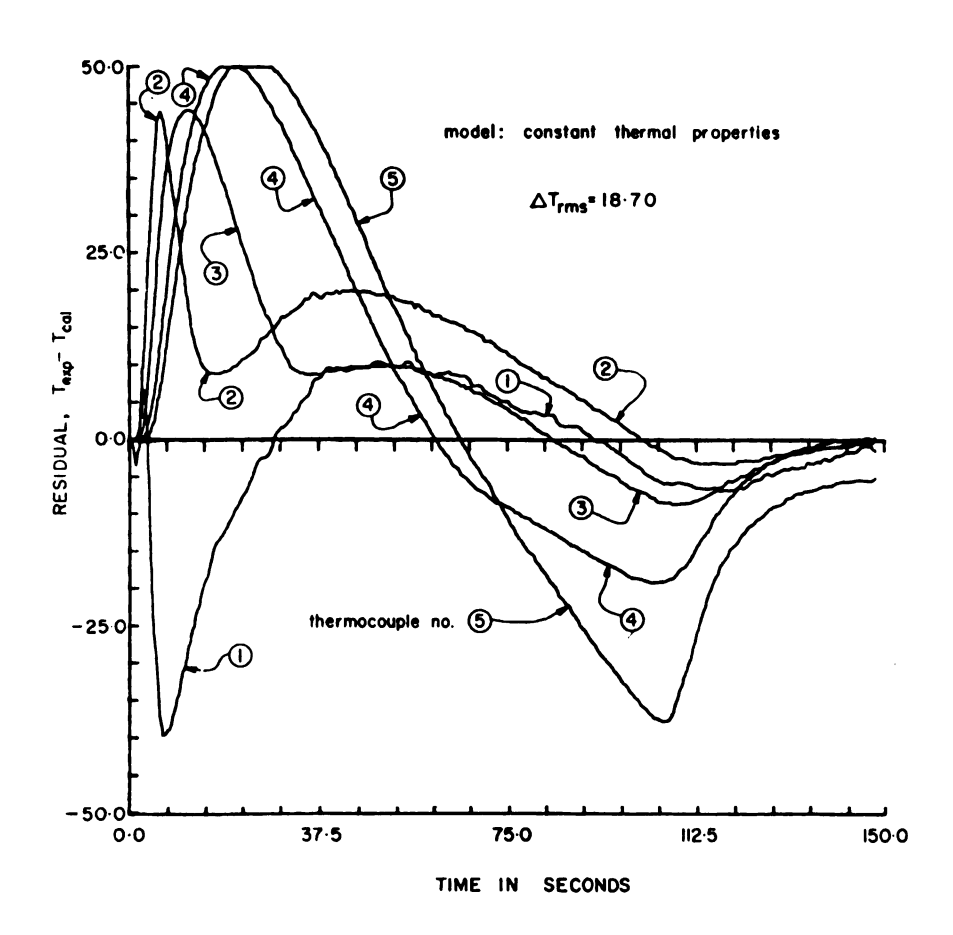


Figure 4.2.2 Residuals for constant thermal conductivity and heat capacity model versus time.

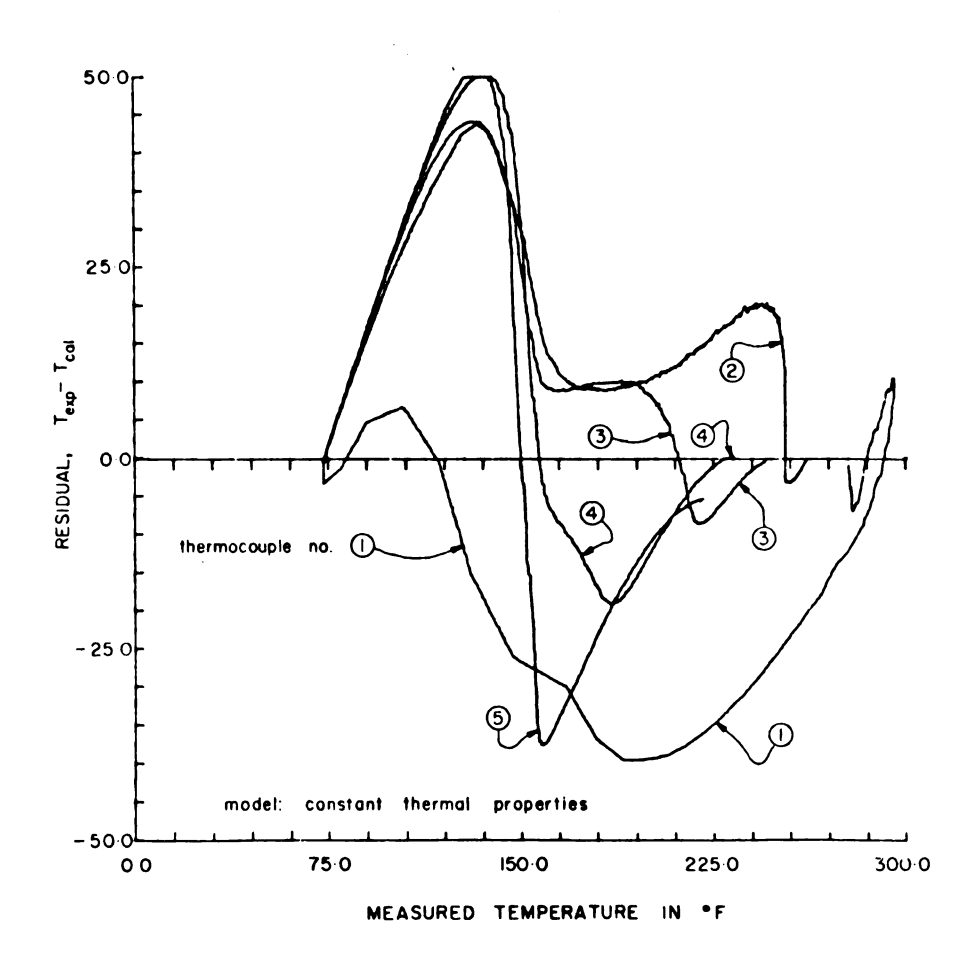


Figure 4.2.3 Residuals for the constant thermal conductivity and heat capacity model versus measured temperature.

magnitude and shape which seems to indicate that the deficiency in the model is temperature dependent.

The decision to be made in Block 6. is an easy one in this case because the model is inadequate. We then proceed to Block 7. of Figure 1.7.1. Because the deficiency in the constant thermal property model seems to be a function of temperature and moves through the body, a model with a step change in thermal properties was proposed. To conserve computation time the temperature at which the step change in thermal properties occurs was set to 160°F (the fusion temperature) and the thermal conductivity and heat capacity for temperatures less than 160°F were evaluated from the solid, non-melting specimen described in Chapter III. The thermal conductivity and heat capacity above 160°F were calculated simultaneously from the data using the method of parameter estimation described in Appendix B.

Instead of actually finding the optimum experiment for this model as in Block 2., it was assumed that the data from the experiment already performed would be sufficient to evaluate the remaining parameters in the model. The properties in this model were calculated to be

$$K(t) = \begin{bmatrix} 12.24; T < 160^{\circ}F \\ 6.27; T > 160^{\circ}F \end{bmatrix}$$
 Btu/hr/ft/°F

$$\rho c_p(T) = \begin{bmatrix} 12.24; T < 160^{\circ}F \\ 182.0; T > 160^{\circ}F \end{bmatrix} Btu/ft^3/{^{\circ}F}$$

Proceed to Block 5. of Figure 1.7.1; Figure 4.2.4 shows the model and the data versus time. The prediction

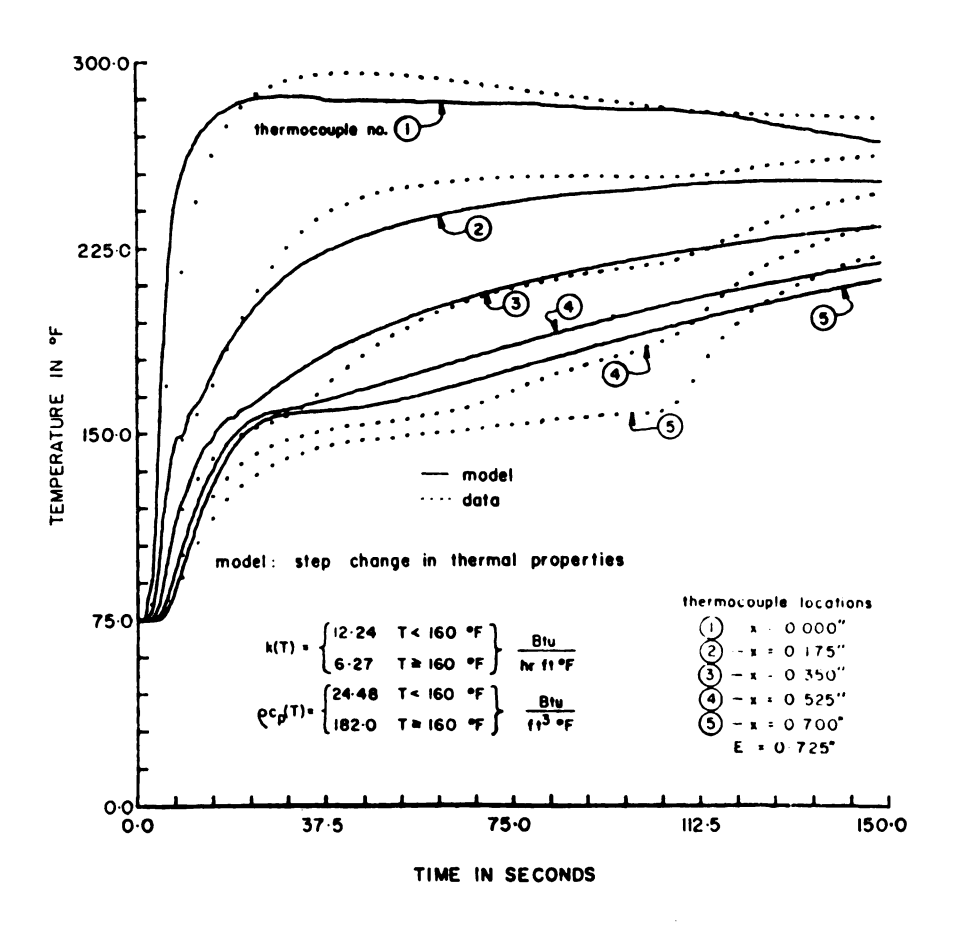


Figure 4.2.4 Step change in thermal properties model and data versus time.

from this model is closer to the data than was the prediction for the constant thermal property model. However, this model still lacks the characteristic shape of the data especially near the insulated surface. This lack of characteristic shape indicates that this model is incapable of accurately describing this heat transfer phenomenon.

Figure 4.2.5 shows the residuals for each thermocouple versus time. This figure is harder to interpret
than the previous examples. With the exception of thermocouple number one at the heated surface, this model is an
improvement over the constant thermal property model except
at later times near the insulated surface. The peaks in
the residuals for each thermocouple still seem to occur in
chronological order but are negative instead of positive.

Figure 4.2.6 shows the residuals for each thermocouple versus the measured temperature for that thermocouple. Note that the peak error for each thermocouple still occurs at approximately the same temperature, near 160°F.

Moving on to Block 6. of Figure 1.7.1; the modification made to the constant thermal property model is insufficient to describe the heat transfer process. There is still some unmodeled phenomenon occurring. The calculated heat capacity for temperatures greater than 160°F is 182.0 Btu/ft<sup>3</sup>/°F. This large value also leads to rejecting this model because it is several times higher than that for any known substance.

With the information gained from the models proposed this far, we move on to Block 7. of Figure 1.7.1 and propose two additional models. Both Figures 4.2.1 and 4.2.4, the data and the predicted responses versus time for both

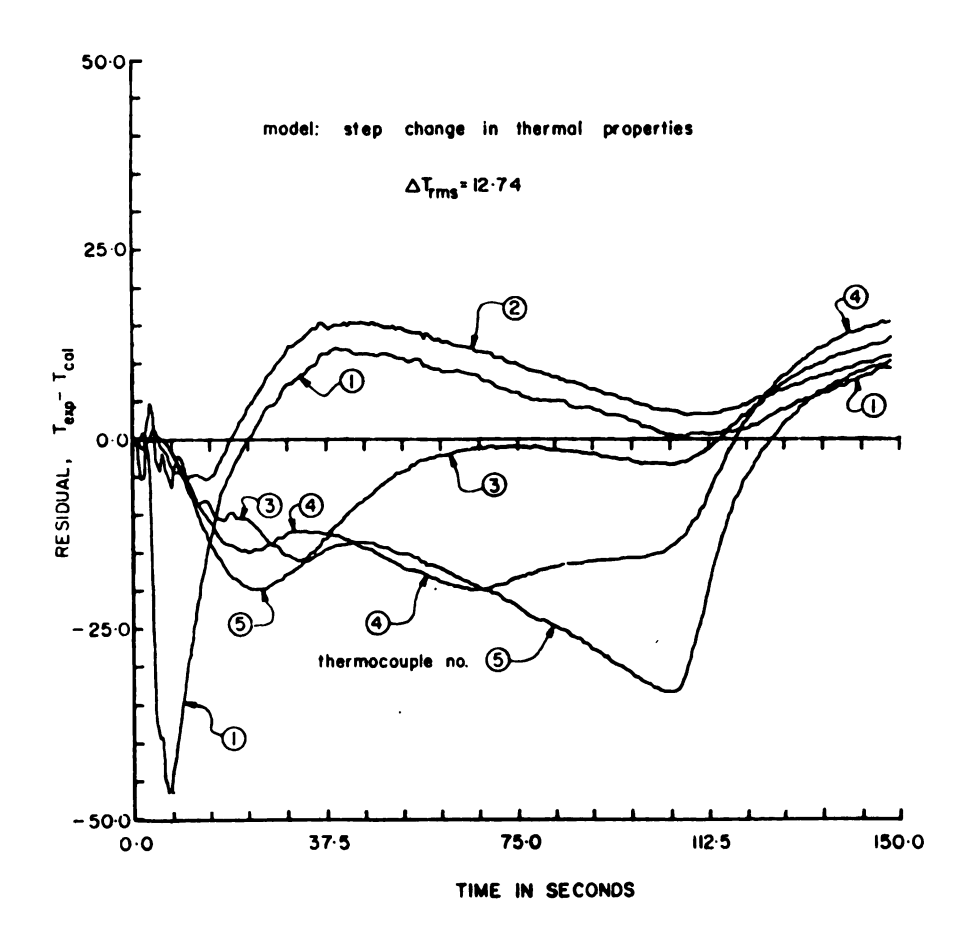


Figure 4.2.5 Residuals for the step change in thermal property model versus time.

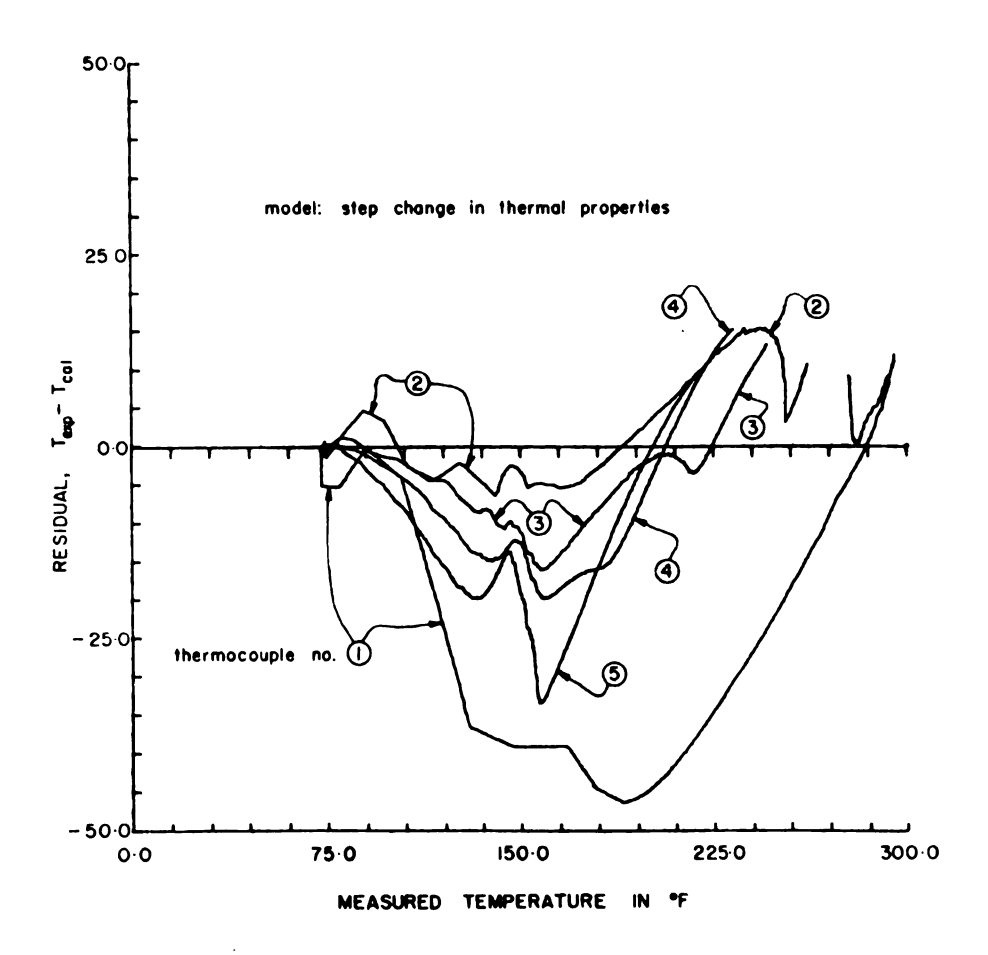


Figure 4.2.6 Residuals for the step change in thermal properties model versus measured temperature.

absorbed and not accounted for by either model. Figure 4.2.6 indicates that the unaccounted for energy is being absorbed in a small temperature range around 160°F. In order to account for this absorbed energy, two different models were proposed; an isothermal change of phase model and a melting over a range of temperature model.

The melting over a range of temperature model was simulated by a triangular pulse in the heat capacity. The solution to temperature variable thermal property problems is discussed in Appendix A. Details of the pulse appear on Figure 4.2.7. The parameters  $k_1$ , the thermal conductivity of the solid, and  $ho c_{pl}$ , the heat capacity of the solid, were evaluated from the solid, non-melting specimen described in Chapter III. The parameters k2, the thermal conductivity of the liquid, and  $\rho c_{p3}$ , the heat capacity of the liquid, were evaluated from a separate experiment using the nylon cup specimen with the sample initially all liquid as described in Chapter III. The experiment performed in Chapter III appears to satisfactorily cover the range of controllable variables so that Block 2. of Figure 1.7.1 can be skipped. The height of the triangular pulse  $\rho_{c_{p2}}$ , the range of melting and the location of the apex of the pulse,  $T_{\mathbf{f}}$ , were calculated from the data shown in Figure 4.2.8. Values for all the parameters obtained are shown on Figure 4.2.8.

The numerical solution of isothermal melting-freezing problems is also discussed in Appendix A. The

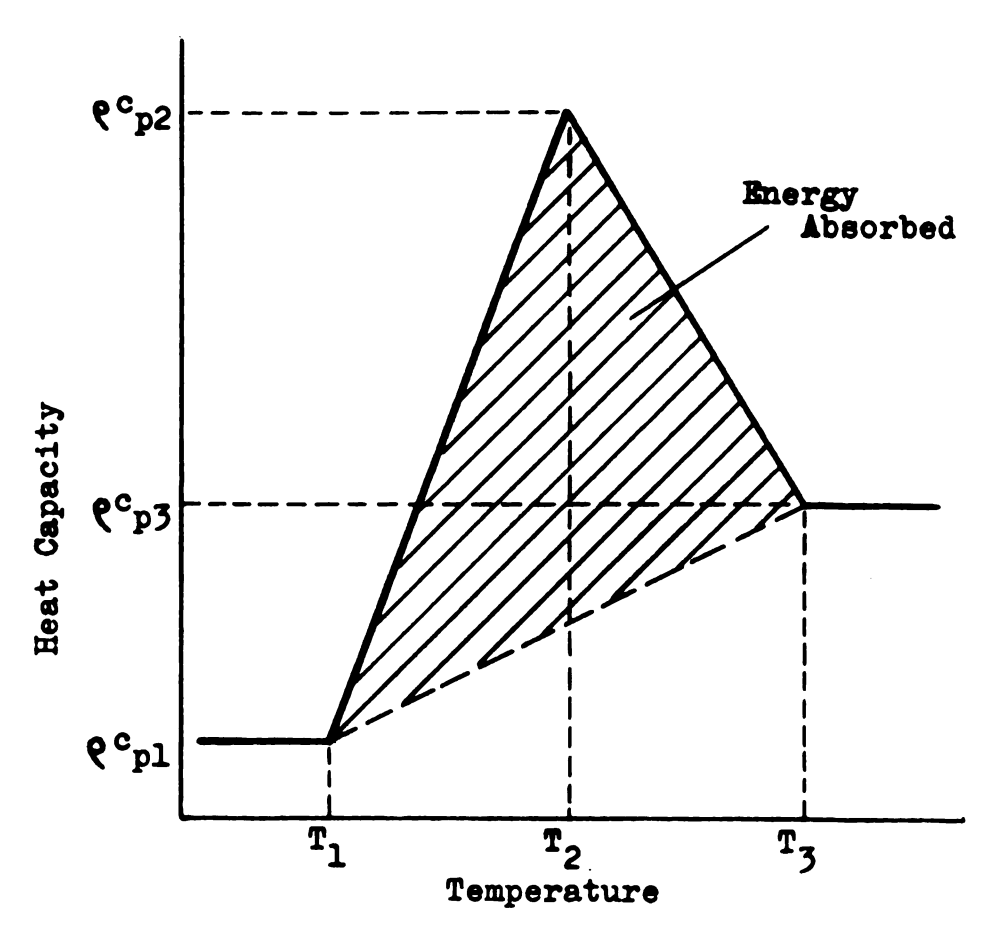
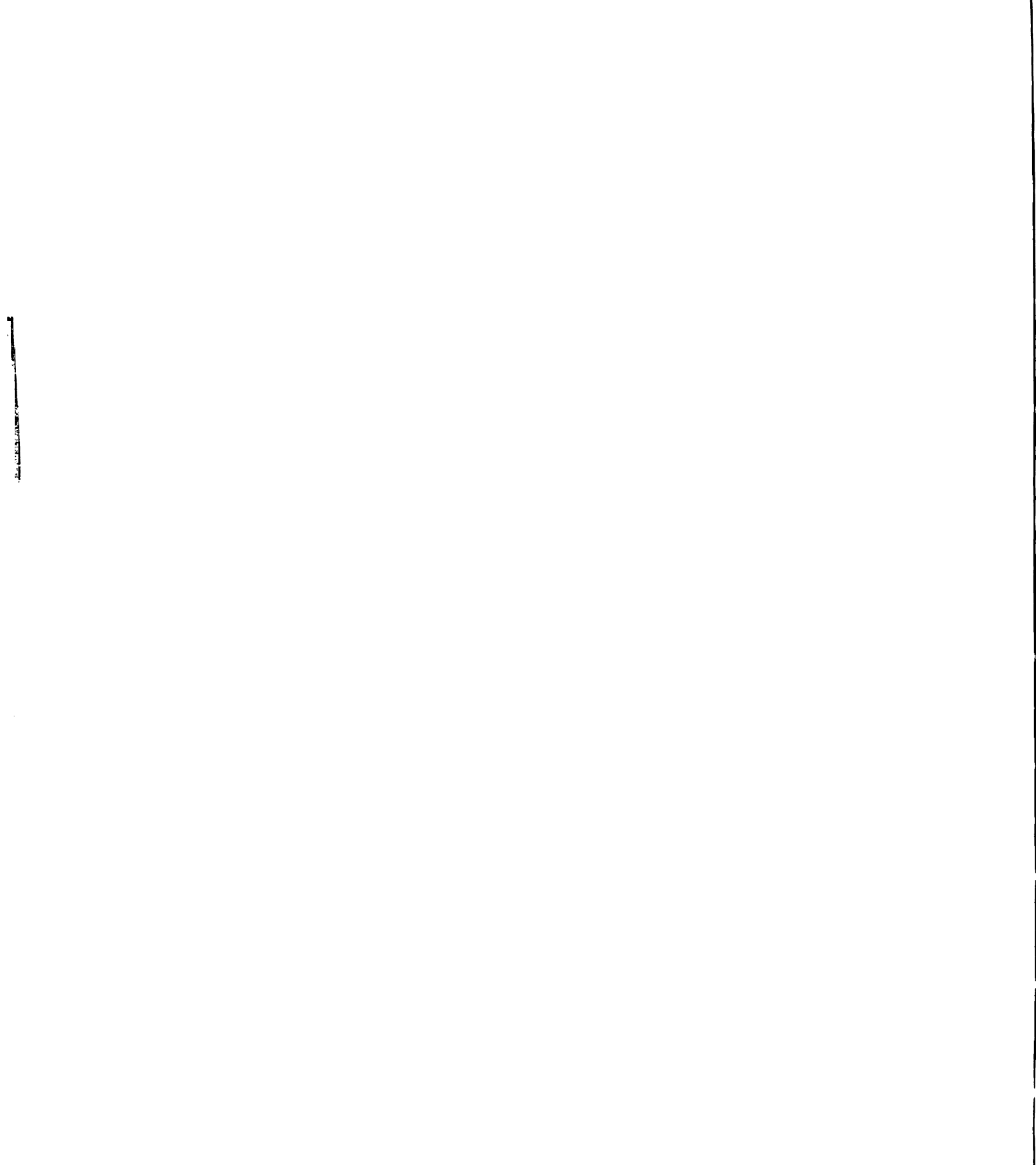


Figure 4.2.7 Energy absorbed by melting over a range of temperature model.



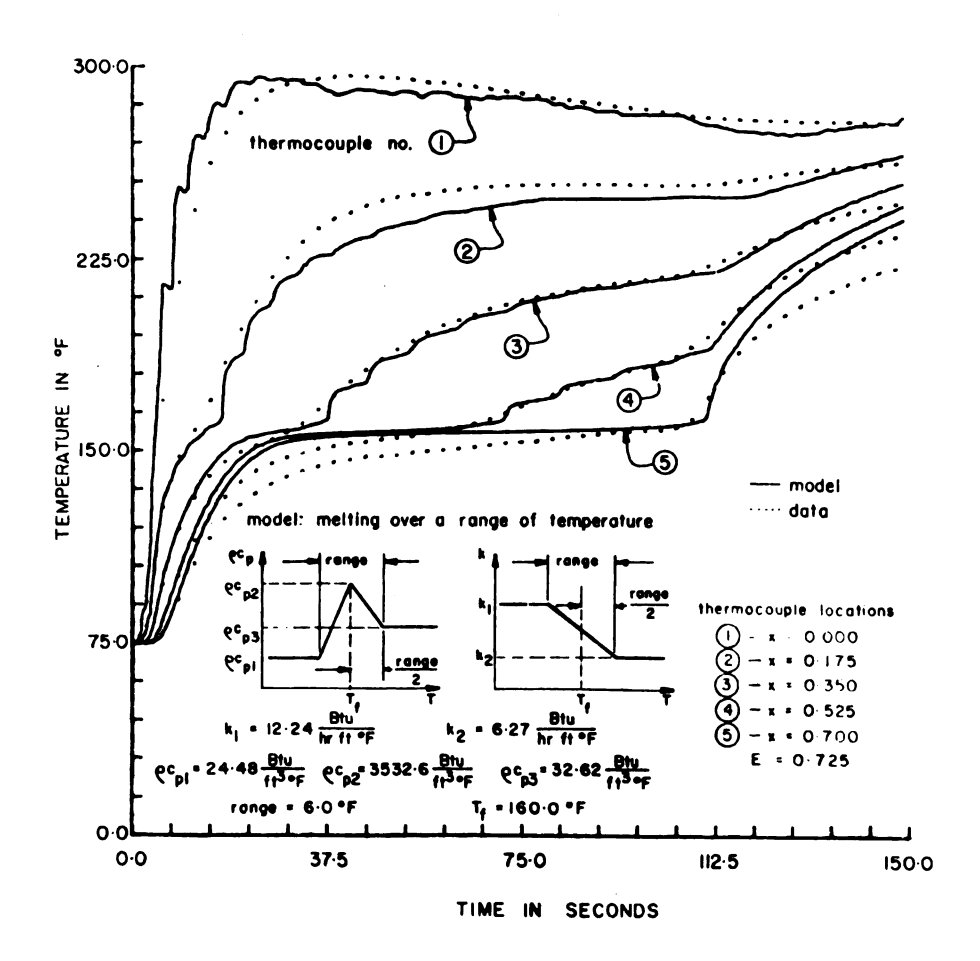


Figure 4.2.8 Melting over a range of temperature model and the data versus time.

parameters  $k_s$  and  $\rho c_{ps}$  were evaluated from the all solid, non-melting specimen. The parameters  $k_L$  and  $\rho c_{pL}$  were evaluated from a separate experiment using the nylon cup specimen initially all liquid as described previously in Chapter III. Optimum experiments for this case are discussed in Chapter II; this satisfies Block 2. of Figure 1.7.1. The parameters  $T_f$  and  $\rho L$  were calculated using the data shown in Figure 4.2.8.

If one calculates the energy absorbed by finding the area under the triangular pulse as shown in Figure 4.2.7., it should be approximately equal to the heat of fusion in the isothermal melting-freezing model. The area under the triangular pulse was calculated to be  $10,683 \, \frac{\text{Btu}}{\text{lbm}}$  and the heat of fusion was estimated from the isothermal melting-freezing model to be  $10,625 \, \frac{\text{Btu}}{\text{lbm}}$ ; thus they agree to within 1%.

Figure 4.2.8 shows the temperature plotted against time. Note that there are oscillations in the calculated temperature; this is due to the sensitivity of the numerical scheme to large changes in the physical properties. The oscillations damp out with time indicating that numerical method remains stable.

Proceed now to Block 5. for the melting over a range of temperature model. The improvment in fit for the thermocouples near the insulated surface is apparent from an inspection of Figure 4.2.9 which shows the residuals versus time for all five thermocouples.

Thermocouple number one which is located at the

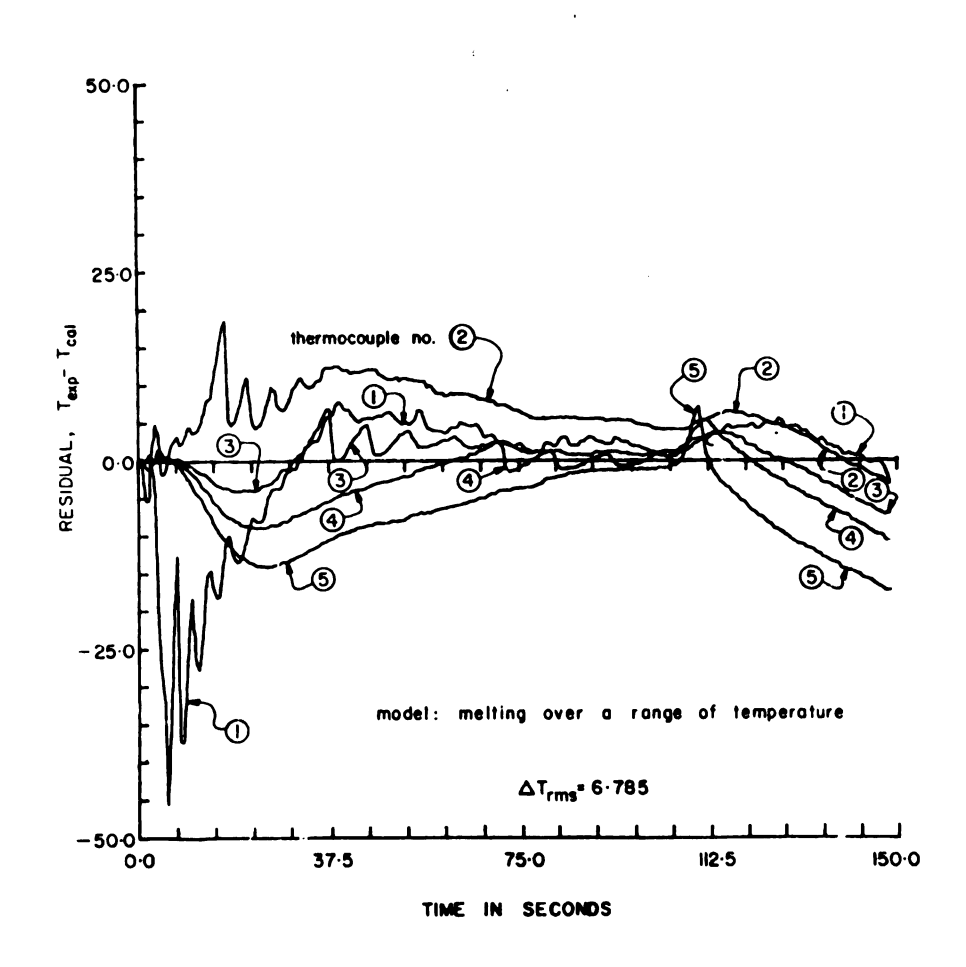


Figure 4.2.9 Residuals for the melting over a range of temperature model versus time.

heated surface has the largest error at the early times. This same residual pattern in thermocouple number 1 was also observed in all previous figures discussed. This pattern has also been noted in many previous experiments conducted at the Michigan State University Thermal Properties Measurement Facility with constant thermal property models. The most probable explanation is non-uniform heat flux across the surface causing three-dimensional effects to influence the measured temperature near this surface. Silicone grease applied carefully and uniformly can help to reduce these effects.

Figure 4.2.10 shows the residuals versus measured temperature. We note that the residuals for thermocouples 3, 4, and 5 show similar characteristics when the material is completely solid, i.e., their sign is negative with a peak in amplitude just before melting begins. After melting these thermocouples exhibit residuals that have the same sign and increasing amplitude. In the melting range we note small spikes in the residuals indicating that the model does not completely describe the complex behavior in the melting range.

For the isothermal melting-freezing model, Figure 4.2.11 shows the data and the model versus time. This model is also a great improvment over the first two. We note that there is no oscillation in this model as in the melting over a range of temperature model. Figures 4.2.12 and 4.2.13 show the residuals versus time and measured temperature for the isothermal melting-freezing model respectively.

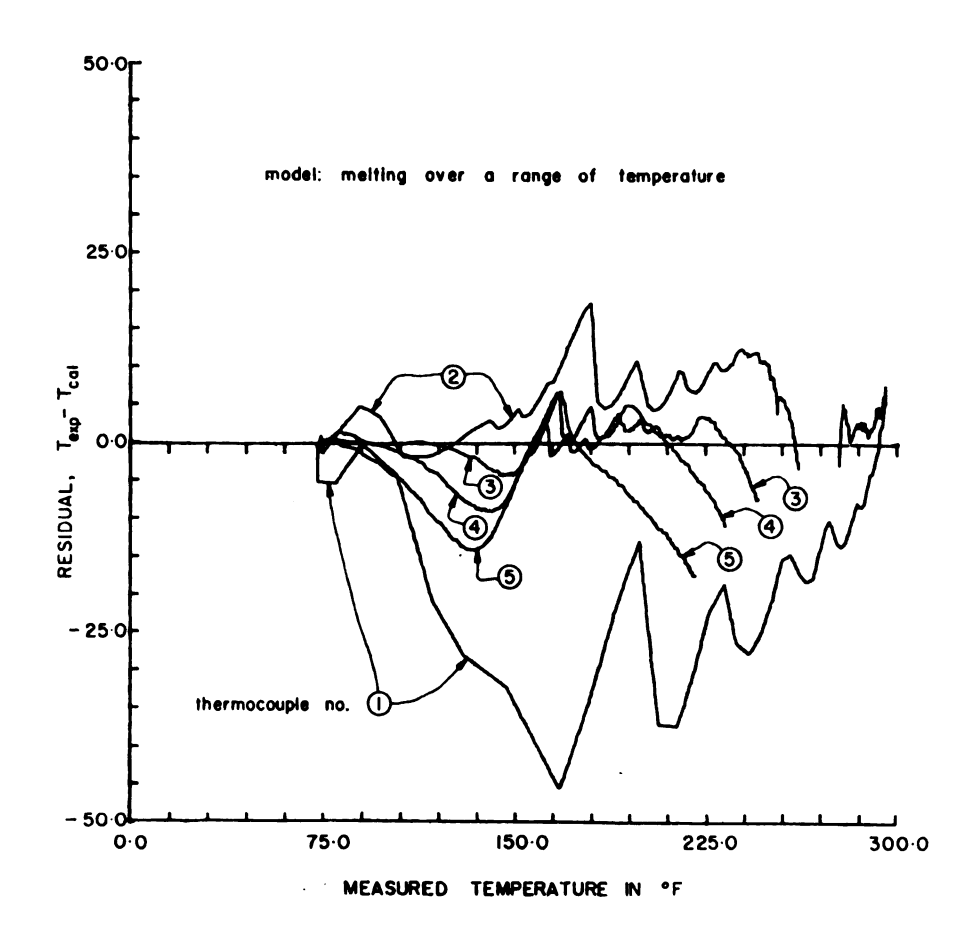


Figure 4.2.10 Residuals for the melting over a range of temperature model versus measured temperature.

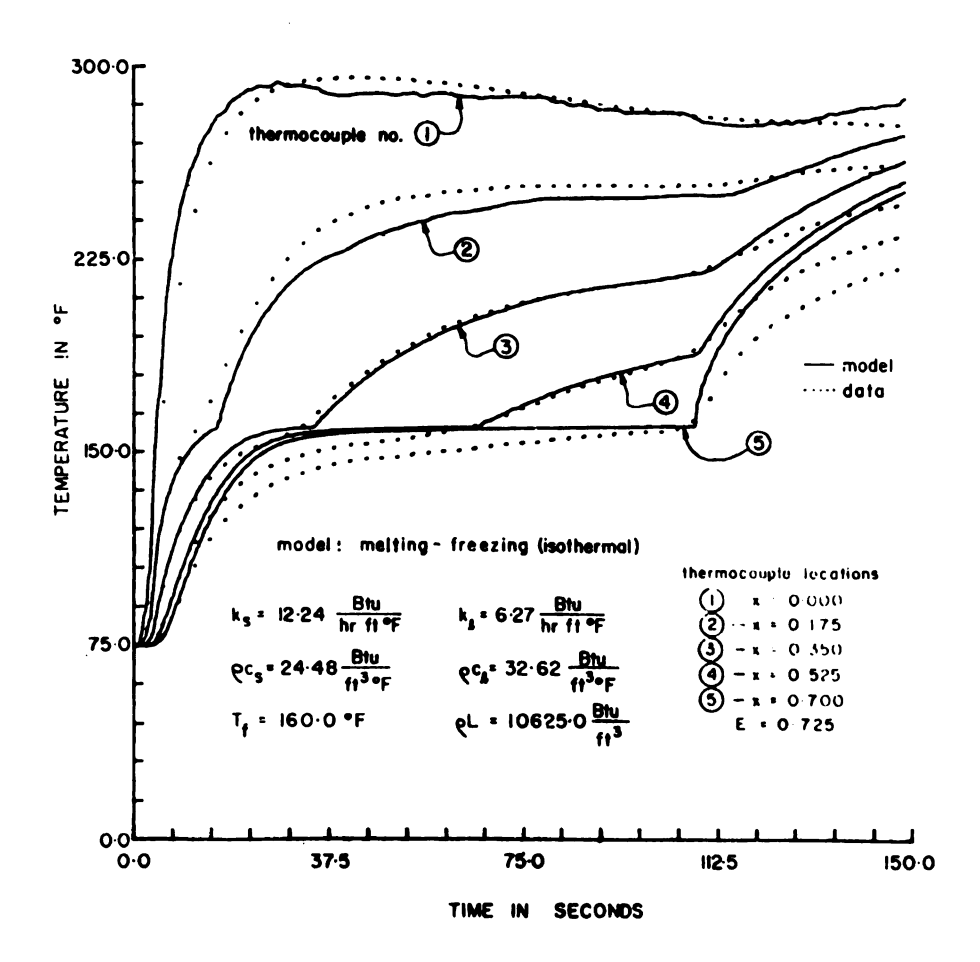


Figure 4.2.11 Isothermal melting-freezing model and the data versus time.

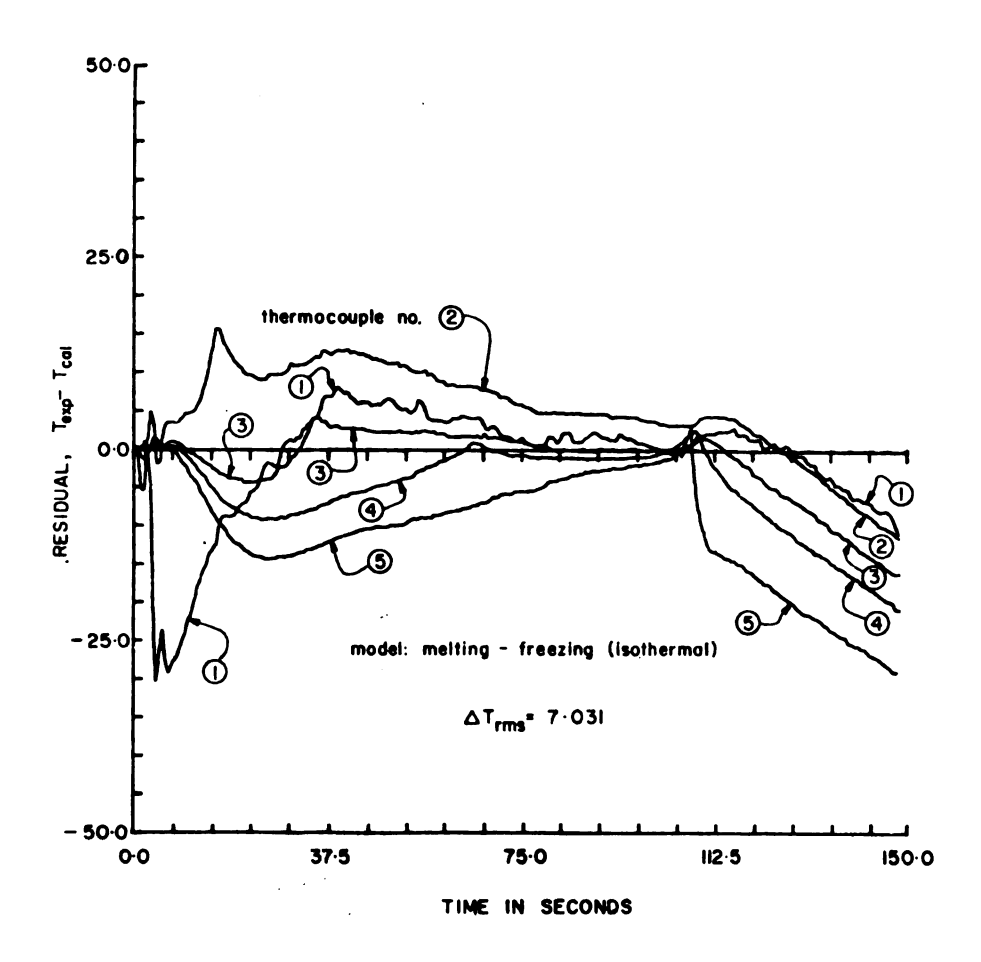


Figure 4.2.12 Residuals for the isothermal melting-freezing model versus time.

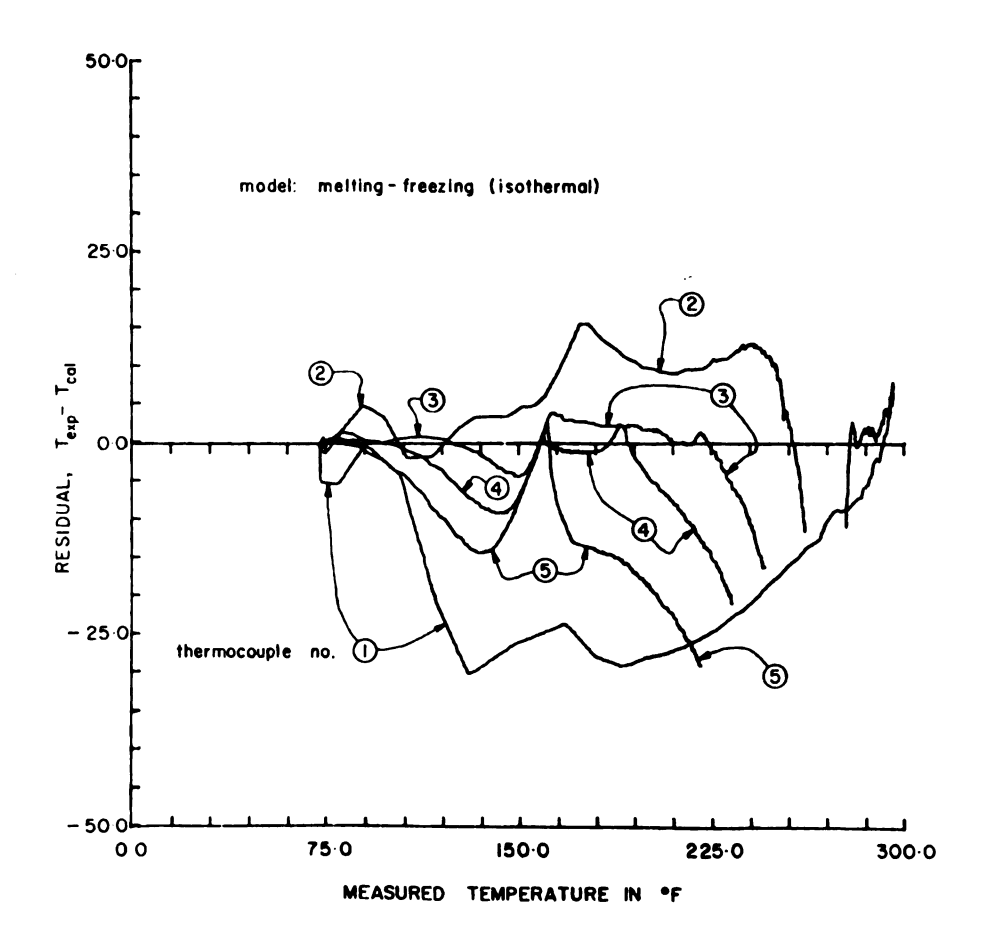


Figure 4.2.13 Residuals for the isothermal melting-freezing model versus measured temperature.

The residuals are very similar in character to those for the melting over a range of temperature model.

Both the melting over a range of temperature and isothermal melting-freezing models appear to be inadequate after the entire body has melted; the residuals for all thermocouples versus time have a negative slope. This indicates that the calculated temperatures rise more rapidly than do the measured temperatures. We can conclude that the heat capacity for the liquid phase used in the models is too small. In fact, our early attempts to estimate the thermal conductivity and heat capacity in the liquid phase and the heat of fusion and fusion temperature simultaneously gave values for the heat capacity of the liquid which seemed erroneously large; for this reason it was decided to estimate the properties of the liquid phase from a separate experiment. It was possible to run only one experiment to evaluate the properties of the liquid phase because the specimen was accidentally overheated and the nylon cup destroyed. cause of the discrepency between the liquid phase properties evaluated from the spearate all liquid experiment and those obtained from the experimental data shown of Figure 4.2.8 is not understood. It was decided to accept the properties calculated from the all liquid experiment because they were closer to published data (36).

We proceed to Block 6. for both models. Examination of Figures 4.2.8 and 4.2.11 shows that both models have the same characteristic shape as the data they are supposed to

represent. That is, both models follow the data reasonably well and are able to absorb energy at nearly a constant temperature as evidenced by the thermocouples near the insulated surface. Since both these models are plausible, we now proceed to the discrimination stage, Block 8. in Figure 1.7.1.

## 4.3 Discrimination between rival mathematical models

To discriminate by the likelihood method described in Chapter I, an estimate of experimental error is needed. One statistically proper way to obtain an estimate of variance is to perform replicate runs. A true replicate run is not just a repeat of the experiment but must be made with completely different specimens and the equipment must also be recalibrated. The experiment is repeated and the differences in the measurements of the two or more replicate runs are then used to estimate the variance. This can be an expensive task but it is usually recommended. Another way to estimate experimental error in temperature measurements is to use an estimate based on previous experience with the experimental equipment. This latter method is the procedure used in this work.

During the course of checking out the experimental equipment, several tests were run to determine the variation in temperature indicated by each of the nine thermocouple-reference junction-data channel combinations. The process Consisted of simply having the computer read the data signal

continuously for an arbitrary length of time while all nine thermocouples were imbedded in an isothermal block of aluminum. Data from these tests showed that the variance between readings on the same data channel was never more than  $0.5^{\circ}F$  and between channels was usually not more than  $5^{\circ}F$ . With this data as a basis,  $5^{\circ}F$  was chosen as an estimate of experimental error.

It should be noted that the test used as a basis for this estimate of experimental error includes only the error introduced by the equipment used to amplify and read the voltage produced by the thermocouples. Errors caused by thermocouple wire variation, inaccurately known thermocouple location, heat losses from the sides and bottom of the specimen, expansion or contraction of the material during melting, and other similar errors are not accounted for in this test. However, these conditions tend to cause biased errors; that is, they tend to be one-sided for a given test. One purpose of replicate runs is to eliminate these biased errors. With a single experiment one has no way to discern these biased errors other than using several thermocouples at each position relative to the heated surface.

For the purpose of comparing likelihood functions we will follow the example set by Reilly (22) and multiply the likelihood functions for each model by an appropriate, common constant to make their magnitudes more tractable.

Table 4.3.1 shows the likelihoods for each model that have been normalized by dividing by the likelihood of the step change in thermal property model. The table of

Table 4.3.1 Comparison of the likelihood functions of the four models.

Model	$\Delta \mathtt{T}_{\mathtt{rms}}$	L(model/data)	L(model 1) L(model 2)	
Constant thermal property	18.70	0.0009	0.0235	
Step change in thermal properties	12.74	0.0389	1.000	
Melting over a range of temperature	6.785	0.3982	10.23	
Isothermal melting- freezing	7.031	0.3721	9.559	

likelihoods shows that the constant thermal property model is an implausible choice as the magnitude of its normalized likelihood is very small. The normalized likelihoods for both the melting over a range of temperature model and the isothermal melting-freezing model show a marked preference for either of these models over the step change in thermal properties model. The normalized likelihoods for the melting over a range of temperature model and the isothermal melting-freezing models show that no discrimination is possible between them, in other words the two models describe the data equally well. This is not an unreasonable conclusion since the isothermal melting-freezing model is really a special case of the melting over a range of temperature model, i.e., the range is zero for the isothermal model. Note that the melting range for the melting over a range of temperature model is only 6°F; the estimate of experimental error was 5°F, thus it is possible that the true melting range could be near zero. For this case both of the two melting-freezing models are capable of describing this complex heat transfer process. Practical considerations lead one to choose the isothermal melting-freezing model because it contains one less parameter and the numerical solution does not oscillate as does the melting over a range of temperature solution.

### CHAPTER V

### CONCLUSIONS

This thesis considers one of the fundamental problems in science - how to build improved mathematical models from observations. This has been given the name of model building and uses concepts of discrimination. A procedure to help an experimenter "build" an adequate mathematical model for cases where there are large amounts of transient data available at relatively low cost has been proposed.

The proposed procedure for model building has been illustrated by finding several rival mathematical models for a complex heat transfer process. The specific heat transfer process chosen to illustrate the procedure was a finite, one-dimensional, solid, melting body. A heat flux boundary condition was applied to one surface of the body while the other surface was insulated. Temperature data was obtained by actual experiment.

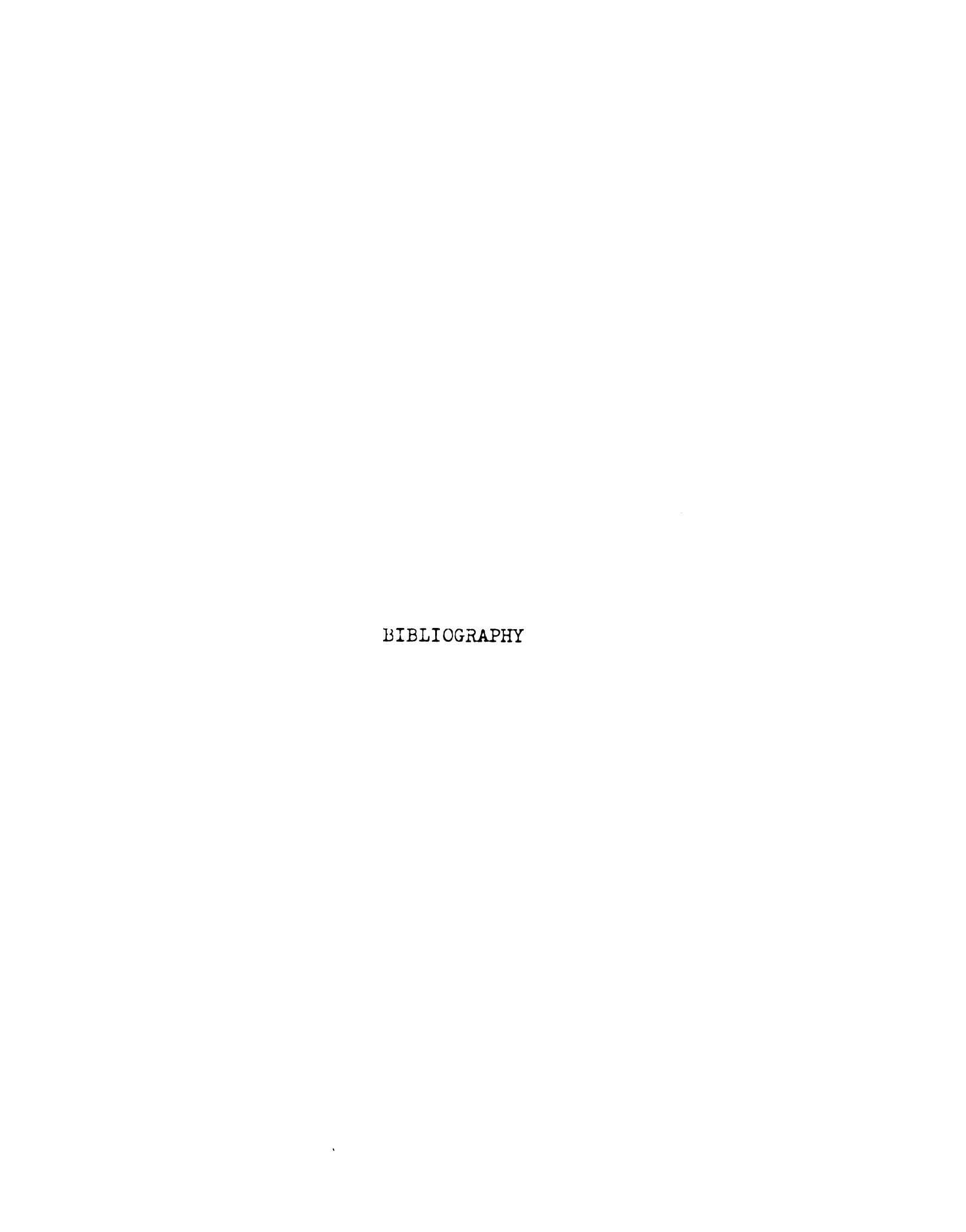
Through the example it was demonstrated that the deficiencies in a mathematical model can be brought to light by examining the model and the residuals. Knowledge of the deficiencies in a model is the information the experimenter needs to propose an improved model.

A method to help an experimenter discriminate between several rival mathematical models has also been incorporated in the model building procedure; it is illustrated using the same experimental data. The discrimination problem is a fundamental and difficult one. Some analytical work has been done on this problem as indicated by the literature review. There is a need, however, of more discrimination studies that attempt to extend and apply the concepts to actual experimental data. This thesis is intended to help satisfy this lack particularly related to heat transfer. It is shown that not all discrimination procedures can be applied to heat transfer problems due to the expense of running each test and the dynamic nature of the tests.

The method proposed for model building including discrimination was successful for the specific case of the melting low temperature alloy. The best mathematical model for this case is the isothermal melting-freezing model. The method presented could be used in other situations to find a mathematical model for a process; that is, under conditions where:

- Large amounts of data can be obtained easily;
   e.g., where there is a transient experiment
   with thermocouples at several positions in the body.
- 2. The optimum conditions for parameter estimation can be found; i.e., the parameters can be estimated.
- 3. A solution to the mathematical model can be found; this may mean that a digital computer is necessary.

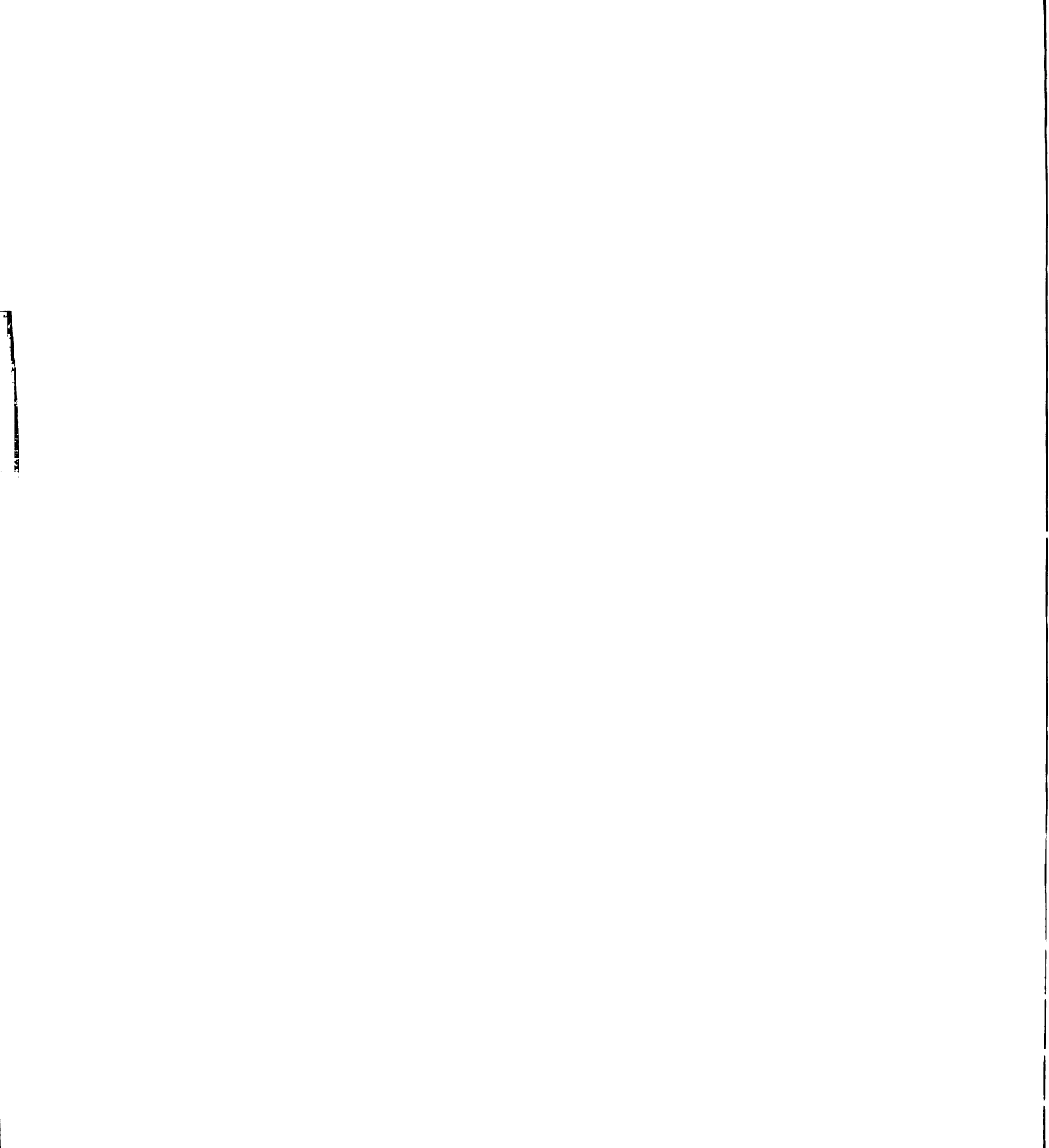
The methods presented must be tempered with practical considerations and common sense. If this rule is observed the methods presented here can be useful tools to the experimenter who is seeking a mathematical model for a process.



### LIST OF REFERENCES

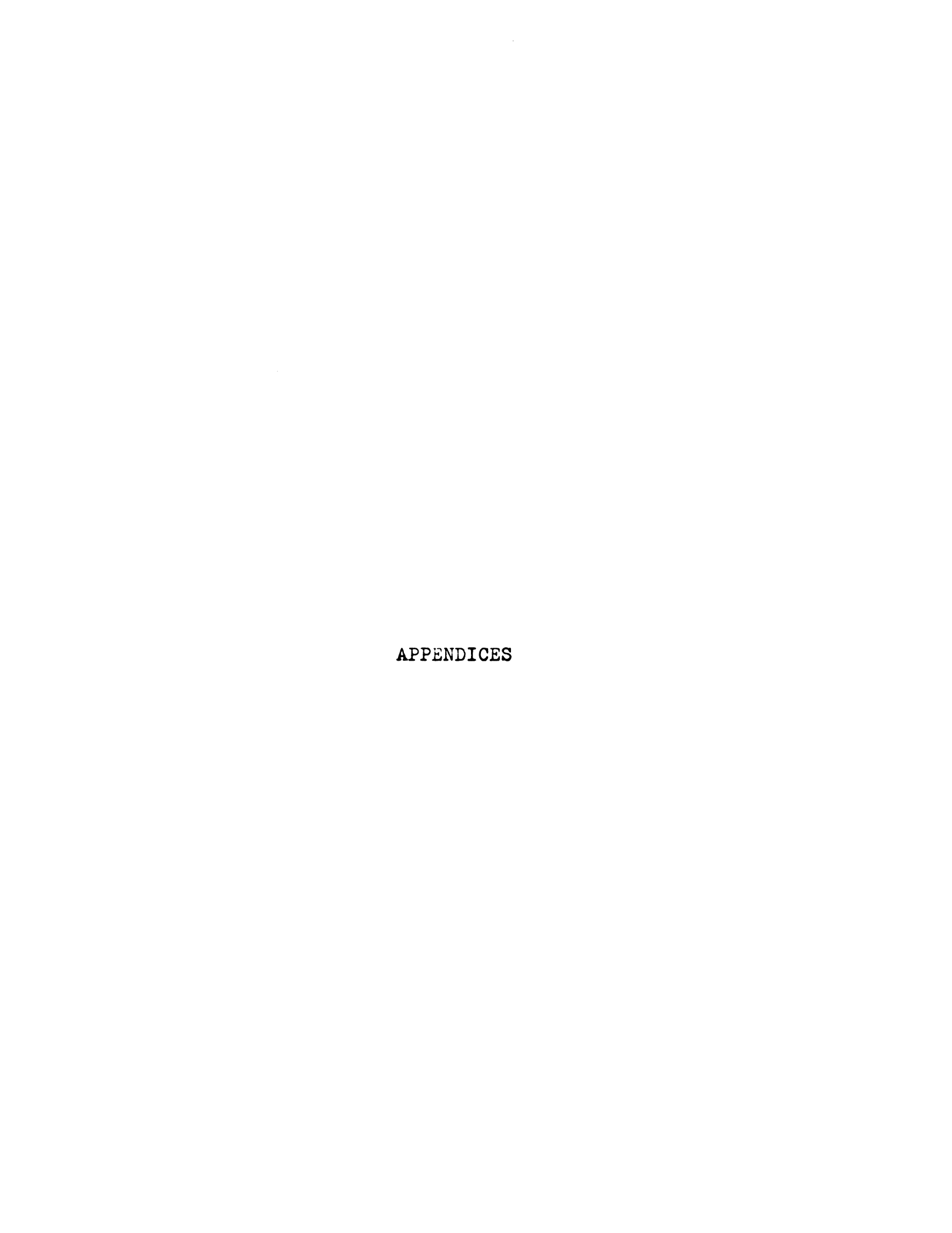
- 1. Box, G.E.P., Hunter, W.G., "An Experimental Study of Physical Mechanisms," <u>Technometrics</u>, VII (1965), 23-42
- 2. Pfahl, R.C., Mitchel, B.J., "Simultaneous Measurement of Six Thermal Properties of a Charring Plastic."
  Int. J. Heat and Mass Transfer, XIII (1969), 275-286
- 3. Box, G.E.P., "Fitting of Empirical Data," Mathematics Research Center, United States Army, The University of Wisconsin, MRC Technical Summary Report #151 (May 1960)
- 4. Box, G.E.P., Coutie, G.A., "Application of Digital Computers in the Exploration of Functional Relationships," Proceedings of the Institution of Electrical Engineers, CIII (1956), 100
- 5. Beck, J.V., "The Optimum Analytical Design of Transient Experiments for Simultaneous Determinations of Thermal Conductivity and Specific Heat," PhD Thesis, Michigan State University (1964)
- 6. Beck, J.V., Dhanak, A.M., "Simultaneous Determinations of Thermal Conductivity and Specific Heat," ASME paper No. 65-HT-14 (1965)
- 7. Pfahl, R.C., "An Experimental and Analytical Investigation of the Internal Mechanisms of Ablative Heat Transfer in Charring Cork," PhD Thesis, Cornell University (1965)
- 8. Pfahl, R.C., "Nonlinear Least Squares: A Method for Simultaneous Thermal Property Determination in Ablating Polymeric Materials," J. of Applied Polymer Science, X (1966)
- 9. Box, G.E.P., Hunter, W.G., "A Useful Method for Model Building," <u>Technometrics</u>, IV (1962), 301-318
- 10. Cochran, W.G., Cox, G.M., Experimental Designs, John Wiley & Sons, Inc. (1950), 122
- 11. Anscombe, F.F., "Examination of Residuals," Proceedings of the Fourth Berkeley Symposium on Mathematical Statistics and Probability, I (1961), 1-37

- 12. Anscombe, F.J., Tukey, J.W., "The Examination and Analysis of Residuals," <u>Technometrics</u>, V (1963), 141-160
- 13. Draper, N., Smith, H., Applied Regression Analysis, John Wiley & Sons, Inc. (1966)
- 14. Hunter, W.G., Reiner, A.M., "Designs for Discrimination Between Two Rival Models," <u>Technometrics</u>, VII (1965). 307-323
- 15. Roth, P.M., "Design of Experiments for Discrimination Among Rival Models," PhD Thesis, Princeton University (1966)
- 16. Box, G.E.P., Hill, W.J., "Discrimination Among Mechanistic Models," <u>Technometrics</u>, IX (1967), 57-71
- 17. Hill, W.J., Hunter, W.G., "A Note on Designs for Model Discrimination: Variance Unknown Case," <u>Technometrics</u>, XI (1969), 396
- 18. Meeter, D., Pirie, W., Blot, W., "A Comparison of Two Model Discrimination Criteria," <u>Technometrics</u>, XII (1970), 457-470
- 19. Chernoff, H., "Sequential Designs of Experiments," Ann. Math. Statistics, XXX (1959), 755-770
- 20. Hill, W.J., Hunter, W.G., Wichern, "A Joint Design Criterion for the Dual Problem of Model Discrimination and Parameter Estimation," <u>Technometrics</u>, X (1968), 145
- 21. Atkinson, A.C., "A Test for Discrimination Between Models," <u>Biometrika</u>, MVI (1969), 337
- 22. Reilly, P.M., "Statistical Methods in Model Discrimination," Third Canadian Symposium on Catalysis, (October (1969)
- 23. Hoel, P.G., "Introduction to Mathematical Statistics," John Wiley & Sons, Inc. (1962), 57
- 24. Beck, J.V., <u>Parameter Estimation in Engineering and and Science</u>, To be published.
- Kmenta, J., Elements of Econometrics, The MacMillan Co., New York, N. Y., (1971).
- 26. Seinfeld, J.H., "Identification of Parameters in Partial Differential Equations," Chemical Engineering Science, XXIV (1969), 65-74



- 27. Carslaw, H.S., Jeager, J.C., <u>Conduction of Heat in Solids</u>, Oxford University Press (1959), 75
- 28. Beck, J.V., "Analytical Determination of High Temperature Thermal Properties Using Plasma. Arcs," Presented to the Eighth Conference on Thermal Conductivity, Purdue University, October 1968
- 29. Box, G.E.P., Lucas, H.L., "Design of Experiments in Nonlinear Situations," <u>Biometrica</u>, MVI (1959), 77
- 30. Stoll, R.R., Linear Algebra and Matrix Theory, McGraw-Hill Book Co., (1959), 89
- 31. Heineken, Tsuchiya, Aris, "On the Accuracy of Determining Rate Constants in Enzimatic Reactions,"

  Mathematical Biosciences, I (1967), 115-141
- 32. Strodtman, C.L., "A Design Optimization Technique Applied to a Squeeze Film, Gas, Journal Bearing," PhD Thesis, Michigan State University, (1968)
- 33. Goodman, T.R., <u>Advances in Heat Transfer</u>, Academic Press, I (1964), 51
- Anon., <u>Instruction Manual for Dana Series 3400 Data Amplifiers</u>, Publication Number DL 370, (1964)
- 35. Beck, J.V., "Nonlinear Estimation Applied to the Nonlinear Inverse Heat Conduction Problem", <u>Int. J. of</u> Heat and Mass Transfer, XIII (1970), 703-716
- 36. Anon., "Cerro Alloy Physical Data and Applications", Cerro Copper and Brass Co., Bellfonte, Pennsylvania
- 37. Smith, G.D., <u>Numerical Solution of Partial Differential Equations</u>, Oxford University Press, (1965), 20
- 38. Murray, W. D., Landis, F., "Numerical and Machine Solutions of Transient Heat-Conduction Problems involving Melting or Freezing", ASME Paper No. 58-HT-16, (1958)
- 39. Heitz, W.L., Westwater, J.W., "An Extension of the Numerical Method for Melting and Freezing Problems", Int. J. of Heat and Mass Transfer, XIII (1970), 1371
- 40. Deutsch, R., <u>Estimation Theory</u>, Prentice-Hall Inc., (1965), 60



#### APPENDIX A

FINITE DIFFERENCE METHOD FOR CALCULATING TEMPERATURE
DISTRIBUTIONS IN ONE-DIMENSIONAL FREEZING-MELTING
AND TEMPERATURE VARIABLE PROPERTY PROBLEMS

### A.1 General finite difference method.

The most flexible method of solving the heat conduction equation for composite bodies with temperature variable properties and general boundary conditions is the method of finite differences. The finite difference equations applying to a general interior node, heat flux boundary condition at x=0 and x=E, and temperature boundary condition at x=0 and x=E are presented.

### A.1.1 General interior node.

An energy balance for node n, shown in Figure A.1, between two dissimilar materials can be written

$$A(n)T_{n-1}^{m+1} + B(n)T_n^{m+1} + C(n)T_{n+1}^{m+1} = D(n)$$
 [A.1.1]

where the coefficients A(n), B(n), and C(n) are defined by

$$A(n) = -\frac{2k_{n-\frac{1}{2}}(1-CNBD)}{(\Delta x_{\perp}^2 + \Delta x_{\perp}\Delta x_{\perp})} \qquad [A.1.1(a)]$$

$$B(n) = \frac{P}{\Delta t} + \frac{2k_{n+\frac{1}{2}}(1-CNBD)}{(\Delta x_{-} \Delta x_{+} + \Delta x_{+}^{2})} + \frac{2k_{n-\frac{1}{2}}(1-CNBD)}{(\Delta x_{-}^{2} + \Delta x_{-} \Delta x_{+})}$$
[A.1.1(b)]

$$C(n) = -\frac{2k_{n+\frac{1}{2}}(1-CNBD)}{(\Delta x_{-} \Delta x_{+} + \Delta x_{+}^{2})}$$
 [A.1.1(c)]

$$D(n) = \left[\frac{2k_{n+\frac{1}{2}}(CNBD)}{(\Delta x_{-} \Delta x_{+} + \Delta x_{+}^{2})}\right] T_{n+1}^{m}$$

$$+ \left[\frac{P}{\Delta t} - \frac{2k_{n+\frac{1}{2}}(CNBD)}{(\Delta x_{-} \Delta x_{+} + \Delta x_{+}^{2})} - \frac{2k_{n-\frac{1}{2}}(CNBD)}{(\Delta x_{-}^{2} + \Delta x_{-} \Delta x_{+})}\right] T_{n}^{m}$$

$$+ \left[\frac{2k_{n-\frac{1}{2}}(CNBD)}{(\Delta x_{-}^{2} + \Delta x_{-} \Delta x_{+})}\right] T_{n-1}^{m} \qquad [A.1.1(d)]$$

 $T_n^m$  is the temperature of node n at time  $t_m$ ,  $k_{n+\frac{1}{2}}$  is the thermal conductivity evaluated between nodes n and n+1,  $\Delta x_+$  and  $\Delta x_-$  are defined on Figure A.1. CNBD is a finite difference parameter that may take on values between zero a and one. If CNBD is set equal to one, the explicit forward difference method results; CNBD being set equal to zero results in the implicit backward difference method. If CNBD is set equal to  $\frac{1}{2}$  the Crank-Nicolson implicit method is obtained. P is the average heat capacity of node n and is given by

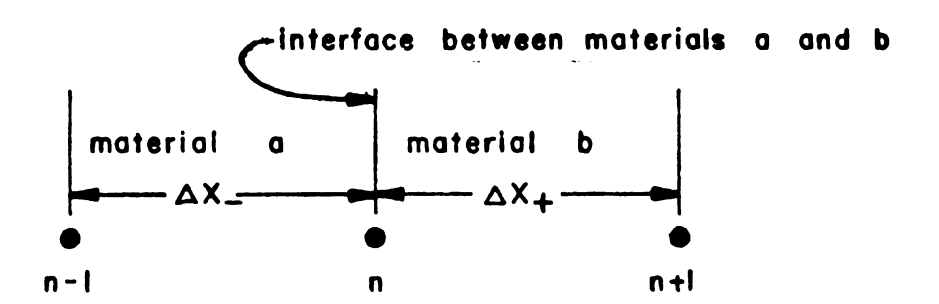


Figure A.1 Node geometry and nomenclature for the finite difference solution to the heat conduction equation at the interface between dissimilar materials.

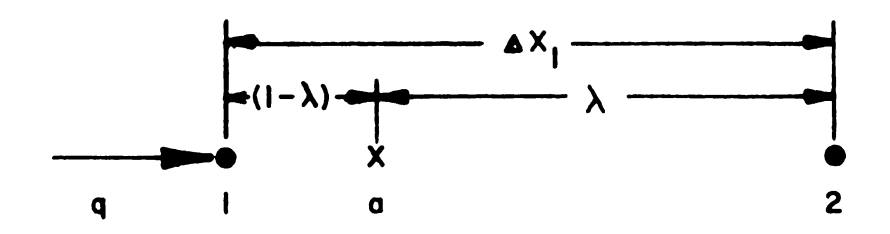


Figure A.2 Node geometry and nomenclature for the finite difference solution to the heat conduction equation at the heated surface with a known heat flux.

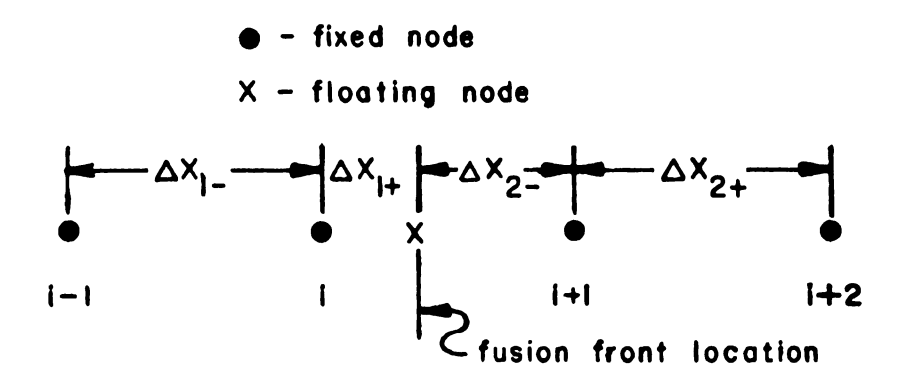


Figure A.3 Node geometry and nomenclature for the floating node used in the finite difference solution of the freezing-melting problem.

$$P = \frac{\Delta x_{-}(\rho c_{p})_{-} + \Delta x_{+}(\rho c_{p})_{+}}{\Delta x_{-} + \Delta x_{+}} \qquad [A.1.1(e)]$$

 $(\rho c_p)_-$  and  $(\rho c_p)_+$  are the heat capacities corresponding to materials a and b in Figure A.l respectively.  $\Delta t$  is the time step i.e., the difference between times  $t_m$  and  $t_{m+1}$ .

If node n is not between two different materials then P simply becomes  $(\rho_c)_n$ , the heat capacity of node n. If the node spacing to the right and left of node n is equal then  $\Delta x_- = \Delta x_+$ . Thus this single equation applies to any interior node, that is, any node not on a boundary.

# A.1.2 Heat flux boundary condition at x=0.

An approximation used by Beck<sup>(5)</sup> to improve the accuracy of finite difference calculations involving heat flux boundary conditions will be presented here. The method will be referred to as the quarter point method.

Referring to Figure A.2, the temperature at point a can be approximated as

$$T_a^m = \lambda T_1^m + (1 - \lambda) T_2^m \qquad [A.1.2]$$

The temperature at point a will be used in the approximation for the time derivative instead of the temperature at point 1. An energy balance on node 1 then gives

$$B(1)T_1^{m+1} + C(1)T_2^{m+1} = D(1)$$
 [A.1.3]

The coefficients B(1), C(1), and D(1) are defined by

$$B(1) = 2 \frac{(1-CNBD)k_{1+\frac{1}{2}}}{\Delta x_{1}^{2}} + \frac{\lambda(\rho c_{p})_{1}}{\Delta^{t}} \qquad [A.1.3(a)]$$

$$C(1) = \frac{(1-\lambda)(\rho c_p)_2}{\Delta t} - 2 \frac{(1-CNBD)k_{1+\frac{1}{2}}}{\Delta x_1^2} [A.1.3(b)]$$

$$D(1) = \left[\frac{\lambda(\rho c_p)_1}{\Delta t} - 2 \frac{(CNBD)k_{1+\frac{1}{2}}}{\Delta x_1^2}\right] T_1^m$$

$$+ \left[\frac{(1-\lambda)(\rho c_p)_2}{\Delta t} + \frac{2(CNBD)k_{1+\frac{1}{2}}}{\Delta x_1^2}\right] T_1^m$$

$$+ \frac{2(1-CNBD)q^{m+1}}{\Delta x_1} + \frac{2(CNBD)q^m}{\Delta x_1} \qquad [A.1.3(c)]$$

 $\Delta x_1$  is the distance between node 1 and node 2,  $k_{1+\frac{1}{2}}$  is the thermal conductivity evaluated between nodes 1 and 2, and  $q^m$  and  $q^{m+1}$  are the heat fluxes at times  $t_m$  and  $t_{m+1}$  respectively. The parameter  $\lambda$  was found by experiment to have a best value of 0.75, thus the term "quarter point method". If q is set to zero, the heat flux boundary condition becomes an insulation boundary condition at x=0.

## A.1.3 Heat flux boundary condition at x=E.

The quarter point method is also used at x=E. The resulting equation for node N at x=E is

$$A(N)T_{N-1}^{m+1} + B(N)T_N^{m+1} = D(N)$$
 [A.1.4]

The coefficients A(N), B(N), and D(N) are defined by

$$A(N) = \frac{(1-\lambda)(\rho c_p)_N}{\Delta t} - \frac{2(1-CNBD)k_{N-\frac{1}{2}}}{\Delta x_N^2}$$
 [A.1.4(a)]

$$B(N) = \frac{\lambda(\rho c_p)_N}{\Delta t} + \frac{2(1-CNBD)k_{N-\frac{1}{2}}}{\Delta x_N^2} \qquad [A.1.4(b)]$$

$$D(N) = \left[\frac{\lambda(\rho c_p)_N}{\Delta t} - \frac{2(CNBD)k_{N-\frac{1}{2}}}{\Delta x_N^2}\right] T_N^m$$

$$+ \left[\frac{(1-\lambda)(\rho c_p)_{N-1}}{\Delta t} + \frac{2(CNBD)k_{N-\frac{1}{2}}}{\Delta x_N^2}\right] T_{N-1}^m$$

$$- \frac{2q^{m+1}(1-CNBD)}{\Delta x_N} - \frac{2q^m(CNBD)}{\Delta x_N} \qquad [A.1.4(c)]$$

 $\lambda$  is again 0.75 and if q=0, we have an insulated boundary at x=E.

# A.1.4 Temperature boundary condition.

For the case in which the boundary temperature is a known function of time we need not write an energy balance for nodes 1 or N, since the new temperature at node 1 or node N is simply equated to the known function.

$$T_1^{m+1} = D(1) \qquad \qquad \left[A.1.5(a)\right]$$

or

$$T_{N}^{m+1} = D(N) \qquad [A.1.5(b)]$$

where D(1) and D(N) are the known functions evaluated at time  $\mathbf{t}_{m+1}$ .

A.1.5 Solution of the finite difference equations.

The result of the energy balances at all N nodes can be written in matrix notation as follows:

$$\begin{bmatrix} B(1) & C(1) & 0 & 0 & \cdots & 0 \\ A(2) & B(2) & C(2) & 0 & \cdots & 0 \\ 0 & A(3) & B(3) & C(3) & \cdots & 0 \\ \vdots & \vdots & \vdots & \vdots & \vdots \\ 0 & \cdots & A(N-1) & B(N-1) & C(N-1) \\ 0 & \cdots & A(N) & B(N) \end{bmatrix} \begin{bmatrix} T_1^{m+1} \\ T_2^{m+1} \\ T_N^{m+1} \\ T_N^{m+1} \end{bmatrix} = \begin{bmatrix} D(1) \\ D(2) \\ D(3) \\ D(N-1) \\ D(N) \end{bmatrix}$$

$$\begin{bmatrix} A.1.6(a) \end{bmatrix}$$

or in short form

$$\underline{\underline{E}} \ \underline{\underline{T}}^{m+1} = \underline{\underline{D}} \qquad \qquad \left[ A.1.6(b) \right]$$

The solution for the temperature distribution at time  $t_{m+1}$  is very efficiently obtained by Guass's elimination method. For a discussion of this method see Smith<sup>(37)</sup>.

- A.2 The solution of freezing-melting problems.
  - A.2.1 Mathematical statement of the problem.

The temperature distribution in a substance that melts or freezes isothermally such as a eutectic alloy or water can be described mathematically by (27).

$$\rho_{\text{ps}} = \frac{\partial_{\text{ps}}}{\partial t} = \frac{\partial_{\text{x}}}{\partial x} \left( k_{\text{s}} \frac{\partial_{\text{x}}}{\partial x} \right) \qquad [A.2.1]$$

in the solid region, and by

$$\rho_{c_{p_{\ell}}} = \frac{\partial_{x}}{\partial t} = \frac{\partial_{x}}{\partial x} \left( k_{\ell} \frac{\partial_{x}}{\partial x} \right) \qquad [A.2.2]$$

in the liquid region if natural convection can be neglected. At the interface between solid and liquid

$$T_g(\epsilon,t) = T_g(\epsilon,t) = T_f$$
 [A.2.3]

where  $\epsilon$  is the position of the interface and  $T_f$  is the fusion temperature. An energy balance at the interface between solid and liquid yields t

$$\frac{d\epsilon}{dt} = \frac{1}{\rho L} \left[ k_s \frac{\partial T_s}{\partial x} \middle|_{x=\epsilon_-} - k_{\parallel} \frac{\partial T}{\partial x} \middle|_{x=\epsilon_+} \right] \quad [A.2.4]$$

where  $\frac{d\mathcal{E}}{dt}$  is the velocity of the interface and  $\rho L$  is the heat of fusion. Equation [A.2.4] couples equations [A.2.1] and [A.2.2] in a highly nonlinear manner.

<sup>1.</sup> This equation is written for a freezing problem; the interface is moving in the positive x-direction with solid to the left of x=€ and liquid to the right of x=€. Melting can be treated by interchanging the subscripts s and A.

A.2.2 Numerical solution of freezing-melting problems.

The first method of Murray and Landis.

Murray and Landis (38) presented two methods that have general practical application for finite difference solutions of freezing-melting problems. In the first method, the body to the left of the solid-liquid interface is divided into r lumps or nodes. The body to the right of the solid-liquid interface is divided into N-r nodes. The number of nodes in liquid and solid remains fixed and as the interface moves to the right the r nodes to the left on the interface are stretched while the N-r nodes to the right are compressed. The temperature history of these traveling nodes is determined by using the substantial derivative.

$$\frac{dT}{dt} = \frac{\partial T}{\partial x} \frac{dx}{dt} + \frac{\partial T}{\partial t} \qquad [A.2.5]$$

where  $\frac{d\mathbf{x}}{dt}$  is determined from the fusion front velocity  $\frac{d\mathbf{E}}{dt}$ . If equation [A.2.5] is substituted into equations [A.2.1] and [A.2.2] with constant properties in both solid and liquid and  $\frac{d\mathbf{x}}{dt}$  determined from the relationship for equally spaced nodes,

$$\frac{d\mathbf{x}}{d\mathbf{t}} = \frac{\mathbf{x}}{\mathbf{\epsilon}} \frac{d\mathbf{\epsilon}}{d\mathbf{t}} , \qquad [A.2.6]$$

we obtain the substantial derivative representing the rate of change of temperature at any point in the body

$$\frac{dT_s}{dt} = \frac{x_s}{\epsilon} \frac{\partial T_s}{\partial x} \frac{d\epsilon}{dt} + \alpha_s \frac{\partial^2 T_s}{\partial x^2} \qquad [A.2.7]$$

in the solid, and

$$\frac{dT_{\ell}}{dt} = \frac{E-x}{E-\epsilon} \frac{\partial T_{\ell}}{\partial x} + C_{\ell} \frac{\partial^{2}T_{\ell}}{\partial x^{2}} \qquad [A.2.8]$$

in the liquid.  $a_s$  and  $a_s$  are the thermal diffusivity of solid and liquid respectively. E is the length of the finite body. In a forward finite difference form equations [A.2.7] and [A.2.8] become

$$\frac{\mathbf{T}_{\mathbf{n}}^{\mathbf{m}+\mathbf{l}} - \mathbf{T}_{\mathbf{n}}^{\mathbf{m}}}{\Delta \mathbf{t}} = \frac{\mathbf{n} \Delta \mathbf{x}_{\mathbf{s}}}{\epsilon_{\mathbf{m}}} \frac{\mathbf{T}_{\mathbf{n}+\mathbf{l}}^{\mathbf{m}} - \mathbf{T}_{\mathbf{n}-\mathbf{l}}^{\mathbf{m}}}{2 \Delta \mathbf{x}_{\mathbf{s}}} \frac{\Delta \epsilon}{\Delta \mathbf{t}} + \alpha_{\mathbf{s}} \frac{\mathbf{T}_{\mathbf{n}-\mathbf{l}}^{\mathbf{m}} - 2\mathbf{T}_{\mathbf{n}}^{\mathbf{m}} + \mathbf{T}_{\mathbf{n}+\mathbf{l}}^{\mathbf{m}}}{\Delta \mathbf{x}_{\mathbf{s}}^{2}}$$

$$\mathbf{n}=1,2,3,\ldots,\mathbf{r}-\mathbf{l}$$

$$[\mathbf{A}.2.9]$$

in the solid, and

$$\frac{T_{n}^{m+1}-T_{n}^{m}}{\triangle t} = \frac{(N-n)\triangle x_{\ell}}{E-\epsilon_{m}} \frac{T_{n+1}^{m}-T_{n-1}^{m}}{2\triangle x_{\ell}} \frac{\triangle \epsilon}{\triangle t} + \alpha_{\ell} \frac{T_{n-1}^{m}-2T_{n}^{m}+T_{n+1}^{m}}{\triangle x_{\ell}^{2}}$$

$$= n=r+1, r+2, ..., N-1.$$
[A.2.10]

in the liquid. The numerical approximation to equation [A.2.4] used by Murray and Landis is

$$\frac{\Delta \epsilon}{\Delta t} \Big|^{m} \simeq \frac{\epsilon_{m+1} - \epsilon_{m}}{\Delta t} = \frac{1}{\rho L} \left[ k_{s} \frac{T_{r-s}^{m} - 4T_{r-1}^{m}}{2\Delta x_{s}} - k_{s} \frac{T_{r+2}^{m} - 4T_{r+1}^{m}}{2\Delta x_{s}} \right]$$
[A.2.11]

where

$$\Delta x_8 = \frac{\epsilon}{r}$$
 and  $\Delta x_2 = \frac{E-\epsilon}{n-r}$  [A.2.12]

Nodes O and N can be treated in a similar manner by applying

whatever boundary conditions are needed. Since this is a forward difference method, the time step must be governed by the choice of node spacing to insure stability. When  $\epsilon$  =0, equation [A.2.9] does not apply and the problem must be started by assuming a value for  $\epsilon = \epsilon_0$ . A starting temperature distribution must also be assumed for points to the left of  $x = \epsilon_0$ . This procedure introduces a considerable starting error if  $\epsilon_{o}$  and the temperature distribution are not chosen carefully. If  $\epsilon_0$  is chosen too small,  $\Delta x_s$ the node spacing to the left of  $\epsilon_0$  becomes very small as seen from equations [A.2.12]. Stability requirements dictate that  $\Delta t$  be correspondingly small and thus the computer solution time goes up substantially. The solution must be stopped before € =E for the same reason and the results extrapolated to find the remainder of the solution. Heitz and Westwater modification

Heitz and Westwater  $^{(39)}$ , in a study of freezing water, used this method but proposed a method of obtaining reasonable starting values. They assume that the body was initially semi-infinite and at the fusion temperature,  $T_f$ , and the boundary condition was a step change in surface temperature. The heat removed from the body in time  $t_o$  is then

$$\int_{0}^{t_{0}} Qdt = 2k_{R} \left[T_{f} - T(0, t_{0})\right] \left[\frac{t_{0}}{\pi \alpha_{R}}\right]^{\frac{1}{2}}$$
[A.2.13]

This heat removal results in subcooling the liquid. They assumed that all the heat of subcooling was instantaneously converted to latent heat of fusion resulting in a solid thickness  $\epsilon_0$  at time  $t_0$  given by

$$\epsilon_{o} = \frac{2k_{R}}{\rho} \left[ T_{f} - T(0, t_{o}) \right] \left[ \frac{t_{o}}{\pi \alpha_{R}} \right]^{\frac{1}{2}}$$
[A.2.14]

They then assumed a linear temperature distribution in the solid to begin calculation by the Murray-Landis method. Heitz and Westwater state that it is only necessary to obtain reasonable estimates of the starting values because to is a very small fraction of the total elapsed time. Pfhal and Mitchel modification

In a study of ablating materials, Pfhal and Mitchel (2) used a modified Murray-Landis method. They applied a non-linear transformation to the grid in both the virgin and char materials. This transformation allowed them to have more nodes near the virgin-char interface where more accurate temperatures are required to predict the motion of the interface. They also used an implicit method similar to that in secion A.l. The implicit method allowed the stability restriction on the time step to be relaxed. Pfhal and Mitchell did not give a comparison of their results with those of uniform grid spacing so no conclusion as to the merit of this procedure is available.

This first proposal of Murray and Landis can treat temperature variable properties and any boundary condition.

It may be quite difficult; however, to

apply the method to composite bodies. Despite its disadvantages this method seem to be widely used and gives good results once the starting error has damped out.

## Murray and Landis second method

The second method proposed by Murray and Landis utilizes a fixed space network. At some time the fusion front,  $\epsilon$ , will be in the i<sup>th</sup> lump or node. For all node points except 0, i, and N the finite difference form of equations [A.2.1] and [A.2.2] for constant properties apply. That is

$$\frac{T_{n}^{m+1}-T_{n}^{m}}{\Delta^{t}}=\alpha_{s}\frac{T_{n-1}^{m}-2T_{n}^{m}+T_{n+1}^{m}}{\Delta^{x}}$$
 [A.2.15]

for  $n = 1, 2, \ldots, i-1$  in the solid, and

$$\frac{T_{n}^{m+1}-T_{n}^{m}}{\Delta t}=\alpha_{1}\frac{T_{n-1}^{m}-2T_{n}^{m}+T_{n+1}^{m}}{\Delta x^{2}}$$
 [A.2.16]

for n = i+1, i+2, ..., N-1 in the liquid. Equations [A.2.15] and [A.2.16] are equivalent to [A.1.1] with CNBD = 1.0. For nodes 0 and N one of the boundary equations in section A.1 with CNBD = 1.0 will apply. In node i a discontinuity in the temperature distribution occurs at  $x=\epsilon$ . Two temperatures are calculated for node i, one by interpolation from temperatures in the solid region and one by interpolation from temperatures in the liquid region. In each case the location of the fusion front,  $\epsilon$ , and the fusion temperature,  $T_f$ , are used in the interpolation procedure. The temperature obtained by interpolation from the left of

 $\epsilon$  is used in the finite difference equation for node i-land the temperature obtained by interpolation from the right of  $\epsilon$  is used in the equation for node i+l. The space derivatives in equation [A.2.4] were approximated by Murray and Landis as

$$\frac{\partial T_{\mathbf{s}}}{\partial \mathbf{x}}\Big|_{\mathbf{x}=\boldsymbol{\epsilon}_{-}} \frac{T_{\mathbf{1}\mathbf{s}}^{\mathbf{m}} - T_{\mathbf{1}-2}^{\mathbf{m}}}{2\Delta \mathbf{x}} + (\Delta \mathbf{x} + \delta \mathbf{x}) \frac{T_{\mathbf{1}-2}^{\mathbf{m}} - 2T_{\mathbf{1}-1}^{\mathbf{m}} + T_{\mathbf{1}\mathbf{s}}}{\Delta \mathbf{x}^{2}}$$

$$[\mathbf{A}.2.17]$$

in the solid, and

$$\frac{\partial^{T} \ell}{\partial x}\Big|_{x=\epsilon_{+}} \frac{T_{i+2}^{m} - T_{i}^{m}}{2\Delta x} - (\Delta x - \delta x) \frac{T_{i}^{m} - 2T_{i+1}^{m} + T_{i+2}^{m}}{\Delta x^{2}}$$
[A.2.18]

in the liquid.  $T_{is}^m$  is the temperature determined by interpolation from the solid at time  $t_m$ ,  $T_{i,\ell}^m$  is the temperature determined by interpolation from the liquid at time  $t_m$ , and  $\delta x$  is the distance of the fusion front from node i (note that  $-\frac{\Delta x}{2} \leq \delta x \leq \frac{\Delta x}{2}$ ). When these approximations are substituted into equation [A.2.4] the position of the fusion front at time  $t+\Delta t$  may be determined by integration. When i=0, 1, N-1, or N a lower order approximation for the space derivatives must be substituted for equations [A.2.17] and [A.2.18].

Again the fusion front must be started at some finite distance from the boundary with the starting value  $\epsilon_0$ . With this method, however, the space network remains fixed, thus

the time step does not have to be reduced when € or E-€ is small. Because of the fixed space network, composite bodies will be much simpler to treat with this second method of Murray and Landis. Despite the advantages of the second method over the first, it does not seem to be as widely used as the first.

## A.2.3 Implicit moving node method

After careful review of the various methods available for the solution of freezing-melting problems, a modification of the second method proposed by Murray and Landis was chosen. A fixed space network was chosen because of the ease of treating composite bodies. Instead of finding two temperatures for the lump which contains the fusion front as Murray and Landis suggested, a single floating node located at the fusion front which travels within the fixed space network was used. Figure A.3 shows the relationship between the floating node and the fixed nodes. When the fusion front comes within  $\pm 0.0001 \Delta x_1$  of node i, where  $\Delta x_1$  is the grid spacing of the fixed network, the floating node is removed until the fusion front passes out of this band. When this happens, the temperature of node is set equal to the fusion temperature,  $T_r$ .

Equation [A.1.1] applies to both fixed nodes i and i+1 with  $\Delta x_{-} = \Delta x_{1-}$  and  $\Delta x_{+} = \Delta x_{1+}$  for node i and  $\Delta x_{-} = \Delta x_{2-}$  and  $\Delta x_{+} = \Delta x_{2+}$  for node i+1; the subscripts 1 and 2 refer to the left and right of the fusion front respectively.

Murray and Landis suggested a forward difference approximation to the heat conduction equation, however, the completely implicit backward difference method (CNBD=0.0 in equation [A.1.1]) was chosen because this method allows greater freedom in the choice of calculation time steps and also gave the best comparison with results from an exact solution to the freezing-melting problem.

When the body is initially above or below the fusion temperature, the temperature distribution is calculated by the standard method of finite differences as outlined in section A.1 until the temperature at x=0 passes the fusion temperature. If the temperature at x=0 is within one degree of the fusion temperature, calculation procedes from this point by the implicit moving node method. If the temperature at x=0 passes the fusion temperature by more than one degree, the calculation is backed up one time step and the time step halved. The calculation is allowed to proceed with the new time step and this process is repeated until the boundary temperature is within plus or minus one degree of the fusion temperature. At this time, the freezing-melting calculation by the implicit moving node method begins.

The space derivatives in equation [A.2.4] are approximated by passing a quadratic through nodes i-1, i and the floating node (referring to Figure A.3) for the derivative to the left of the fusion front and nodes i+1, i+2, and the

floating node for the derivative to the right of the fusion front. The approximations are then

$$\frac{\partial T_{1}}{\partial x}\Big|_{x=\epsilon_{-}} = \frac{(T_{1-1}^{m} - T_{f}) \triangle x_{1+}^{2} - (T_{1}^{m} - T_{f})(\triangle x_{1-} + \triangle x_{1+})^{2}}{\triangle x_{1+}^{2}(\triangle x_{1-} + \triangle x_{1+}) - (\triangle x_{1-} + \triangle x_{1+})^{2} \triangle x_{1+}}$$
[A.2.19]

and.

$$\frac{\partial T_{2}}{\partial x}\Big|_{x=\epsilon_{+}} = \frac{(T_{1+2}^{m} - T_{f}) \triangle x_{2-}^{2} - (T_{1+1}^{m} - T_{f}) (\triangle x_{2-} + \triangle x_{2+})^{2}}{(\triangle x_{2-} + \triangle x_{2+}) \triangle x_{2-}^{2} - (\triangle x_{2-} + \triangle x_{2+})^{2} \triangle x_{2-}}$$

$$[A.2.20]$$

If the fusion front is between nodes 0 and 1 or between nodes N-1 and N a linear approximation must be used. The position of the fusion front at time  $t_{m+1}$  can be calculated as

$$\epsilon_{m+1} = \epsilon_m + \frac{\Delta t}{\rho L} \left[ k_1 \frac{\partial T_1}{\partial x} \Big|_{x=\epsilon_-} - k_2 \frac{\partial T_2}{\partial x} \Big|_{x=\epsilon_+} \right] \left[ A.2.21 \right]$$

In the case of a flux boundary condition the procedure is started at time  $t_0$  by replacing  $k_1 \frac{\partial T_1}{\partial x}_{x=\epsilon}$  in equation [A.2.21] by  $q_1$  the average heat flux between time  $t_0$  and time  $t_1$ ; this continues until  $\Delta x_{1+} \ge 0.0001 \Delta x_1$  where  $\Delta x_1$  is the distance between nodes 0 and 1. In the case of a temperature boundary condition an estimate of the fusion front position must be made to start the procedure. In order to obtain this estimate an exact solution for a semi-infinite body subjected to a step change in surface temperature was employed. This solution gives

$$\epsilon_1 = 2 \lambda \sqrt{a_1 t_1}$$
 [A.2.22]

where  $\epsilon_1$  is the estimate of the fusion front location at time  $t_1$ ,  $\alpha_1$  is the thermal diffusivity of the material to the left of the fusion front, and  $\lambda$  is a constant determined by solving for the root of equation [2.4.4]. Equation [2.4.4] can be solved easily by the Newton-Raphson iterative method. The time step should be small enough so that  $\epsilon_1$  from equation [A.2.22] is much less than  $x_1$ , the distance from the surface to the first node. The temperature of the boundary node is determined from the given boundary temperature and the temperature of the floating node is fixed at the fusion temperature.

The calculation procedure for a single time step is then:

- 1. Using the fusion front location at time t<sub>m</sub>, calculate the temperature distribution for time t<sub>m+1</sub>. The body is treated as two separate bodies, one to the left of the fusion front and one to the right; the finite difference equations of section A.l are applied to both. The rear boundary condition of the body to the left of the fusion front is that of constant temperature, i.e. the fusion temperature. The front boundary of the body to the right of the fusion front is also held at the fusion temperature.
- 2. Calculate the fusion front location for time  $t_{m+1}$  using equations [A.2.19], [A.2.20], and [A.2.21].

- 3. Calculate  $\Delta x_{1-}$ ,  $\Delta x_{1+}$ ,  $\Delta x_{2-}$ , and  $\Delta x_{2+}$  for use in calculation of the next time step.
- 4. Return to step 1.

Calculation proceeds in this manner until the fusion front crosses the entire body, then the calculation procedure returns to the standard finite difference methods of section A.1.

Several test cases were run to check the accuracy of the method and the computer program. Comparison was made with the results of an exact solution for a semi-infinite body initially at a uniform temperature above the fusion temperature with a step change in surface temperature and an approximate solution for a finite slab initially at the fusion temperature with a constant heat flux boundary condition at x=0 and an insulation boundary condition at x=0.

The exact solution is given in Chapter II by equations [2.4.1] through [2.4.9]. A comparison of results from the finite difference solution for both Crank-Nicolson (CNBD=0.5) and backward difference (CNBD=0.0) methods and the exact solution is shown in Figure A.4. The backward difference method seems to be superior to the Crank-Nicolson method for this problem.

The approximate solution used to check the accuracy of the computer program was found using an integral energy method similar to that used in Chapter II. The body is considered to be initially completely solid at the fusion temperature; thus, no heat passes the interface between

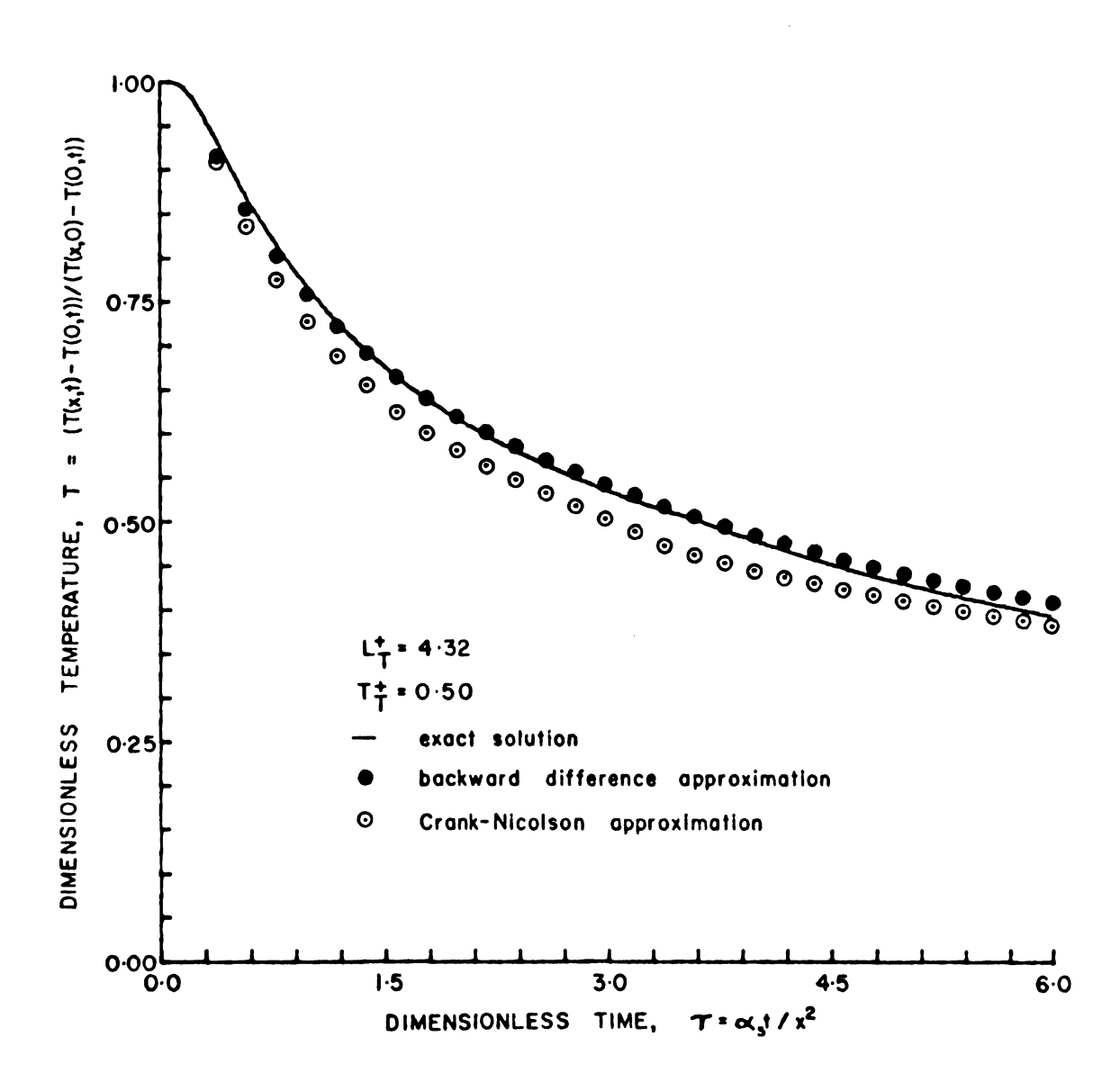


Figure A.4 A comparison of finite difference solutions to an exact solution of the freezing-melting problem.

solid and liquid and only the properties of the liquid and the heat of fusion become involved in the solution. After the fusion front moves across the entire body, an exact solution for a finite slab with a constant heat flux at x=0 and insulated at x=E was used to describe the temperature distribution. The solution is

$$\bar{T}_{\mathcal{L}} = \frac{T - T_{\mathcal{L}}}{qE/k_{\mathcal{L}}} = A\left[\frac{x}{E} - \frac{\epsilon}{E}\right] + B\left[\frac{x}{E} - \frac{\epsilon}{E}\right]^{2}; \quad \tau \leq \tau_{m}, \quad 0 \leq \frac{x}{E} \leq \frac{\epsilon}{E}$$

$$\left[A.2.23(a)\right]$$

$$\bar{T}_{s} = \frac{T - T_{\mathcal{L}}}{qE/k_{\mathcal{L}}} = 0; \quad \tau \leq \tau_{m}, \quad \frac{\epsilon}{E} \leq \frac{x}{E} \leq 1$$

$$\left[A.2.23(b)\right]$$

where A and B are given by

$$A = \frac{L_{q}^{+}}{2} - \left[ \frac{L_{q}^{+}}{(\epsilon/E)} + \frac{L_{q}^{+^{2}}}{4(\epsilon/E)^{2}} \right]^{\frac{1}{2}}$$
 [A.2.23(c)]

and

$$B = \frac{1}{2} \left[ \frac{1}{(\epsilon/E)} + \frac{L_{q}^{+}}{2(\epsilon/E)} \right] - \frac{1}{2} \left[ \frac{L_{q}^{+}}{(\epsilon/E)^{3}} + \frac{L_{q}^{+^{2}}}{4(\epsilon/E)^{4}} \right]^{\frac{1}{2}}$$
[A.2.23(d)]

The location of the fusion front  $\epsilon/E$  is found by solving the algebraic equation

$$\tau = \frac{1}{6} \left( \frac{\epsilon}{E} \right)^2 + \frac{5}{6} L_q^+ \left( \frac{\epsilon}{E} \right) + \frac{1}{3} \left[ \frac{1}{4} L_q^{+2} \left( \frac{\epsilon}{E} \right)^2 + L_q^{+} \left( \frac{\epsilon}{E} \right)^3 \right]^{\frac{1}{2}} \left[ A.2.24 \right]$$

The time  $au_{\mathrm{m}}$  is the time for the entire body to melt and is given by

$$\tau_{\rm m} = \frac{5}{6} L_{\rm q}^{+} + \frac{1}{3} \left[ L_{\rm q}^{+} + \frac{1}{4} L_{\rm q}^{+2} \right]^{\frac{1}{2}} + \frac{1}{6}$$
 [A.2.25]

After the entire body melts  $( au> au_{\mathrm{m}})$ , the solution is given by

$$\bar{T}_{2} = \frac{T-T_{f}}{qE/k_{2}} = \tau + \frac{1}{2} \left(\frac{x}{E}\right)^{2} - \frac{x}{E} - A + B + \frac{7}{6}$$

$$+ \frac{2}{\pi^{2}} \sum_{n=1}^{\infty} \frac{2B-1}{n^{2}} e^{-n^{2}\pi^{2}\tau} \cos\left[n\pi\left(1-\frac{x}{E}\right)\right]$$
[A.2.26]

Results of the approximate solution and the finite difference solution using the backward difference approximation are shown in Figure A.5. There seems to be quite good agreement between the two solutions.

ı			

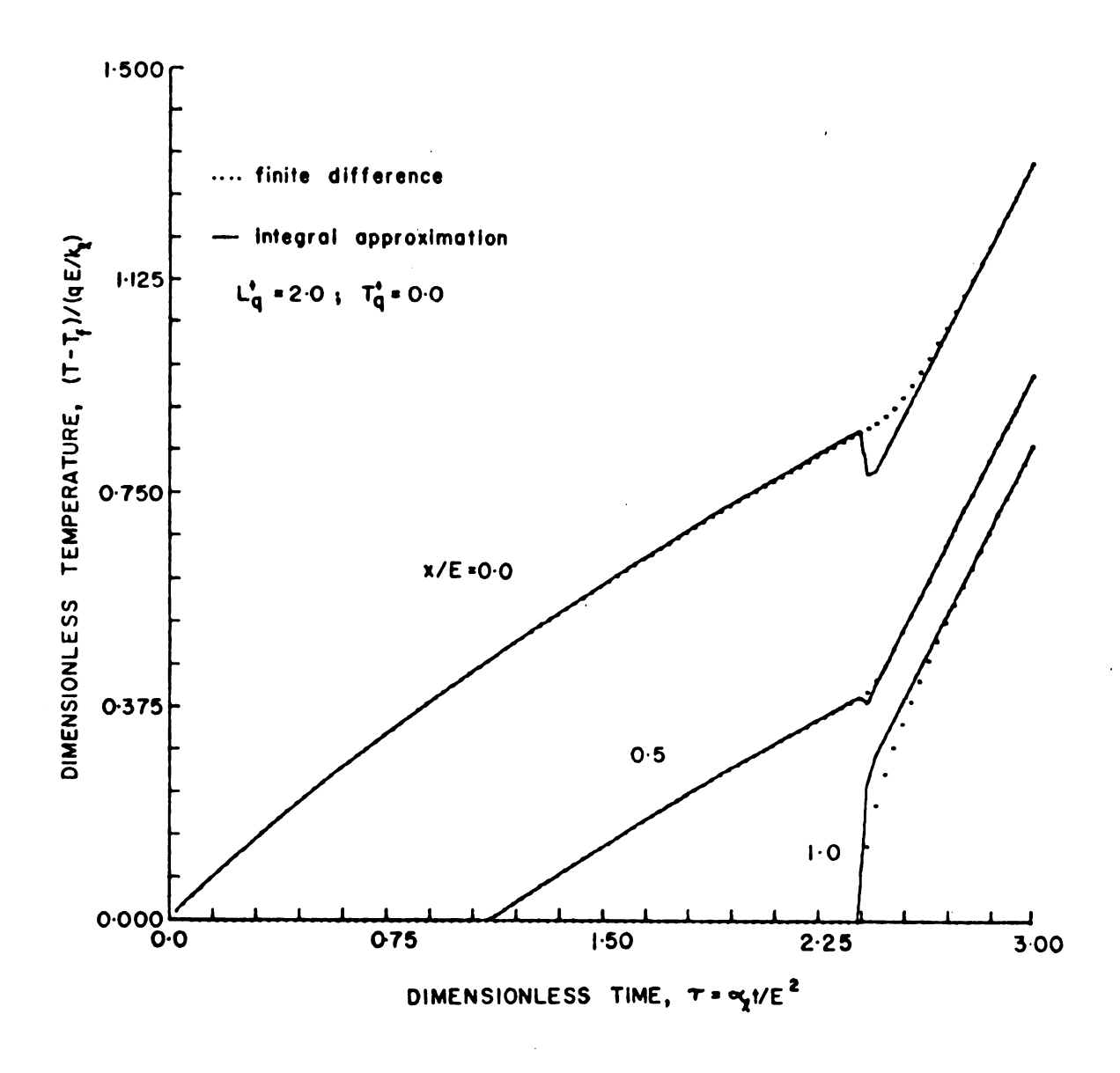


Figure A.5 A comparison of the finite difference solution to an approximate solution of the freezing-melting problem.

#### APPENDIX B

# THE PARAMETER ESTIMATION PROCEDURE AND THE CALCULATION OF SENSITIVITY COEFFICIENTS

B.1 The Gauss-Newton or linearization method of minimizing the sum of squares function

The sum of squares function is (40)

$$F(\underline{P}) = \left[\underline{Y} - W(\underline{P})\right]\underline{\Psi}^{-1}\left[\underline{Y} - W(\underline{P})\right] \qquad [B.1.1]$$

where  $\underline{Y}$  is the vector of observations of n thermocouples and m time steps.

$$\underline{\underline{Y}^{(nm \times 1)}} = \begin{bmatrix} \underline{\underline{Y}_{1}^{(m \times 1)}} \\ \underline{\underline{Y}_{2}^{(m \times 1)}} \\ \vdots \\ \underline{\underline{Y}_{n}^{(m \times 1)}} \end{bmatrix}$$
 [B.1.1(a)]

 $\underline{\underline{W}}(\underline{P})$  is the vector of predictions from the mathematical model for n locations and m time steps,

$$\underline{\underline{w}^{(nm \times 1)}(\underline{P})} = \begin{bmatrix} \underline{\underline{w}_{1}^{(m \times 1)}(\underline{P})} \\ \underline{\underline{w}_{2}^{(m \times 1)}(\underline{P})} \\ \vdots \\ \underline{\underline{w}_{n}^{(m \times 1)}(\underline{P})} \end{bmatrix}$$
[B.1.1(b)]

P is the vector of parameters in the mathematical model,

$$\underline{P} = \begin{bmatrix} p_1 \\ p_2 \\ \vdots \\ p_k \end{bmatrix}$$
 [B.1.1(c)]

and  $\Psi$  is a weighting matrix.

For the most accurate parameter estimates \( \bar{Y} \) should be made the covariance matrix of the observation errors (see Deutsch (40), p. 60, for proof). Unfortunately we have no way to determine the covariance matrix at this time; thus the weighting matrix will be defined as

$$\underline{\Psi} = \sigma^2 \underline{I}$$
 [B.1.1(d)]

Where  $\sigma^2$  is the constant variance of the observations and  $\underline{\mathbf{I}}$  is the identity matrix. The sum of squares function then becomes

$$F(\underline{P}) = \frac{1}{\sigma^2} \sum_{u=1}^{N} (y_u - w_u)^2 \qquad [B.1.1(e)]$$

Where  $y_u$  is the  $u^{th}$  measurement and  $w_u$  is the corresponding prediction. N is the total number of observations which is equal to the product nm.

One of the simplest and most efficient methods of minimizing the sum of squares function is called the Gauss-Newton or linearization method. It is assumed that an initial estimate,  $\underline{P}^0$ , of the parameter vector  $\underline{P}$  is available and of sufficient accuracy to allow  $\underline{W}(\underline{P}^*)$ , where  $\underline{P}^*$  is the parameter vector that minimizes  $\underline{F}$  in equation

[A.3.1], to be approximated by the truncated Taylor series

$$\underline{\underline{W}}(\underline{\underline{P}}^*) = \underline{\underline{W}}(\underline{\underline{P}}^{\circ}) + \left[\underline{\underline{\nabla}}_{\underline{p}}\underline{\underline{W}}^{\bullet}(\underline{\underline{P}}^{\circ})\right]^{\bullet}(\underline{\underline{P}}^* - \underline{\underline{P}}^{\circ}) \qquad \left[\underline{B.1.2}\right]$$

where

$$\underline{\nabla}_{p} = \begin{bmatrix} \frac{\partial}{\partial p_{1}} \\ \frac{\partial}{\partial p_{2}} \\ \vdots \\ \frac{\partial}{\partial p_{k}} \end{bmatrix}$$
[B.1.2(a)]

The sum of squares function  $F(\underline{P})$ , is minimized by differentiating with respect to  $p_i$  and equating to zero

$$2\underline{Z} \ \Psi^{-1} \left[ \underline{Y} - \underline{W}(\underline{P}^*) \right] = \underline{0} \qquad [E.1.3]$$

where

$$Z'(\underline{P}) = \underline{\nabla}_{\underline{p}}\underline{w}'(\underline{P})$$
 [B.1.3(a)]

If we substitute equation [B.1.2] into equation [B.1.3], we obtain

$$\underline{z}^{\bullet}\underline{\Psi}^{-1}\left[\underline{Y}-\underline{W}(\underline{P}^{\circ})\right]+\underline{z}(\underline{P}^{\circ})(\underline{P}^{*}-\underline{P}^{\circ})=\underline{0}\quad \left[\text{B.1.4}\right]$$

Solving for  $\underline{P}^*$  in equation [B.1.4]

$$\underline{P}^* = \underline{P}^o + \underline{N}^{-1}\underline{Z}'(\underline{P}^o)\underline{\Psi}^{-1}\left[\underline{Y} - \underline{w}(\underline{P}^o)\right] \qquad \left[B.1.5\right]$$

<sup>1.</sup> Note the prime (') denotes transposition.

where the square matrix N is defined by

$$\underline{\mathbf{N}} = \underline{\mathbf{Z}} \cdot \underline{\mathbf{Y}}^{-1} \underline{\mathbf{Z}}$$
 [B.1.6]

The true value of  $\underline{P}^*$  is usually not reached on the first iteration so the iterative formula

$$\underline{P}^{k} = \underline{P}^{k-1} + \underline{N}^{-1}\underline{Z}'(\underline{P}^{k-1})\underline{\Psi}^{-1}[\underline{Y} - \underline{W}(\underline{P}^{k-1})] \quad [B.1.7]$$

is applied. The iteration can be stopped when all the  $p_{\text{i}}^{k}-p_{\text{i}}^{k-1} \text{ have satisfied some predetermined criterion such as}$ 

$$\frac{p_{1}^{k} - p_{1}^{k-1}}{p_{1}^{k}} < 0.001$$

## B.2 Calculation of sensitivity coefficients

The matrix Z is called the matrix of sensitivity coefficients. The sensitivity coefficients are an important part of parameter estimation, not only in the Gauss-Newton algorithm but in the determination of optimum experiments. The numerical approximation of these derivatives is not difficult once the mathematical model has been programmed; the differentiation can be approximated as

$$\frac{\mathbf{a}^{w(\underline{P},x_{i},t_{i})}}{\mathbf{a}^{p_{j}}} \simeq$$

$$\frac{w(p_{1},...,p_{j}+\delta p_{j},...p_{k},x_{i},t_{i})-w(p_{1},...,p_{j},...,x_{i},t_{i})}{\delta p_{j}}$$
[B.2.1]

where  $\delta$  is some small value, say 0.001.

In order to test the method and the computer program, sensitivity coefficients for a test case were computed using the computer program and compared with sensitivity coefficients calculated using the exact solution. The test case used a finite body exposed to a constant heat flux at one surface (x=0) and insulated at the other (x=E). The exact solution for the dimensionless sensitivity coefficients is

$$\frac{k}{qE/k} \frac{\delta T}{\delta k} = -\frac{3(E-x)^2 - E^2}{6E^2} + \frac{2}{\pi^2} \sum_{n=1}^{\infty} \frac{1}{n^2} e^{-n^2 \pi^2 \tau_{\cos(\frac{n\pi x}{E})}}$$

$$+ 2\tau \sum_{n=1}^{\infty} e^{-n^2 \pi^2 \tau_{\cos(\frac{n\pi x}{E})}}$$
[B.2.2]

$$\frac{\rho c_p}{qE/k} \frac{\partial T}{\partial (\rho c_p)} = \tau \left[1 + 2 \sum_{n=1}^{\infty} e^{-n^2 \pi^2 \tau} \cos \left(\frac{n \pi x}{E}\right)\right] \quad [B.2.3]$$

The results are shown in Figure B.1 and Figure B.2; the numerical approximation to the derivatives seems to work quite well for the case of no change of phase.

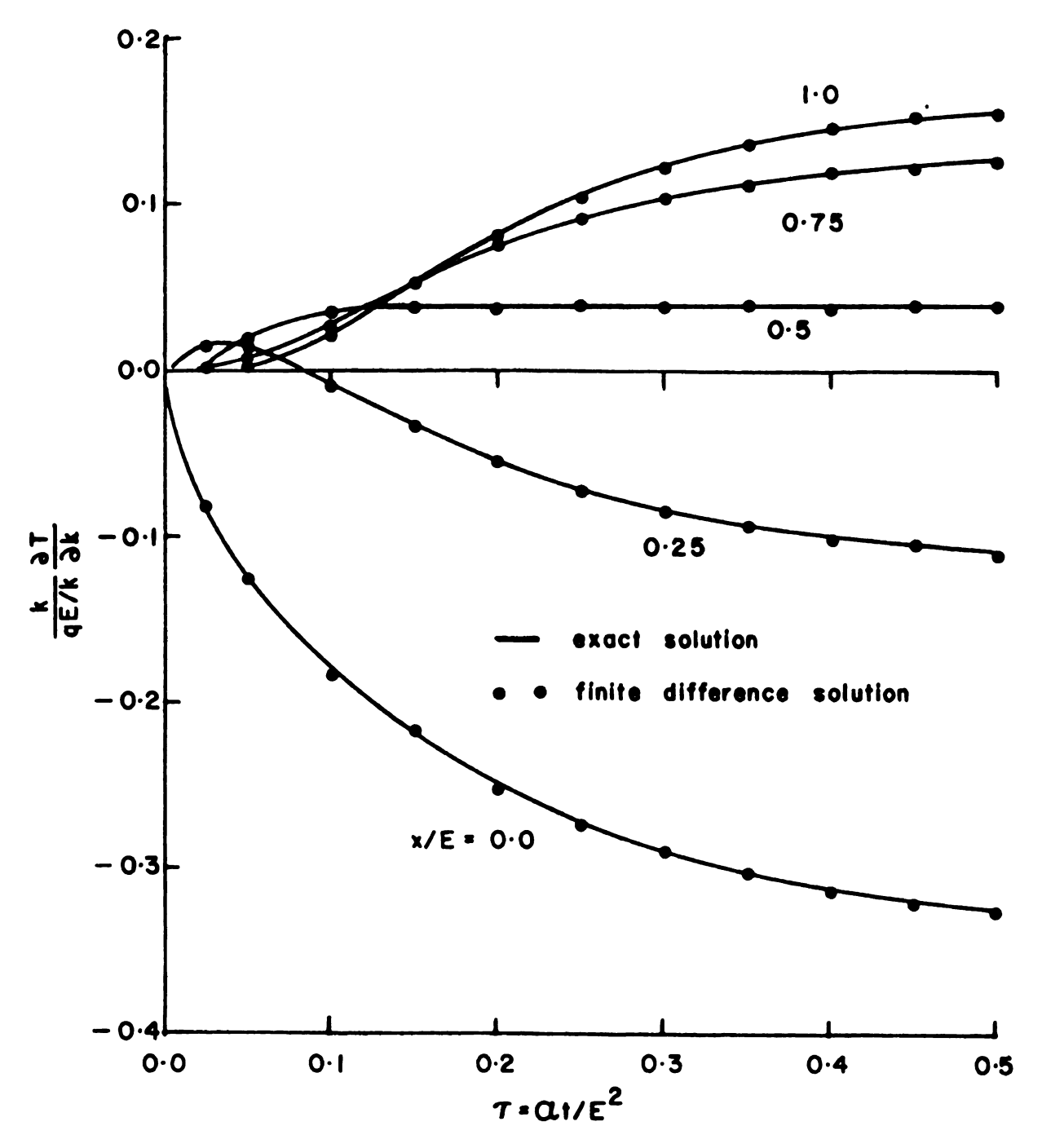


Figure B.1 A comparison of exact and numerical approximation of the dimensionless sensitivity coefficient  $S_k^T(x,t)$  for a finite body with constant heat flux, q, at x=0 and insulated at x=E.

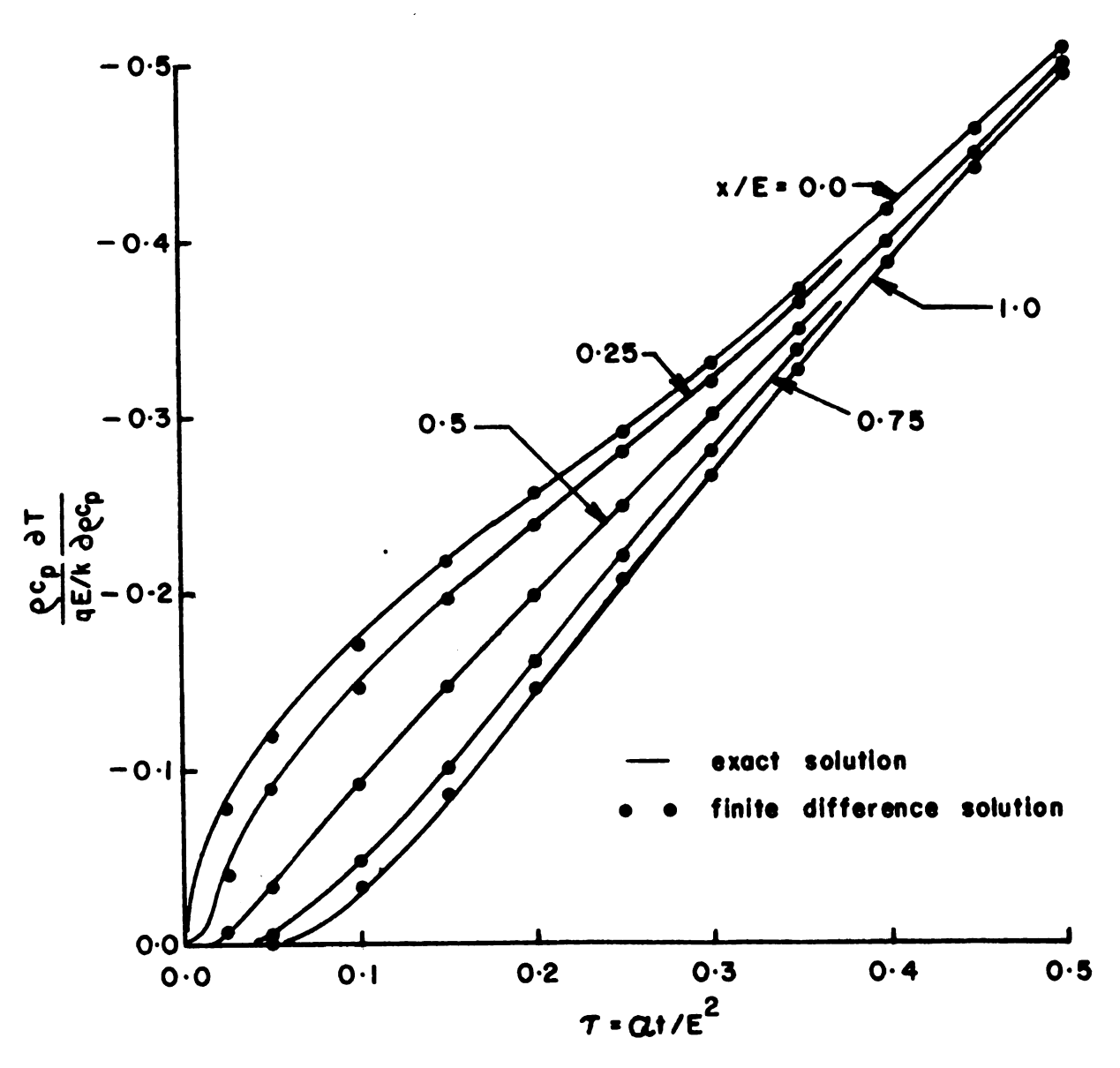


Figure B.2 A comparison of exact and numerical approximation of the dimensionless sensitivity coefficient  $S_p^T(x,t)$  for a finite body with constant heat flux, q, at x=0 and insulated at x=E.

### APPENDIX C

## THE CALCULATION OF SURFACE HEAT FLUX FROM AN INTERNAL TEMPERATURE HISTORY

The problem of finding the surface heat flux given the temperature history of a body at some internal point is known as the inverse heat conduction problem. That is, the boundary condition at one surface (the heat flux) is unknown, while the temperature (or solution to the normal boundary value problem) at some internal point is known.

The heat conduction equation for a one dimensional homogeneous body is

$$\frac{\partial}{\partial x} \left( k \frac{\partial T}{\partial x} \right) = \rho c_{p} \frac{\partial T}{\partial t}$$
 [C.1]

and the boundary and initial conditions for the inverse problem, assuming for simplicity the body to be insulated at x=E, and the temperature history for some point x=e is known, are

$$T(e,t) = T_e(t)$$
 [C.2]

$$\frac{\partial T(B,t)}{\partial x} = 0 \qquad [C.3]$$

$$T(x,0) = T_{1}(x) \qquad [C.4]$$

The problem is to calculate

$$q(0,t) = -k \frac{\partial T(0,t)}{\partial x} \qquad [C.5]$$

For a review of the various methods, the reader is referred to the paper by Beck (35). To illustrate the difficulty encountered by most methods of solving the inverse problem, Beck considered the effect of a short heat pulse of duration  $\tau_{p}$  at x=0 upon the temperature rise at x=E, the insulated surface of the body. The ratio of the temperature rise to the maximum temperature rise [T(E,t)-T,]/ $T(E)_{max}-T_i$  versus  $\tau/\tau$  p for several values of  $\tau_p$  is shown in Figure C.1. Note that the ratio of temperature rise to maximum temperature rise at time  $\tau/\tau_{\rm p}$ =1 becomes very small as  $au_{p}$  decreases below 0.1. Thus very little information about the heat pulse reaches the insulated surface in time  $\tau_{p}$  for  $\tau_{p}$  less than 0.1. As  $\tau/\tau_{p}$ becomes larger than 1; however, more information becomes available about the heat pulse. Beck used this fact in his concept of "future temperatures". That is, to calculate the average heat flux over the time interval  $\boldsymbol{\tau}_{\mathrm{p}}$  he employed temperatures at times  $2\tau_p$ ,  $3\tau_p$ ,... The temperatures at times  $2\tau_p$ ,  $3\tau_p$ ,... are called future temperatures. In general, the smaller  $au_{p}$  the more future temperatures are needed.

The procedure to solve the inverse problem for an arbitrarily varying heat flux is to divide the heat flux into a finite number of heat pulses. The duration of pulse  $q_m$  is from time  $t_{m-1}$  to time  $t_m$ . This is illustrated in Figure C.2. The duration of the various pulses need not be same.  $q_1$  is found by minimizing the sum of squares function

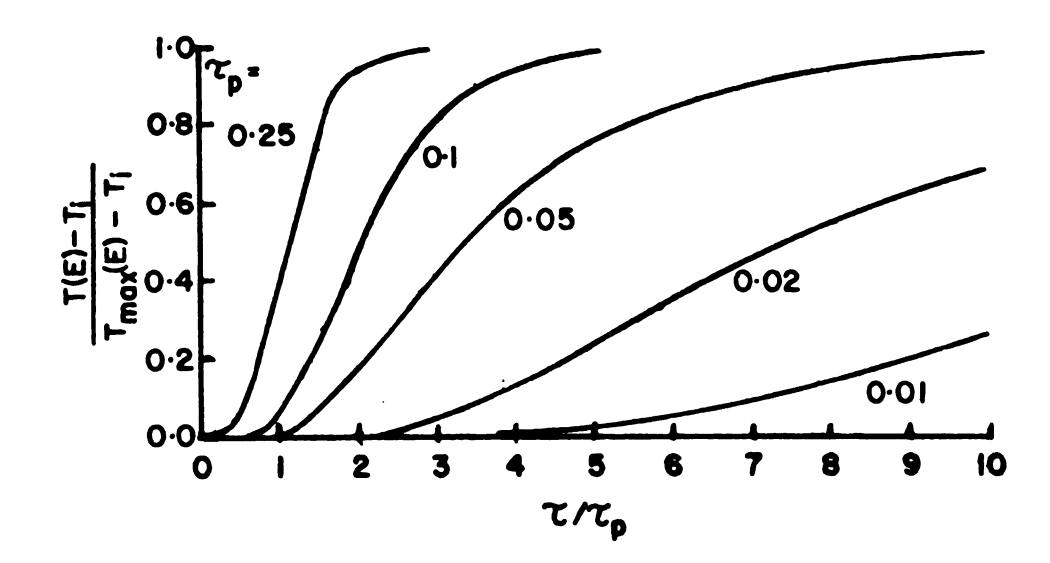


Figure C.1 Ratio of temperature rise to maximum temperature rise versus ratio of dimensionless time to dimensionless duration of heat pulse at the insulated surface of a plate with a heat pulse applied to the other surface.

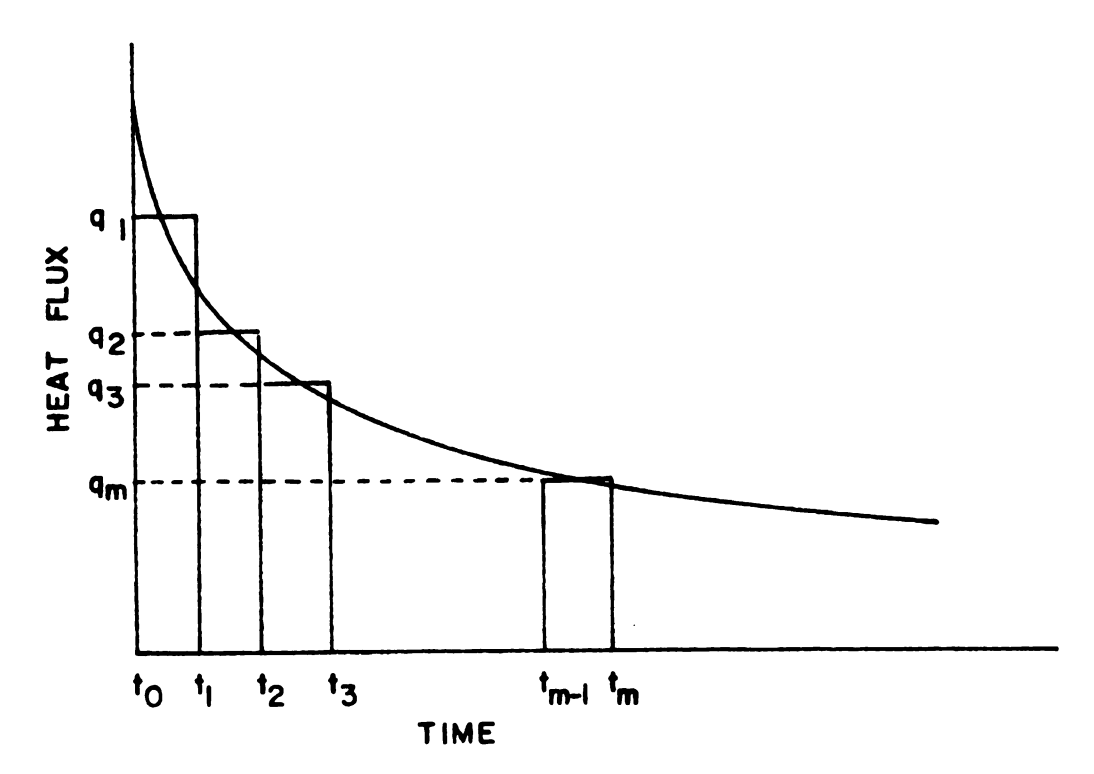


Figure C.2 Illustration of how a time varying heat flux is broken up into a series of heat pulses.

$$F(q_1) = \sum_{i=1}^{I} \left[T_e^{1+i}(q_1) - T_{exp}^{1+i}\right]^2$$
 [C.6]

where  $T_e^{l+i}(q_l)$  is the calculated temperature at location x=e and time  $t_{l+i}$ ,  $T_{exp}^{l+i}$  is the experimentally measured temperature at the same time and location, and I is the number of future temperatures used.

Once  $q_1$  is found,  $q_2$  is found in the same manner using the calculated temperatures at time  $t_1$  as the initial conditions in the mathematical model. The sum of squares function then becomes

$$F(q_2) = \sum_{i=1}^{I} \left[T_e^{2+i}(q_2) - T_{exp}^{2+i}\right]^2$$
 [C.7]

Thus the solution is marched out in time until all the heat pulses are found.

The power of this method now becomes apparent. The calculated temperature in the sum of squares function can be supplied from any solution of the heat conduction equation; thus, finite difference solutions which can treat composite bodies and temperature variable properties can be employed. The sum of squares function can be extended to include measurements from thermocouples at several different locations in the body, thus helping to minimize the effect of errors due to inaccurately known thermocouple locations.

A computer program was written for this algorithm using the Crank-Nicolson finite difference method to solve the heat conduction equation for composite bodies with temperature variable properties. Two test cases were solved

using the program and are presented here. Several different cases can be found in the paper by Beck. The first case is that of a finite slab with a step change in heat flux at x=0 and insulated at x=E. The data used in this case is the temperature of the insulated surface and it is accurate to six places. The results are shown in Figure C.3. for values of I=1, 2, and 3. The dimensionless time step for the  $q_i$  was  $\Delta \tau_E$ =0.05. Note the improved response time between values of I=1 and I=2. The second case has the same geometry as the first, but with noisy data The data from case 1 was truncated to three being used. places without rounding. Two future temperatures were used in the calculation and the time step for the  $q_4$  remained at  $\Delta \tau_{\rm E}$ =0.05. The results of this test are shown in Figure C.4. They make it evident that this method of solving the inverse heat conduction problem is very successful.

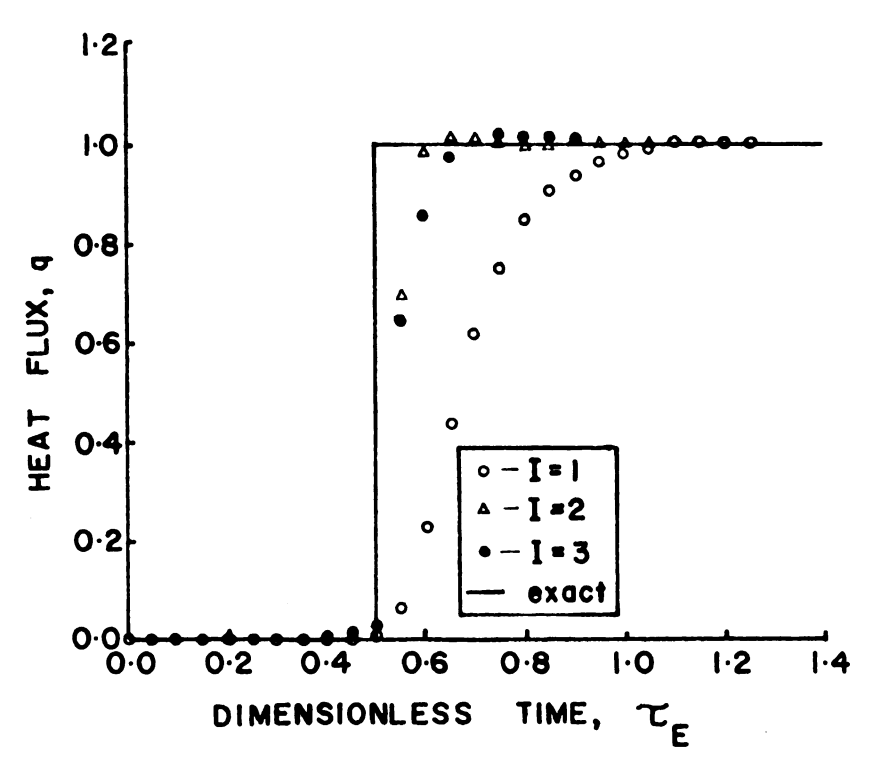


Figure C.3 Comparison of heat flux calculated from temperature data accurate to six places for 1,2, and 3 future temperatures for a slab with a step in flux at one surface and the other surface insulated.

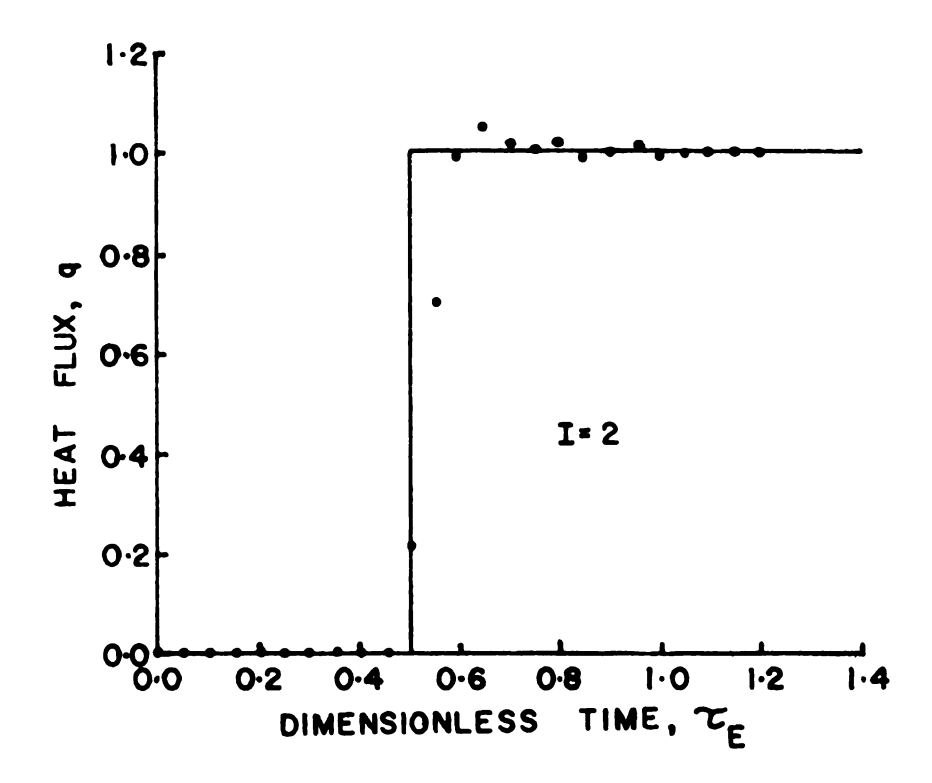


Figure C.4 Heat flux calculated from noisy data for 2 future temperatures for a slab with a step in flux at one surface and insulated at the other surface.

